INSTITUTO NACIONAL DE PESQUISAS DA AMAZÔNIA - INPA
PROGRAMA DE PÓS-GRADUAÇÃO EM BOTÂNICA

Alterações no pulso de inundação: como reagem os igapós da Amazônia Central?

ANGÉLICA FARIA DE RESENDE

Manaus, Amazonas
Maio de 2019

Angélica Faria de Resende

Alterações no pulso de inundação: como reagem os igapós da Amazônia Central?

ORIENTAÇÃO:
DR. JOCHEN SCHÖNGART

Coorientação:
Dr. Thiago Sanna Freire Silva
Dra. Susan E. Trumbore

Fontes financiadoras: CNPq, CAPES, FAPEAM.

Tese de doutorado, apresentado ao Programa de Pós-Graduação em Botânica, do Instituto Nacional de Pesquisas da Amazônia, como parte dos requisitos para obtenção do título de Doutora em Botânica.

Manaus, Amazonas
Maio de 2019

INPA
INSTITUTO NACIONAL DE PESQUISAS DA AMAZÔNIA

PÁTRIA AMADA BRASIL

Curso de Pós-Graduação em Botânica • INPA

ATA DEFESA PÚBLICA DE TESE DE DOUTORADO DISCENTE DO PROGRAMA DE PÓS-GRADUAÇÃO EM BOTÂNICA DO INSTITUTO NACIONAL DE PESQUISAS DA AMAZÔNIA.

Aos vinte e quatro dias do mês de maio de 2019 às 09:00 horas, no auditório da Pós-graduação do INPA-Campus I, reuniu-se a Comissão Examinadora da Defesa Pública, composta pelos seguintes membros: Dr. Giuliano Maselli Locosselli, da Universidade de São Paulo (USP), Dr. Bruce Rider Forsberg, do Instituto Nacional de Pesquisas da Amazônia (INPA), Dra. Veridiana Vizoni Scudeller, da Universidade Federal do Amazonas (UFAM), Dr. Daniel Magnabosco Marra, do Instituto Nacional de Pesquisas da Amazônia (INPA/Max Planck), e Dr. Adriano Costa Quaresma, do Instituto Nacional de Pesquisas da Amazônia (INPA), tendo como suplentes: Dr. Adrian Paul Ashton Barnett, do Instituto Nacional de Pesquisas da Amazônia (INPA) e Dr. Eduardo Magalhães Borges Prata, do Instituto Nacional de Pesquisas da Amazônia (INPA), sob a presidência do primeiro, a fim de proceder a arguição pública da **TESE DE DOUTORADO**, intitulada: **"Alterações no pulso de inundação: como reagem os igapós da Amazônia Central?"** discente: **Angélica Faria de Resende**, sob orientação: Dr. Jochen Schongart. Após a exposição, dentro do tempo regulamentar, a discente foi arguida oralmente pelos membros da Comissão Examinadora, tendo recebido o conceito final:

EXAMINADORES	PARECER		ASSINATURA
ADRIANO COSTA QUARESMA	(X) APROVADO	( ) REPROVADO	
BRUCE RIDER FORSBERG	(X) APROVADO	( ) REPROVADO	
DANIEL MAGNABOSCO MARRA	(X) APROVADO	( ) REPROVADO	
GIULIANO MASELLI LOCOSSELLI	(X) APROVADO	( ) REPROVADO	
VERIDIANA VIZONI SCUDELLER	(X) APROVADO	( ) REPROVADO	
ADRIAN PAUL ASHTON BARNETT	( ) APROVADO	( ) REPROVADO	
EDUARDO MAGALHÃES BORGES PRATA	( ) APROVADO	( ) REPROVADO	

Manaus (AM), 24 de maio de 2019

OBS: _____

Nada mais havendo, foi lavrado a presente ata, que, após lida e aprovada, foi assinada pelos membros da Comissão Examinadora.

Dr. Michael John Gilbert Hopkins
Coordenador do Programa de
Pós-Graduação em Botânica
PO. 116/2017 - DIBOT/INPA

INPA
INSTITUTO NACIONAL DE PESQUISAS DA AMAZÔNIA

DIVISÃO DOS CURSOS DE PÓS-GRADUAÇÃO

AULA DE QUALIFICAÇÃO

Curso de Pós-Graduação em Botânica ★ INPA

P A R E C E R

Aluna: **ANGÉLICA FARIA DE RESENDE**
Curso: BOTÂNICA
Nível: Doutorado
Orientador: Dr. Jochen Schongart, Coorientação: Dr. Thiago Sanna Freire Silva e Dra. Susan Trumbore

Título:

"Influência de Alterações no Regime Hidrológico e Eventos Climáticos Extremos em Igapós da Amazônia Central"

BANCA JULGADORA:

TITULARES:
RAFAEL ASSIS
BRUCE WALKER NELSON
HENRIQUE NASCIMENTO
PHILIP FEARNSIDE
MARIA TERESA FERNANDEZ PIEDADE

SUPLENTES:
JULIANA SCHIETTI
ADRIAN PAUL ASHTON BARNETT

EXAMINADORES	PARECER	ASSINATURA
RAFAEL ASSIS	(X)APROVADO( ) REPROVADO	
BRUCE WALKER NELSON	(X)APROVADO( ) REPROVADO	
HENRIQUE NASCIMENTO	(X)APROVADO( ) REPROVADO	
PHILIP FEARNSIDE	(X)APROVADO( ) REPROVADO	
MARIA TERESA FERNANDES PIEDADE	(X)APROVADO( ) REPROVADO	
JULIANA SCHIETTI	( )APROVADO( ) REPROVADO	
ADRIAN PAUL ASHTON BARNETT	( )APROVADO( ) REPROVADO	

Manaus (AM), 19 de Agosto de 2015.

OBS:_____

p/ Dr. Michael John Gilbert Hopkins
Coordenador do Programa de Pós Graduação em Botânica
PO. 258/2014

Ficha catalográfica

R433a RESENDE, ANGELICA FARIA DE
Alterações no pulso de inundação: como reagem os igapós da Amazônia Central? / ANGELICA FARIA DE RESENDE; orientador Jochen Schöngart; coorientadores Thiago S. F. Silva & Susan E. Trumbore. -- Manaus:[s.l], 2019.
126 f.

Tese (Doutorado - Programa de Pós Graduação em Botânica) -- Coordenação do Programa de Pós-Graduação, INPA, 2019.

1. alterações no regime hídrico. 2. florestas alagáveis. 3. hidrelétricas. 4. dendroecologia. 5. sensoriamento remoto. I. Schöngart, Jochen, orient. II. Susan E. Trumbore, Thiago S. F. Silva &, coorient. III. Título.

CDD: 580

Sinopse

Sinopse:
Estudou-se como as alterações do pulso de inundação afetam as florestas sazonalmente alagadas por água-preta (igapó) na Amazônia Central em sistemas não perturbados (Parque Nacional do Jaú - PNJ) e impactados pela usina hidrelétrica (UHE) de Balbina (Reserva de Desenvolvimento Sustentável do Uatumã - RDSU). Por meio de sensoriamento remoto os igapós do Rio Uatumã foram classificados e mapeados para estudar o impacto da alteração do regime hidrológico, afetando principalmente os macro-habitats dominados pela espécie arbórea *Eschweilera tenuifolia* a jusante da barragem. Cronologias de anéis de crescimento de *E. tenuifolia* no PNJ e RDSU indicam mudanças nas relações entre crescimento arbóreo e clima durante o período de intensificação do ciclo hidrológico induzido por mudanças climáticas (PNJ) e pela UHE (RDSU). Abordagens dendroecológicas relatam mudanças no crescimento populacional da espécie em igapós impactados pela UHE de Balbina em comparação com os macro-habitats no PNJ.

Palavras-chave: Intensificação do regime hídrico, florestas alagáveis, hidrelétricas, dendroecologia, sensoriamento remoto.

Agradecimentos

Esse trabalho é fruto de muito tempo de dedicação, quase exclusiva, a algo que amo de forma incondicional: a Floresta, ou melhor dizer "As Florestas", que formadas por incontáveis elementos e suas variáveis tanto me encantam e despertam a curiosidade, essa que me levou a seguir os sinuosos trilhos da ciência no Brasil. De todas as incríveis florestas que estive, as árvores são os seres mais magníficos que já conheci, não apenas pela beleza ou pelos incontáveis benefícios que trazem ao mundo, mas também pela resistência ao tempo e a enorme capacidade que têm em se adaptar ao ambiente. Sinto gratidão por viver em um planeta com árvores e ter o privilégio de estudá-las.

Meus mais de quatro anos de doutorado foram despendidos entre Manaus, Rio Jaú, Rio Uatumã, a cidade de Rio Claro (UNESP, São Paulo), Fayetteville (Arkansas, EUA), Jena (Turíngia, Alemanha) e ao final em Belém. Não faltaram mãos para me apoiar, a começar pelo meu sábio orientador Dr. Jochen Schöngart, que esteve indescritivelmente presente em cada detalhe desta tese, os queridos e competentes coorientadores (oficiais e extraoficiais) Dr. Thiago S. F. Silva, Dra. Susan E. Trumbore, Dr. David W. Stahle e Dra. Maria Teresa F. Piedade, todos de extrema importância não apenas na concepção desta tese, mas principalmente na minha formação profissional e pessoal, todos me receberam em seus respectivos laboratórios e me ensinaram muito.

Houve muita gente envolvida na complexa logística de se realizar trabalhos de campo na Amazônia. Houve os que levantaram a verba, compraram insumos e organizaram as excursões, os que cozinharam para pudéssemos trabalhar, houveram aqueles que me acompanharam em campo e suaram a camisa furando e cortando árvores, Sr. Raimundo do Jaú, Josué e Sr. Domingos do Uatumã, Celso, Mário, Val, Jaime, Victor Lery, Yuri Feitosa, Alberto Peixoto, Eduardo Rios, Layon O. Demarchi, Jekiston, Anderson, Gildo, entre outros.

Mas tudo isso só foi possível pelo esforço e apoio de minha mãe e da minha família; cada um tem sua enorme contribuição em toda minha vida, até mesmo pelo simples fato de existir, Francisco, Selvita, Lourdes, Catarina, Lívia, Téo, Marília, Malu, João Pedro, Mayra, Geisels, Miguel, Matthew e muitos outros familiares. Foi essencial o enorme apoio do meu

companheiro Pedro, que sempre teve papel não apenas de namorado, marido, mas também de amigo, irmão, pai, conselheiro e algumas vezes de coorientador.

Amigos, então, é difícil colocar todos os nomes no papel, foi tanta gente me dando força e esperança, isso foi essencial ao meu crescimento pessoal. E dentre os que estiveram mais próximos nesses dias de calor manauara eu não poderia deixar de citar Sabine, Carol, Thaiane, Aline, Igor, Danilo Pulga, Izabela, Lydiane, Flávia D., César, Luciana E., Ana Cláudia, Raffaello, Maíra da Rocha, Gisele, Bianca, Luciana M., Maria, todos do MAUA: Layon, Adriano, Abner, Vivi, Gildo, Luciana C., em especial Aline Lopes que sempre me ajudou na parte escrita, e muitos outros que tiveram seu papel.

Os companheiros de laboratório que acabaram virando família, merecem aqui ser citados, quando eu cheguei na casa 20 (nosso laboratório de dendroecologia) eu fui muito bem recebida pelo Bruno, Cyro e pelo Bóris, a Eliane e até o Victor Hugo já aparecia as vezes por ali. Depois vieram muitos alunos que aumentaram a família: Tito, Beto, Yuri, Jailane (que hoje mora num lugar melhor), Maíra, Juliana, Jekiston e Fernanda (meus Pibics favoritos), Tayane, Janaína, Priscila, Anderson e Kézia. E nosso técnico Sr. Gilson.

Agradeço muito a todos que de alguma maneira me apoiaram e incentivaram. Agradeço ainda aos pesquisadores que muito colaboraram na revisão do meu plano, e também do artigo, e ainda aos membros da banca que engrandeceram esse trabalho com suas valiosas contribuições. Não posso deixar de agradecer ao INPA e sobretudo ao PPG em Botânica, que me deu toda a estrutura e o incentivo necessários para vencer esta etapa, cada funcionário que ajudou e fez parte dessa história. Ao Ibama, SISBio, SISGen, DEMUC/SEMA, órgãos que me permitiram desenvolver a pesquisa em unidades de conservação, coletar e transportar material botânico para o INPA e ao exterior. Agradeço muito aos financiamentos do CNPq, CAPES, FAPEAM, Max Planck de Biogeoquímica e qualquer outra fonte de financiamento que indiretamente tenha contribuído nessa tese.

Espero que este trabalho contribua com a ciência da mesma maneira em que tantos artigos, livros, teses e dissertações contribuíram na construção do meu conhecimento e forneceram a base para este trabalho.

Epígrafe

Velhas Árvores

Olha estas velhas árvores, mais belas
Do que as árvores novas, mais amigas:
Tanto mais belas quanto mais antigas,
Vencedoras da idade e das procelas...

O homem, a fera, e o inseto, à sombra delas
Vivem, livres de fomes e fadigas;
E em seus galhos abrigam-se as cantigas
E os amores das aves tagarelas.

Não choremos, amigo, a mocidade!
Envelheçamos rindo! Envelheçamos
Como as árvores fortes envelhecem:

Na glória da alegria e da bondade,
Agasalhando os pássaros nos ramos,
Dando sombra e consolo aos que padecem!

Olavo Bilac, in "Poesias"

Esse poema me lembra não somente das árvores, mas do INPA, pois está gravado aos pés da Tanimbuca, velha árvore do bosque da ciência. São lembranças que vou levar para toda a vida.

Resumo

Os igapós de águas pretas são cobertos por florestas alagadas por águas ácidas e pobres em nutrientes, que ocorrem às margens de grandes rios como o Rio Negro, Rio Uatumã e outros da Bacia Amazônica, perfazendo mais de 140,000 km^2. Naturalmente, esses ambientes possuem uma fase de águas altas (fase aquática) e uma fase de águas baixas (fase terrestre), caracterizando um pulso de inundação monomodal e previsível, o que permitiu a especialização e dependência da flora a condições semiaquáticas. Este trabalho buscou compreender como os igapós de duas sub-bacias na Amazônia Central se comportam em condições normais; sob influência de eventos hidro climáticos extremos que aumentaram drasticamente nas últimas três décadas (Rio Jaú, afluente do Rio Negro) e em condições severas de alteração no pulso de inundação (Rio Uatumã, afluente do Rio Amazonas) induzidas pela hidrelétrica de Balbina instalada nos anos 80. Para tal, a jusante do Rio Uatumã, no capítulo 1 mapeamos e classificamos os igapós para identificar áreas onde houve a mortalidade massiva de árvores e onde a mortalidade ainda está ocorrendo. O mapeamento foi feito com 56 imagens de radar de abertura sintética (ALOS/PALSAR) adquiridas em diferentes níveis de inundação entre 2006 e 2011. A classificação pelo algoritmo supervisionado (*Random Forests*) apresentou acurácia geral de 87,2%. Foi observada a mortalidade de 12% da floresta de igapó após os primeiros 43 km a jusante, ao longo de um trecho de 80 km. Com base nas imagens e dados hidrológicos, detectamos que 29% dos remanescentes de igapó vivos podem estar atualmente sofrendo mortalidade. Os resultados indicaram que principalmente as topografias baixas caracterizadas por macro-habitats dominadas pela espécie arbórea *Eschweilera tenuifolia* (O. Berg) Miers (Lecythidaceae) foram os mais impactados. Para estudar em mais detalhe a ecologia desta espécie arbórea os capítulos 2 e 3, comparam os macro-habitats nas duas áreas de estudo, visando compreender como e quando os distúrbios no pulso de inundação afetaram as populações desta espécie, altamente adaptada às condições de inundações prolongadas de até 10 meses por ano em média. Nos igapós do Rio Uatumã, coletamos discos de 30 árvores mortas e bastões de madeira (duas amostras por árvore retirados com trado dendrocronológico) de 62 indivíduos vivos. Em florestas de igapó adjacentes ao Rio Jaú, coletamos 21 discos de indivíduos mortos e bastões de madeira de 31 indivíduos vivos. O segundo capítulo aborda as relações entre crescimento arbóreo e fatores climáticos em ambientes naturais (Parque Nacional do Jaú - PNJ) e perturbados (Reserva de Desenvolvimento Sustentável do Uatumã - RDSU). Para isso foram construídas cronologias de anéis de crescimento em cada sítio de estudo que apresentam estatísticas robustas para os períodos 1927-1999 (PNJ) e 1920-2006 (RDSU). As cronologias foram relacionadas com parâmetros regionais de hidrologia (nível mensal da água) e clima (precipitação mensal) e com anomalias de temperaturas superficiais do mar (TSM) do Pacífico Equatorial e Atlântico Tropical. Os resultados sugerem fortes mudanças nas respostas das árvores de *Eschweilera tenuifolia* à intensificação do ciclo hidrológico, caracterizado pelo aumento da frequência e magnitude de cheias severas no sistema natural (PNJ) e pelo aumento do nível mínimo da água durante o período da operação da barragem de Balbina (RDSU). No PNJ as árvores indicam um aumento nas respostas às anomalias de TSM dos dois oceanos (correlação positiva) em resposta da intensificação do ciclo hidrológico, causada pelo aquecimento do Atlântico Tropical e o simultâneo esfriamento do Pacífico Equatorial

resultando na intensificação da circulação de Walker, forte convecção de nuvens e aumento de precipitação nas secções norte e central da Bacia Amazônica. Na RDSU, os impactos das mudanças do regime hidrológico induzidas pela barragem de Balbina resultaram em respostas do crescimento arbóreo opostas ao período pré-barragem. O terceiro capítulo aborda o crescimento arbóreo e a mortalidade da espécie nos dois sítios por meio de análises de séries temporais de incrementos diamétricos e datação com radiocarbono para detectar mudanças nos padrões de crescimento e mortalidade e suas causas. Os resultados mostram que o incremento diamétrico médio (IMD) e a idade média para árvores do PNJ foram 2,04 ± 0,39 mm e 201 ± 103 anos (DAP médio: 43,9 ± 21,7 cm) , respectivamente, enquanto para árvores da RDSU o IMD foi 2,28 ± 0,69 mm e a idade média 213 ± 103 anos (DAP médio: 45,9 ± 24,6 cm). A trajetória de crescimento acumulado entre os dois sítios de estudo foi similar, ao considerarmos um período de 500 anos de modelagem do crescimento. O IMD foi comparado entre os dois sítios de estudo e entre períodos antes e após (a partir de 1982) das mudanças do ciclo hidrológico induzidas por mudanças de clima (PNJ) e UHE (RDSU). O período anterior à construção da usina hidrelétrica (UHE) de Balbina indica que o crescimento das árvores não diferiu entre os dois sítios de estudo. Da mesma forma, o IMD das árvores no PNJ não apresentou diferença entre os períodos antes e depois de 1982. Em contraste, a manipulação do pulso de inundação ocasionada pela operação da UHE resultou na diferenciação do IMD entre as duas áreas e entre os períodos no Rio Uatumã. As árvores do Rio Uatumã morreram cerca de dez anos após o início da construção da barragem enquanto as árvores do Rio Jaú não apresentaram um padrão distinto de mortalidade ao longo da cronologia avaliada. As árvores vivas do Rio Uatumã apresentaram um aumento no incremento entre 1982 e 2000 e um abrupto e forte declínio de IMD após o ano 2000, que perdura até hoje, caracterizando um padrão de supressão de crescimento induzido pelas condições permanentes de inundação que possivelmente resultará em mortalidade. Com isso, concluímos que a alteração do pulso de inundação, causou e continua causando anomalias no crescimento e mortalidade de *Eschweilera tenuifolia*, mesmo em mais de 30 anos após a perturbação. A espécie é altamente sensível às mudanças na amplitude e duração da inundação que impactam os macro-habitats dominados por ela. A mortalidade massiva de árvores pode levar a perda destes macro-habitats, serviços ecossistêmicos e até a extinção regional da espécie. É necessário que as leis para a instalação e funcionamento de UHEs na Amazônia sejam criteriosamente revisadas com base em estudos feitos em áreas alagáveis a jusante das barragens.

Abstract

Igapós are floodplain forests inundated by acidic and nutrient-poor waters and occur along the black-water rivers, such as the Negro River and its tributaries, the Uatumã River and others in the Amazon Basin, covering more than 140,000 km^2. Under natural conditions, the flood-pulse is monomodal and predictable, which drives the specialization and dependence of the flora to semiaquatic conditions. This work sought to understand how the *igapós* of two sub-basins in Central Amazonia perform under 1) normal conditions; 2) under the influence of extreme hydroclimatic events which increased dramatically during the last three decades (Jaú River, Negro River tributary); and 3) under flood-pulse disturbances (Uatumã River, Amazon River tributary) where the Balbina hydroelectric power plant was installed in the 1980s. For this, the *igapó* forests downstream the Uatumã River were classified and mapped to identify areas with massive tree mortality and where mortality is still occurring (first chapter). The mapping was done using 56 synthetic aperture radar images (ALOS/PALSAR) acquired at different flood levels between 2006 and 2011. The results showed that the application of object-based image analysis (OBIA) methods and the random forests supervised classification algorithm generated an overall accuracy of 87.2%. The mortality of 12% of the *igapó* forest was observed after the first 43 km downstream, along a stretch of 80 km. Based on the images and hydrological data, we detected 29% of the living igapó forests might be currently suffering mortality. Low topographies in the floodplains characterized by macrohabitats dominated by the tree species *Eschweilera tenuifolia* (O. Berg) Miers (Lecythidaceae) were the most impacted. To further study the ecology of this species, chapters 2 and 3 compare the macrohabitats in the two study areas to understand how and when flood pulse disturbances affected the growth and mortality of populations of this species, highly adapted to prolonged flooding conditions with flood durations of up to 10 months per year on average. Therefore, we collected discs of 30 dead individual trees and cylindrical cores (two per tree) from 62 living individuals in the Uatumã River *igapós*. In forests adjacent to the Jaú River, with natural tree mortality, we collected 21 discs from dead individuals and 31 cores from living trees. The second chapter discusses how the relationship between tree growth and climatic factors changed with the intensification of the hydrological cycle in natural environments (Jaú National Park - JNP) and the disturbed system (Uatumã Sustainable Development Reserve - USDR). For that, tree-ring chronologies were constructed at each study site, which presented robust statistics for the periods 1927-1999 (JNP) and 1920-2006 (USDR). The chronologies were related to regional parameters of hydrology (monthly water level) and climate (monthly precipitation) and with sea surface temperature anomalies (SST) of the Equatorial Pacific and Tropical Atlantic. The results suggest strong changes in the responses of *Eschweilera tenuifolia* trees to the intensification of the hydrological cycle, characterized by the increase in the frequency and magnitude of severe floods in the natural system (JNP) and by the increase of the minimum water level during the

operational period of the Balbina dam (USDR). In the JNP, the trees indicate an increasing strength in the responses to the SST anomalies of both oceans, which reflects the described mechanisms that results in the intensification of the hydrological cycle, caused by the warming of the Tropical Atlantic and the simultaneous cooling of the Equatorial Pacific resulting in an intensification of Walker's circulation, strong cloud convection and increased precipitation in the northern and central sections of the Amazon Basin. In the USDR, the impacts of changes in the hydrological regime induced by the Balbina dam resulted in opposite responses of tree growth compared to the pre-dam period. The third chapter shows that the mean diameter increment (MDI) and mean age for trees in the JNP are 2.04 ± 0.39 mm and 201 ± 103 years, respectively, while trees at the USDR has MDI of 2.28 ± 0.69 mm and a mean age of 213 ± 103 years. The cumulative growth trajectory is similar between both areas for a 500-year period of growth modeling and the MDI analysis by periods indicates that overall the tree growth did not differ between both sites in the period before the construction of the Balbina hydroelectric power plant. In the same way, tree growth at JNP did show any significant difference between the periods before and after the intensification. Opposingly, the alteration of the flood pulse, caused by the operation of the dam, resulted in the MDI differentiation between the two periods at the USDR. The trees at USDR died about ten years after the beginning of the dam construction, whereas those from the JNP did not show a clear pattern throughout the evaluated periods. The living trees of USDR showed an increase in growth between 1982 and 2000 and an abrupt and strong growth decline after the year 2000, continuing until present day induced by the permanent flooding conditions leading to growth suppression and mortality. The change in the flood-pulse, more than 30 years after the disturbance, continues to cause growth anomalies and mortality in *Eschweilera tenuifolia*, which is highly sensitive to changes in flood amplitude and duration. In summary, the findings indicate the excessive mortality of trees is still occurring in the floodplains of the Uatumã River basin affecting especially macrohabitats dominated by this species, causing losses of ecosystem services and regional extinction of an extraordinary tree species. It is necessary that laws for the installation and norms for the operation of hydroelectric power plants in the Amazon should be carefully reviewed based on studies done in wetland areas downstream of dams.

Sumário

Introdução

As florestas alagáveis que margeiam os grandes rios amazônicos, juntamente com outras fitofisionomias não florestais na interface entre sistemas terrestres e aquáticos, constituem as áreas úmidas e perfazem cerca de 30% da área da Bacia Amazônica (Junk et al. 2011). Esses ecossistemas são amplamente utilizados pelo homem e abrigam alta biodiversidade, com fauna e flora especializadas às condições estabelecidas pela inundação (Ferreira 2000a, Parolin et al. 2004, Wittmann et al. 2006, 2013, Junk et al. 2010, Householder et al. 2012, Luize et al. 2015, 2018).(Ferreira 2000a, Parolin et al. 2004, Wittmann et al. 2006, 2013, Junk et al. 2010, Householder et al. 2012, Luize et al. 2015, 2018). Além de as margens de rios estarem sujeitas aos impactos de mudanças do uso da terra, tais como mineração, desmatamento das cabeceiras e mudanças no clima, os cursos de água amazônicos têm sido o alvo de grandes empreendimentos hidrelétricos, que alteram o pulso de inundação natural dos rios afetando diretamente as florestas alagáveis (Junk and Mello 1990, Castello and Macedo 2015b, Assahira et al. 2017).

As áreas úmidas amazônicas ao longo dos grandes rios são alagadas anualmente de forma previsível por um pulso de inundação monomodal, constituindo as áreas alagáveis, em sua maioria florestadas (Melack and Hess 2010, Junk et al. 2011). As duas principais formações florestais de áreas alagáveis são as várzeas e os igapós (Prance 1979). Nesses ambientes, ao longo do ano, ocorrem duas fases bem definidas: aquática e terrestre (Junk et al. 1989). As várzeas são as áreas alagáveis associadas a rios que têm suas nascentes nas regiões andinas e pré-andinas e, por esse motivo, possuem alta carga sedimentar e têm um pH próximo da neutralidade (Sioli 1984). Várzeas são as áreas alagáveis amazônicas com maior fertilidade dos solos e águas e mais habitadas e exploradas em múltiplas atividades econômicas (Junk et al. 2000). Os rios que formam os igapós drenam pelos escudos Paleozoicos ou Pré-Cambrianos da Guiana e do Brasil Central (Fittkau et al. 1975, Wittmann et al. 2010) e são divididos em dois grandes grupos conforme a cor de suas águas: igapós de águas claras e igapós de águas pretas. Enquanto rios de águas claras têm cor transparente esverdeada, poucos sedimentos dissolvidos, e um pH variado, as águas pretas em geral são mais ácidas e pobres em nutrientes, com alto

teor de ácidos húmicos e fúlvicos dissolvidos (baixo pH), que dão a sua cor preta avermelhada. Igapós são florísticamente mais distintos entre si do que as florestas de várzea, exibindo enormes diferenças em composição mesmo dentro de uma sub-bacia (Ferreira 2000a, Wittmann et al. 2010, Montero et al. 2014, Junk et al. 2015, Scudeller and Vegas-Vilarrúbia 2018).

As florestas alagáveis possuem vegetação adaptada à inundação, com muitas espécies utilizando a fase aquática para a dispersão (Schöngart et al. 2002, Parolin et al. 2010) enquanto a fase terrestre é o momento onde as árvores investem em crescimento secundário (Worbes 1985, Schöngart et al. 2002). Para tolerar o pulso monomodal de inundação (Junk et al. 1989), as espécies arbóreas de áreas alagáveis possuem adaptações anatômicas, morfológicas e fisiológicas, que permitem a sobrevivência em ambientes com pouca disponibilidade de nutrientes e oxigênio, e maiores concentrações de fitotoxinas (Parolin et al. 2004, Parolin 2009). Dentre tais adaptações, podemos destacar a produção diferenciada de fito-hormônios como o etileno, ligado a formação de aerênquima e lenticelas hipertrofiadas em caules e expansão de raízes adventícias e a mudança para um metabolismo anaeróbico eliminando substâncias fitotóxicas como acetaldeído e etanol (Jackson 1990, Armstrong and Drew 2002, Voesenek et al. 2003, Crawford and Braendle 2007, Parolin 2009, Piedade et al. 2010, Sauter 2013). As adaptações da flora ao ambiente, combinadas com estratégias reprodutivas, de crescimento, e interações com a fauna, são devidas a processos evolutivos causado pela inundação anual (Junk 1989, Junk et al. 1989, Parolin et al. 2004).

Há uma diferenciação das comunidades de plantas dentro de cada tipologia de florestas alagáveis. Isto acontece em decorrência de diferenças geomorfológicas que alteram a profundidade e duração da inundação gerando ambientes específicos, definidos como macro-habitats (Junk et al. 2018). Somente na bacia do Rio Negro, a maior sub-bacia amazônica banhada majoritariamente por águas pretas, foram definidos 25 macro-habitats de igapós, variando em atributos geomorfológicos e florísticos (Junk et al. 2015). Dentre os macro-habitats de igapó, o nível mais baixo ocupado por árvores é formado por formações de florestas dominadas por *Eschweilera tenuifolia* (O. Berg) Miers, árvores capazes de suportar até dez meses de inundação anual (Junk et al. 2015).

Em florestas alagáveis tropicais, o pulso de inundação causa diferenciação nas fases de vida das árvores levando à desaceleração do metabolismo e a inatividade temporária do cambio secundário durante a fase aquática, resultando na formação de anéis de crescimento, sendo que em muitas árvores esses anéis são anuais (Worbes 1985, Schöngart et al. 2002, Worbes 2002,

Schöngart et al. 2017a). Pelo uso da dendrocronologia, uma análise retrospectiva do tempo por meio dos anéis de crescimento, é possível determinar a idade e taxas de incremento em diâmetro das árvores, relacionar o crescimento com variações climáticas, detectar eventos passados tais como temperaturas e precipitações extremas, incêndios, ataque de insetos e outros distúrbios (Fritts 1976, Speer 2009).

Além da cheia e da seca sazonais comuns e previsíveis que definem as fases aquática e terrestre de florestas alagáveis, fenômenos climáticos recorrentes podem promover eventos extremos causando impactos a esses ecossistemas (Schöngart et al. 2004, Piedade et al. 2013, Junk et al. 2018). O aumento da duração dos períodos de seca em diferentes partes da Amazônia leva à redução dos níveis de água de rios e lagos, prolongando a fase terrestre em suas áreas alagáveis (Schöngart et al. 2004, Schöngart and Junk 2007, Zeng et al. 2008, Tomasella et al. 2010, 2013, Yoon and Zeng 2010, Marengo et al. 2011, 2018). Em contraste às secas, cheias extremas também têm ocorrido com maior frequência nas últimas décadas na Amazônia. Nas últimas décadas foi verificada a intensificação no ciclo hidrológico e o aumento na frequência de cheias extremas, resultando em uma maior amplitude de inundação dos rios (Gloor et al. 2013, Duffy et al. 2015, Barichivich et al. 2018). Esses eventos extremos de cheias alteram o ciclo hidrológico da região (Gloor et al. 2013, Jesús et al. 2014, Marengo and Espinoza 2016, Barichivich et al. 2018) e promovem inundações de maior intensidade nas áreas alagáveis (Schöngart e Junk 2007, Piedade et al. 2013). As mudanças climáticas têm afetado a região amazônica de diferentes maneiras. Na região sul observa-se uma diminuição de chuvas durante a estação seca e o prolongamento desta estação, enquanto na região central e norte da Amazônia está ocorrendo o aumento das chuvas (Espinoza et al. 2018, Marengo et al. 2018).

Os eventos de larga escala envolvidos na intensificação da ocorrência de extremos climáticos são principalmente o ENSO (*El Niño-Southern Oscillation*) e o gradiente meridional de anomalias de TSM sobre o Atlântico Tropical. O ENSO afeta sobretudo o período chuvoso (tendo maior influência a leste, região central e ao norte da bacia), aumentando o volume de chuvas quando há o resfriamento anormal das águas do oceano Pacífico Equatorial (La Niña), ou o declínio das chuvas, quando o oceano apresenta um aquecimento anômalo (El Niño). Já o aquecimento do Atlântico Tropical Norte afeta mais o período seco (atuando ao sul e sudeste da bacia), o que reduz o volume de chuvas (Yoon and Zeng 2010).

Além dos eventos climáticos naturais, um dos principais fatores de ameaça as áreas úmidas são os distúrbios antrópicos (Castello et al. 2013, Castello e Macedo 2016, Junk et al.

2018). O desmatamento para uso de recursos como madeira, mineração, conversão de extensas áreas em plantios e pastagens, construções de estradas e cidades são comumente considerados pela legislação, porém o represamento de enormes rios para a implementação de usinas hidrelétricas (UHE), suprime extensas áreas de florestas acima e causa impacta ecossistemas abaixo das barragens (Timpe and Kaplan 2017).

Entretanto, a maioria dos estudos realizados considera principalmente os danos acima da barragem e os impactos sobre o ambiente alterado (Fearnside 2005, Malhi et al. 2008). As hidrelétricas atingem diretamente o curso dos rios e os ecossistemas ligados a eles. O barramento e represamento de rios não apenas interrompe o fluxo hídrico, transformando ambientes dinâmicos em estacionários na parte de cima, como também desequilibra o ciclo hidrológico através da manipulação do pulso de inundação tanto acima quanto abaixo da barragem, ocasionando severos impactos ao meio ambiente (Junk and Mello 1990, Kemenes et al. 2016, Forsberg et al. 2017, Assahira et al. 2017). Empreendimentos hidrelétricos de larga escala são responsáveis por alterações significativas na paisagem, porém com dimensões ainda pouco conhecidas (Junk and Mello 1990, Fearnside 1995, Junk et al. 2014, Castello and Macedo 2015a, Assahira et al. 2017, Lobo et al. 2019, Neves et al. 2019). A maioria dos estudos contempla apenas as perdas de florestas nas áreas inundadas pelas represas (Cochrane et al. 2017) deixando de quantificar e entender os processos que ocorrem abaixo das barragens, onde o ciclo hidrológico fica comprometido, uma vez que passa a ser regulado pela abertura e fechamento das comportas, deixando de apresentar a sazonalidade natural dos rios (Williams and Wolman 1984, Junk and Mello 1990, Adams 2000, Zahar et al. 2008, Forsberg et al. 2017, Assahira et al. 2017).

No Rio Uatumã o pulso de inundação foi severamente alterado, deixando de ser monomodal e previsível pela instalação da UHE de Balbina (Assahira et al. 2017). Desde o início da construção em 1983 e o fechamento das comportas em 1987 a amplitude média de inundação foi reduzida, enquanto as partes mais altas se tornaram permanentemente secas, as topografias mais baixas do igapó ficaram permanentemente inundadas, o que causou a mortalidade de indivíduos arbóreos da espécie *Macrolobium acaciifolium*, confirmadas por datação de radiocarbono (^{14}C) e dendrocronologia (Assahira et al. 2017).

Entender a extensão dos impactos causados por distúrbios hidrológicos em florestas alagáveis naturais ou impactadas somente é viável com o auxílio de sensoriamento remoto na escala de paisagem. Essa detecção pode ser feita com o auxílio de imagens de radar (banda L)

de diferentes datas, que permitem a visualização e identificação das mesmas no tempo e no espaço (Ferreira-Ferreira et al. 2014, Silva et al. 2015). As imagens fornecidas por sensores de radar de abertura sintética (*Synthetic Aperture Radar*, SAR), como o sensor ALOS/PALSAR, nos permitem detectar com boa precisão a presença de água livre abaixo do dossel, o que facilita o delineamento das áreas alagáveis (Woodhouse 2017). Para compreender como os igapós são afetados por distúrbios no pulso de inundação, sejam eles de origem natural ou antrópica, nós utilizamos o trecho a jusante da barragem na bacia do Rio Uatumã, afetado pela implementação da hidrelétrica de Balbina. No primeiro capítulo da tese, a nível de paisagem, mapeamos e classificamos as áreas de igapó. Localizamos o alcance e quantificamos as áreas de mortalidade massiva de árvores e identificamos locais que, devido à persistência do distúrbio hidrológico, podem no futuro se tornar áreas de mortalidade arbórea massiva.

Principalmente os macro-habitats dominados pela espécie *Eschweilera tenuifolia* sofrem mortalidade em grande escala e massivos distúrbios. Para entender melhor a dinâmica a ecologia das populações os capítulos 2 e 3 comparam estes macro-habitats uma área não afetada por distúrbios antrópicos (Parque Nacional do Jaú – PNJ) e nos igapós da Reserva de Desenvolvimento Sustentável do Uatumã (RDSU) a jusante da UHE de Balbina. Desta forma, utilizamos no segundo capítulo árvores das duas áreas de estudo para descrever a formação de anéis de crescimento da espécie *E. tenuifolia*, e construir cronologias de anéis de crescimento para verificar se as relações entre crescimento arbóreo e clima mudaram em consequência da alteração do ciclo hidrológico ocasionada pela UHE de Balbina no Rio Uatumã ou em consequência da intensificação do ciclo hidrológico nas árvores do PNJ. No terceiro capítulo analisamos as taxas de incremento e datamos a morte de indivíduos amostrados com o intuito de melhor compreender os padrões de mortalidade e crescimento e sua relação com as mudanças induzidas pela UHE de Balbina no Rio Uatumã.

Objetivos

Geral

Compreender como os distúrbios hidrológicos afetam as florestas de igapó a jusante da barragem da usina hidrelétrica de Balbina (Reserva de Desenvolvimento Sustentável do Uatumã) e comparar essas florestas a suas equivalentes no Parque Nacional do Jaú, ambiente protegido integralmente de impactos antrópicos.

Específicos

1. Determinar espacialmente a área de igapó atual e perdida (mortalidade massiva) após a instalação da barragem de Balbina (Cap. 1);
2. Verificar se existem áreas que ainda sofrem com o distúrbio hidrológico em Balbina, podendo acrescer as áreas de mortalidade massiva (Cap. 1);
3. Estudar mudanças das relações entre crescimento arbóreo e clima da espécie *Eschweilera tenuifolia* nos mesmos macro-habitats do sistema natural e alterado, avaliando os impactos da intensificação do ciclo hidrológico (Cap. 2);
4. Compreender como ocorre o crescimento secundário (incremento anual médio) da espécie *Eschweilera tenuifolia* nos dois ambientes (com e sem alteração do regime hidrológico) (Caps. 2 e 3);
5. Verificar se o padrão de crescimento de árvores vivas foi alterado com a instalação da hidrelétrica (Rio Uatumã) (Cap. 3);
6. Datar o ano de morte de árvores de *Eschweilera tenuifolia* e relacionar a mortalidade com distúrbios hidrológicos naturais e antropogênicos nos dois ambientes (Cap. 3).

Capítulo 1

Resende, A. F.; Schöngart, J.; Streher, A. S.; Ferreira-Ferreira, J.; Piedade, M. T. F.; Silva, T. S. F. **Massive tree mortality from flood pulse disturbances in Amazonian floodplain forests: The collateral effects of hydropower production**. *Science of the Total Environment* (659: 587-598) (DOI: 10.1016/j.scitotenv.2018.12.208)

Massive tree mortality from flood pulse disturbances in Amazonian floodplain forests: the collateral effects of hydropower production

Angélica Faria de Resende[a*], Jochen Schöngart[a], Annia Susin Streher[b], Jefferson Ferreira-Ferreira[b,c], Maria Teresa Fernandez Piedade[a], Thiago Sanna Freire Silva[b]

[a] National Institute for Amazonian Research (INPA), Coordination of Environmental Studies (CODAM), Av. André Araújo 2936, 69060-001 Manaus, Brazil
[b] Universidade Estadual Paulista (Unesp), Instituto de Geociências e Ciências Exatas, Ecosystem Dynamics Observatory, Avenida 24-A 1515, 13506-900, Rio Claro, Brazil.
[c] Instituto de Desenvolvimento Sustentável Mamirauá, Estrada do Bexiga, 2584, Bairro Fonte Boa, Tefé, AM 69470-000, Brazil
[*] Corresponding author at, National Institute for Amazonian Research (INPA), Av. André Araújo 2936, 69060-001 Manaus, Brazil. E-mail address: gel.florestal@gmail.com

Highlights

- Considerable floodplain forest loss occurred downstream of the Balbina dam from flood pulse changes;
- Several species of trees are still suffering mortality, which may increase dead stand areas;
- Remote sensing methods used here may be applied to other floodplains with massive tree mortality by damming;
- Downstream igapó forests are highly sensitive to the loss of low water periods resulting from flow alteration by dam operations;

Graphical abstract

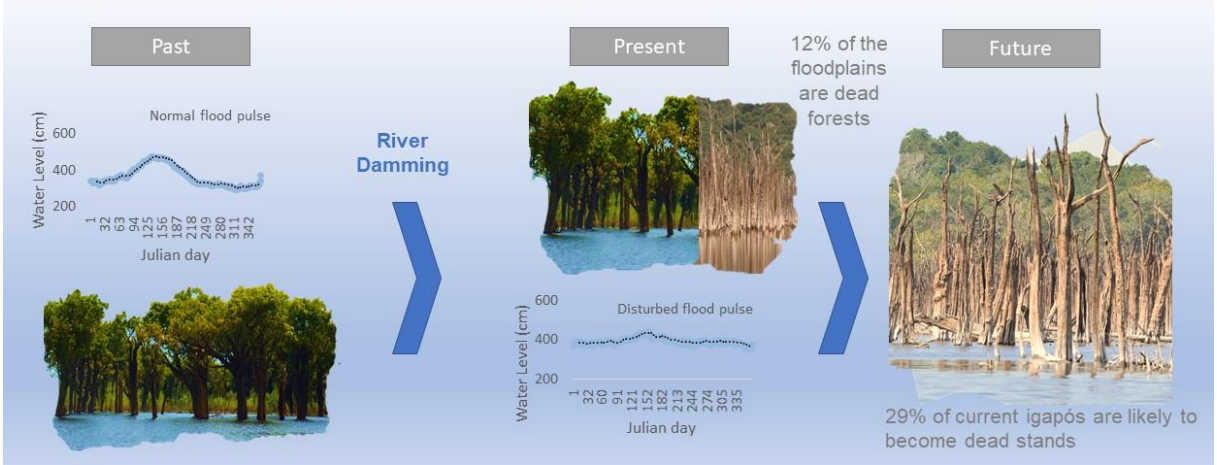

Abstract

Large dams built for hydroelectric power generation alter the hydrology of rivers, attenuating the flood pulse downstream of the dam and impacting riparian and floodplain ecosystems. The present work mapped black-water floodplain forests (*igapó*) downstream of the Balbina Reservoir, which was created between 1983 and 1987 by damming the Uatumã River in the Central Amazon basin. We apply remote sensing methods to detect tree mortality resulting from hydrological changes, based on analysis of 56 ALOS/PALSAR synthetic aperture radar images acquired at different flood levels between 2006 and 2011. Our application of object-based image analysis (OBIA) methods and the Random Forests supervised classification algorithm yielded an overall calibration accuracy of 87.2%. A total of 9,800 km^2 of *igapó* forests were mapped along the entire river downstream of the dam, but forest mortality was only observed below the first 49 km downstream, after the Morena rapids, along an 80-km river stretch. In total, 12% of the floodplain forest died within this stretch. We also detected that 29% of the remaining living *igapó* forest may be presently undergoing mortality. Furthermore, this large loss does not include the entirety of lost *igapó* forests downstream of the dam; areas which are now above current maximum flooding heights are no longer floodable and do not show on our mapping but will likely transition over time to upland forest species composition and dynamics, also characteristic of *igapó* loss. Our results show that floodplain forests are extremely sensitive to long-term downstream hydrological changes and disturbances resulting from the disruption of the natural flood pulse. Brazilian hydropower regulations should require that Amazon dam operations ensure the simulation of the natural flood-pulse, despite losses in energy production, to preserve the integrity of floodplain forest ecosystems and to mitigate impacts for the riverine populations.

Keywords:

PALSAR, synthetic aperture radar, object-based image analysis, *igapós*, black water river, tree mortality, hydropower dam, Balbina, Uatumã River, Amazon, flood pulse.

Introduction

Hydroelectric dams are a growing threat to the extensive Amazon wetlands, having several negative environmental effects and disturbing the hydrological balance that controls the structure and function of these environments (Foote et al. 1996, Kahn et al. 2014, Castello and Macedo 2015a, Latrubesse et al. 2017, Timpe and Kaplan 2017). Although dams are important for electricity production, they also increase greenhouse gas emissions, disrupt indigenous and riverine communities, and lead to forest degradation and losses of biodiversity as a consequence of the large areas artificially inundated by the reservoirs behind storage dams (Junk and Mello 1990, Fearnside 1995, Kemenes et al. 2007, Benchimol and Peres 2015, Cochrane et al. 2017). Most ecological studies of hydropower dam impacts assess only the inundated and surrounding areas of reservoirs, while downstream environmental alterations caused by the hydrological changes created by dams remain poorly understood (Williams and Wolman 1984, Manyari and de Carvalho 2007, Timpe and Kaplan 2017, Assahira et al. 2017).

Dams typically alter the natural "flood pulse" (Junk et al. 1989), negatively affecting the ecological dynamics of downstream floodplain ecosystems (Junk and Mello 1990, Fearnside 1995, Kemenes et al. 2007, Benchimol and Peres 2015). Under natural conditions, the monomodal flood pulse of large rivers is predictable, characterized by an annual cycle of rising, high, receding and low water phases, which can span more than 10 m of amplitude in the case of Central Amazonia (Schöngart and Junk 2007, Junk et al. 2011). This natural water level oscillation floods over 750,000 km^2 annually in the Amazon Basin (Wittmann and Junk 2017), varying in amplitude and duration depending on the amount and seasonality of rainfall within catchments, and on river discharge and topography (Junk et al. 2011). The flood pulse is the main driver of ecological and biogeochemical processes in floodplain forests (Junk 1989, Lewis et al. 2000), where trees display anatomical, morphological, physiological, and biochemical adaptations to survive in this seasonal environment (Junk 1989, De Simone et al. 2003, Parolin et al. 2004, Ferreira and Parolin 2011). For this reason, a large number of tree species are endemic to floodplain environments (Wittmann et al. 2006, 2017, Householder et al. 2012).

Within the Amazonian floodplains, *igapós* are forests influenced by black or clear water (oligotrophic) rivers with catchments in the Precambrian Guiana shield and Central Brazilian

archaic shield, receiving much lower sediment loads than the eutrophic *várzea* forests, which are inundated by sediment-rich white-water rivers with catchments in the Andean region (Prance 1979, Sioli 1984, Junk et al. 2011). Due to their low sediment load, black water and clear water rivers have been the main targets of hydroelectric projects across the Brazilian Amazon. Furthermore, several *igapó* areas along clear water rivers are close to the so-called "Arc of Deforestation", the expanding southwestern agricultural frontier in the Amazon, further compounding the threats to these systems (Lees et al. 2016).

Floodplain forest trees are recognized as good bioindicators of hydrological disturbances, due to their longevity (Schöngart et al. 2005). Many species have a seasonal growth pattern closely linked to the hydrological cycle (Schöngart et al. 2002), and changes in the regularity and duration of the natural flood cycle can lead to growth reduction or interruption and even to mortality. Assahira et al. (2017) found that a substantial increase in annual minimum water levels observed for several consecutive years in the Uatumã River, caused by water released from the Balbina Reservoir for power generation, led to the mortality of large populations of the highly flood-adapted tree species *Macrolobium acaciifolium* (Benth.) Benth. (Fabaceae) (Schlüter and Furch 1992).

The number of hydroelectric power plants in the Amazon has grown steadily in the last 30 years, and this growth is expected to continue because these ventures are considered to be important for economic development, with efforts to understand and manage their socio-ecological implications often rushed and inadequate (Tilt et al. 2009, Tilt 2012). Recent studies show conflicting data on the number of hydroelectric plants in operation, under construction and planned, even for papers published within the same year (Castello et al. 2013, Lees et al. 2016, Latrubesse et al. 2017, Timpe and Kaplan 2017). Latrubesse et al (2017) identified 140 dams in operation or under construction and 288 planned dams in the entire Amazon region. However, Anderson et al. (2018) reported 142 dams in operation or under construction and 160 planned dams for the Andean Amazon alone, implying a considerable underestimation from the remaining studies (Finer and Jenkins 2012, Castello and Macedo 2015a, Forsberg et al. 2017, Anderson et al. 2018).

Disruptions in connectivity are also known to compromise the physical habitat and the ecological integrity of river systems around the world, threatening endemic species and allowing the colonization of invasive ones (Ligon et al. 1995, Ward and Stanford 1995, Nilsson 2000, Mumba and Thompson 2005). In the case of large-scale Amazonian hydroelectric dams, existing studies have a very limited spatial distribution, and thus the true impacts and the extent

of environmental disturbances caused by them remain only partially understood (Junk and Mello 1990, Fearnside 2014, Wittmann and Junk 2017). There is a pressing need to quantify and understand the processes that occur downstream of Amazonian dams, where the natural flood pulse is completely altered by the opening and closing of floodgates, thereby altering the natural seasonality of the rivers (Junk and Mello 1990, Assahira et al. 2017).

The construction of the Balbina Dam (Amazonas, state, Brazil) between 1983 and 1987 led to an abrupt change in the Uatumã River hydrology, which has been maintained for the past 30 years, providing an ideal system to assess ecohydrological responses to damming in *igapó* environments. Therefore, in the present study, we address the following questions: (1) What is the spatial distribution and extent of tree mortality in *igapó* floodplain forests in the Uatumã River, downstream of the Balbina Dam? (2) Which recommendations can be made for future evaluations of environmental impacts of future hydroelectric dams in the Amazon region with focus on downstream areas? (3) Is *igapó* vegetation loss still occurring, and if so, in which areas?

Methods

Study area

We studied a 300-km stretch of the Uatumã River downstream of the Balbina hydroelectric dam, up to its confluence with the Amazon River, including major tributaries (Abacate and Jatapú rivers - see figure S1, showing the non-disturbed Abacate River *igapó*). The Uatumã River has a catchment area of approximately 69,500 km^2, corresponding to nearly 1.2% of the entire Amazon Basin (Melack and Hess 2010).

The Balbina hydroelectric plant, built between 1983 and 1987, is known worldwide as one of the largest ecological disasters in Brazilian history (Fearnside and P.M. 1989). Its damming flooded about 4,437 km^2 (Benchimol and Peres 2015), but due to the low slope of the relief, the 250 MW of nominal energy produced is extremely low in relation to the flooded area. Compared to the Tucuruí hydroelectric dam on the Tocantins River, whose reservoir is nearly 100 km^2 smaller, the Balbina hydroelectric power plant produces almost 33 times less energy (International Rivers and ECOA, 2017).

Our study area is located approximately 150 km east of the capital city of Manaus (Amazonas state), within the Uatumã Sustainable Development Reserve (RDS Uatumã) (Figure

1). Four distinct forest types are described for this region: upland forests (*terra firme*), oligotrophic floodplain forests (*igapó*), and two white-sand open vegetation (*campinas* and *campinaranas*) (IDESAM 2009, Andreae et al. 2015, Targhetta et al. 2015, Adeney et al. 2016). According to data acquired between 2013 and 2015 from the Amazon Tall Tower Observatory (ATTO) project, the area has an average annual temperature of 27ºC and an average annual total rainfall of 1920 mm, with August and September being the driest months.

According to the Shuttle Radar Topography Mission (SRTM) global digital elevation model, the first 22 km of the Uatumã River downstream of the dam have an average width of 200 m (Figures 1 and 2). For the next 13 km downstream, the river and its associated floodplain widen progressively, coinciding with a change from a rectilinear to a meandering pattern. The topographic profile from the dam to the Uatumã river mouth shows a steep descending gradient, with the steepest portions occurring up to 35 km downstream of the dam (Figure 2), thus matching the geomorphological pattern described above.

In contrast to *várzea* habitats and most Andean rivers, the Uatumã River originates from the Guiana Shield, like most black water rivers in the middle portion of the Amazon basin (northern rivers) (Sioli 1984, IDESAM 2009, Abad et al. 2013). Black water rivers are stable and have slow geomorphologic and floristic dynamics, which can be associated with the presence of monodominant populations of ancient trees (Junk et al. 2015).

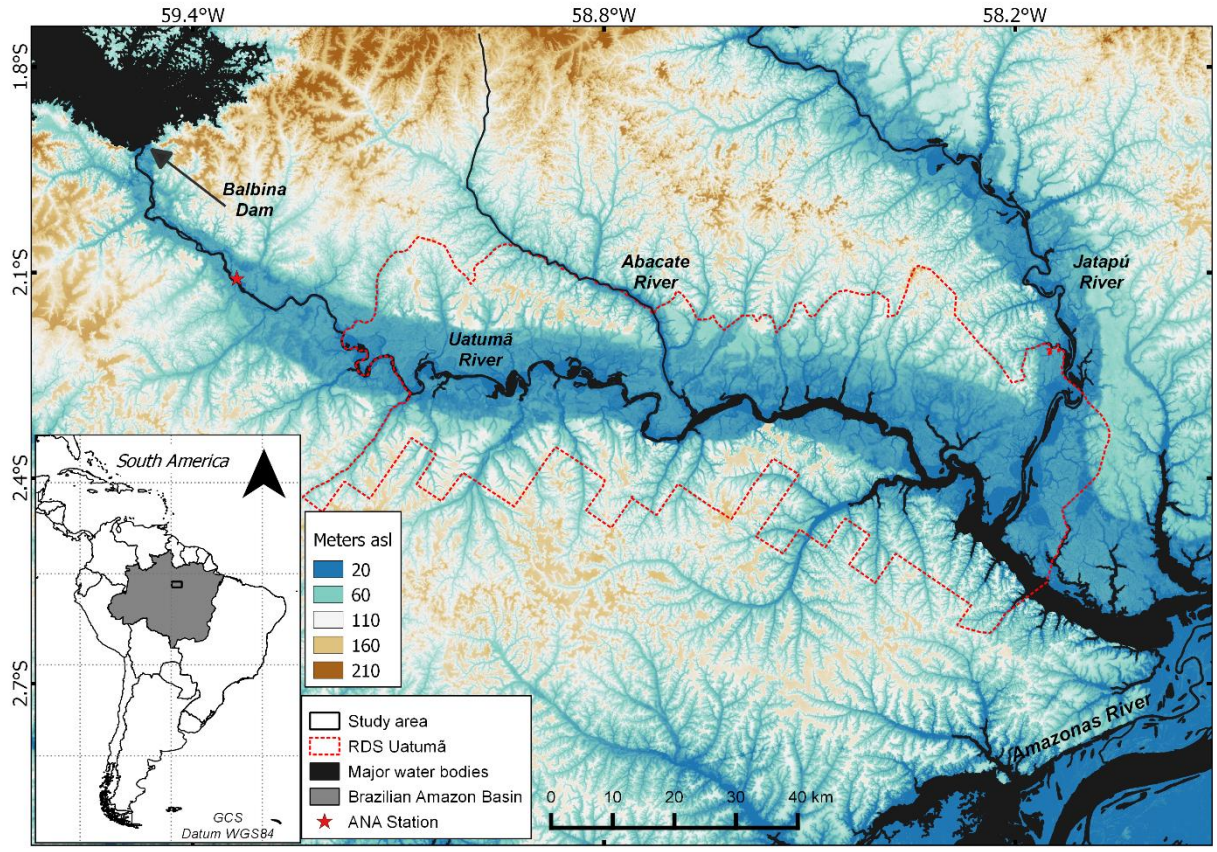

Figure 1 - Location of the study area in the Brazilian Amazon Basin, and detail of the study site, from the Balbina dam to the mouth of the Uatumã River. Background: Shuttle Radar Topography Mission (SRTM) digital elevation model showing the topographic variation with red outlines showing the areas mapped by remote sensing.

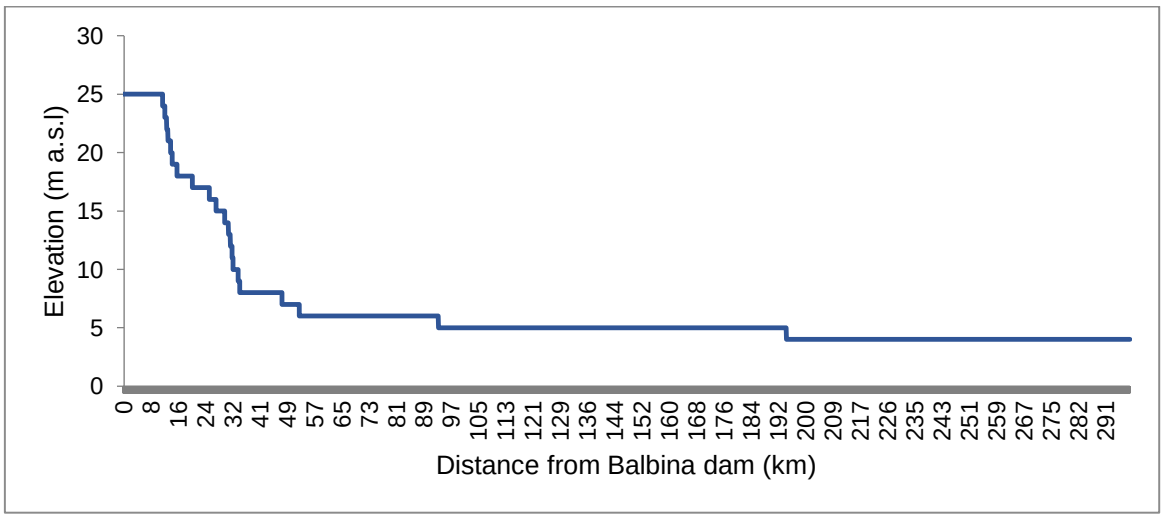

Figure 2 - Longitudinal elevation profile along the main Uatumã river channel (in February 2000) showing the steeper slope along the first 35 to 50 km downstream of the Balbina dam (SRTM data obtained from earthexplorer.usgs.gov).

Since the damming of the Uatumã River by the Balbina hydroelectric plant, the annual predictable flood pulse has been modified (Timpe and Kaplan 2017, Assahira et al. 2017).

However, the only available water level monitoring station for the Uatumã River downstream of the dam is the Cachoeira Morena gauging station, operated by the Brazilian Geological Service/ Brazilian National Water Agency (CPRM/ANA) (Cachoeira Morena Station - number 16100000). However, because this station sits on a terrace, near rapids, its data do not reflect the range of absolute river stage variation (see Figure 2), and its overall measured stage amplitude (ca. 2 m) is much smaller than the observed amplitudes downriver (up to 9 m, field measurements). The lack of proper monitoring stations downriver makes it difficult to characterize the absolute magnitudes of changes in the water level regime post-damming.

Furthermore, as the hydrological regime is presently irregular, care must be taken to separate abnormal events caused by the dam from those induced by extreme climatic events. As a consequence of the strong El Niño event in 1997/98 reducing rainfall in the Central Amazon region (Foley et al. 2002, Marengo and Espinoza 2016), all *igapós* were dry, followed by a 13-year period between 1999 and 2012, where all lower elevation *igapós* and some intermediate elevation *igapós* were completely flooded. In May 2000, water levels flooded all *igapós* for at least six days, reaching upland forests and riverine houses. During the severe El Niño event in 2015/16, water levels were so low that even the lowest areas including dead stands remained dry. This shows how unpredictable and irregular the flood pulse has become after starting hydropower operations, and the full consequences of such events remain unknown (Figure 3).

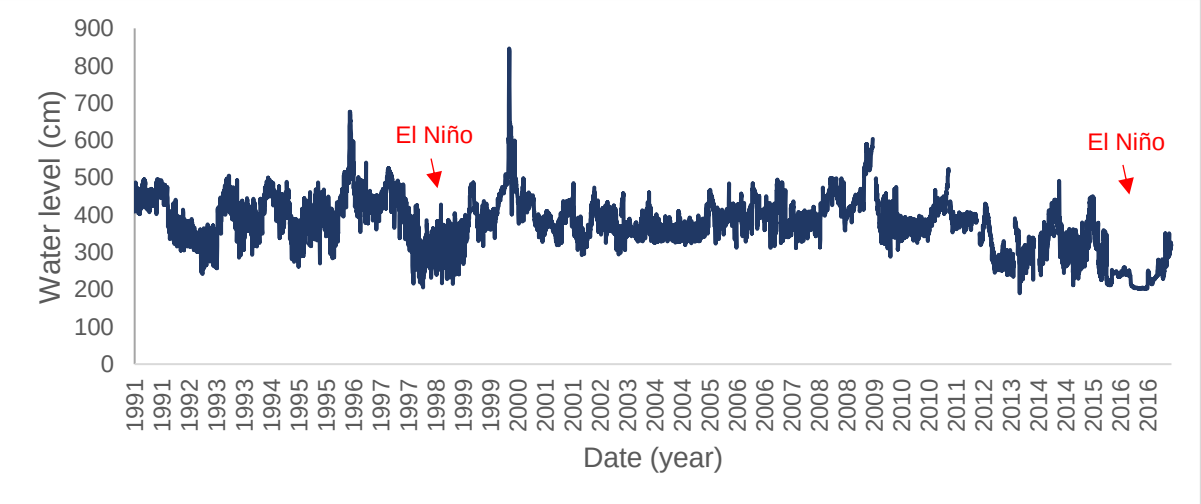

Figure 3 - The line shows the average water level during the post-dam period.

Remote sensing data

We used L-band synthetic aperture radar (SAR) satellite images, as they have the ability to penetrate forest canopies and detect the flooding beneath, producing an increase in the returned signal (radar backscattering) known as "double-bounce" (Silva et al. 2015). Furthermore, L-band radar is insensitive to cloud cover and other atmospheric interferences like gases, smoke, and illumination (Woodhouse 2017). For our study, the detection of areas with high tree mortality is based on the even stronger SAR return signal caused by double-bounce between the free water surface and the standing dead trees, without the attenuation caused by volumetric scattering from canopies that is observed for live forest stands (Hess et al. 2002, Silva et al. 2008). In general, dead tree stands under flooded conditions have higher SAR returns than living flooded stands, which are still brighter than upland, non-flooded forests.

We acquired 56 SAR images from the Phased Array Type L-band Synthetic Aperture Radar (PALSAR) sensor, onboard the Advanced Land Observing Satellite-1 (ALOS-1), operated by the Japanese Aerospace Exploration Agency (JAXA), including 14 images for each of the following frame/path numbers: 7130/71, 7140/72, 7140/73, and 7140/74 (Table S1). The ALOS-1 mission operated between 2006 and 2011, carrying several sensors including PALSAR-1, a synthetic aperture radar operating at L-band with a wavelength of 23.5 cm. All images were acquired at the finest available resolution, in two polarization modes: Fine Beam Single (FBS) with HH polarization, and Fine Beam Dual (FBD) with HH and HV polarizations. The nominal spatial resolution after pre-processing was 25 m, and each scene covers a swath of approximately 70 km. All images were obtained from the Alaska Satellite Facility (vertex.daac.asf.alaska.edu/), at the Radiometric Terrain Corrected (RTC) processing level (ASF DAAC 2015). Since the ALOS/PALSAR mission did not perform regular observations of the Earth surface, unlike systems such as the well-known Landsat series, PALSAR images were selected from the historical record to maximize the range of flood amplitudes observed for our study site, based on the association between water stage heights observed in the Cachoeira Morena gauging station and image acquisition dates.

Image processing and classification

We used the approach previously used to classify Amazonian *várzea* environments, developed by Arnesen et al (2013), Ferreira-Ferreira et al (2014) and Silva et al (2010). To adapt it for *igapó* forests, we had to consider the presence of a different floodplain structure,

with the occurrence of almost monospecific stands in lower topographies, capable of withstanding long periods of flooding (Junk et al. 2015).

Our approach is based on Object-Based Image Analysis (OBIA), where the image is first segmented into homogeneous groups of pixels (objects), which correspond to different elements of the landscape (Blaschke 2010). Prior to segmentation, three seasonal descriptor images were calculated: (1) TBM - temporal backscattering mean, (2) TSD - temporal standard deviation of backscattering, and (3) BLW - backscattering at the lowest water level (Arnesen et al. 2013). These descriptors aid in the segregation of important landscape characteristics during segmentation, and they separate areas where there is less temporal variation from areas that change more in response to water level variation. The descriptors were converted to an 8-bit scale and filtered 3 times by a 3x3 window of a Gamma filter (Shi and Fung 1994) to reduce speckle noise and increase the efficiency of the segmentation algorithm.

We used these three seasonal descriptors as inputs for the multi-resolution segmentation algorithm from Benz et al. (2004), iteratively optimizing the algorithm parameters as scale = 70, shape = 0.1 and compactness = 0.5, to better represent homogeneous landscape units. After segmentation, we computed the mean and standard deviation of SAR backscatter for each object in each acquired image and for the three original untransformed and unfiltered seasonal descriptors (Figure 4).

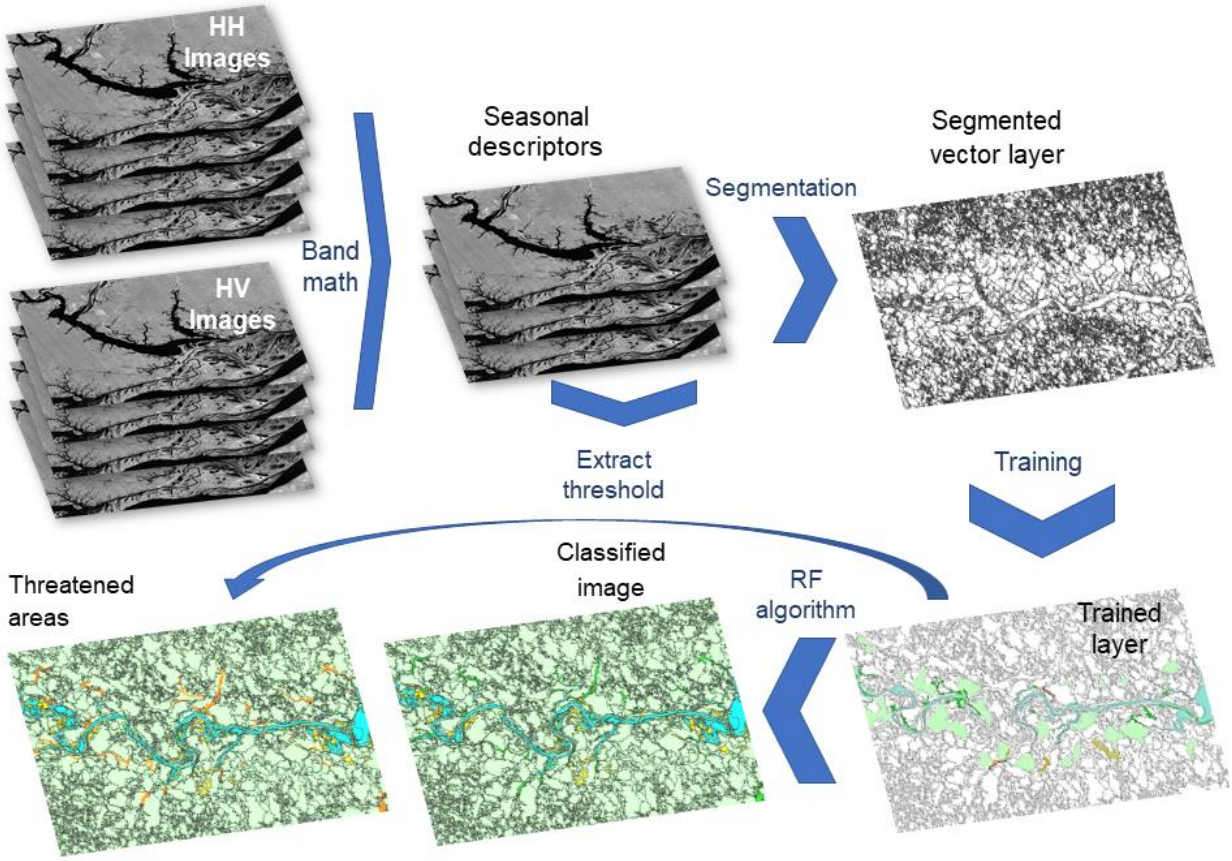

Figure 4 - Systematization of the stages of image processing, analysis and classification.

To train the classification algorithm, we used high-resolution images from Google Earth™ and Bing Maps™, loaded into the QGIS 2.18 software using the *Open Layers Plugin*, combined with field GPS points and field knowledge, to select about 80 training samples for each of the five pre-defined land cover classes (Table 1).

Table 1 – Land cover classes defined and used to train the Random Forests algorithm to identify igapó forests and tree mortality in the Uatumã River (Amazon, Brazil) using ALOS/PALSAR data.

Land Cover Class	Standing water presence	Canopy presence	Other characteristics
Dead Stands	Yes	No	Mostly dense, dead standing trees under long periods of flooding (Figure 5).
Flooded Forests	Yes	Yes	Living trees at varying densities.
Non-Forest	Occasionally	No	Grasslands, shrublands, woodlands, settlements (small villages and farms), sand banks and river

			beaches, campinas (herbaceous vegetation/ shrubs in sandy soil).
Open water	Yes	No	Permanently open water surfaces
Upland	No	Yes	Any type of forest vegetation with a closed canopy (including some campinaranas) that never flood, this class was defined as mask, and not further quantified, although in some places this category included former floodplain no longer subject to inundation.

We then used the sampled training objects as inputs to the Random Forests (RF) classification algorithm, implemented in the RF package of the open-source software R (Liaw and Wiener 2002, R Core Team 2018). This algorithm categorizes the segments using a "forest" of predictive trees, based on independent randomized samples (Breiman 2001). The RF algorithm was applied following Ferreira-Ferreira et al. (2014), with the parameters *Number of Trees* (*ntree*) and *Number of Variables Tried at Each Split (mtry)* set as *ntree* = 15000 and *mtry* = 20.

One important limitation of our method is that it relies on the increased double-bounce scattering caused by flooding to separate floodplain forests from upland forests. We are therefore unable to detect former floodplain areas that are no longer subject to regular flooding, and some of the areas classified as upland might represent additional lost *igapó* regions, assuming the loss of flooding will lead to changes in forest structure and composition over time.

*Figure 5 - Dead forest stands in the floodplains of the Uatumã River, below the blue line. Behind the dead stands, between the orange and blue lines, the igapó forest is observable, followed by upland (*terra firme*) forest above the orange line.*

Forecasting future forest mortality

In addition to mapping dead forest stands, we used remote sensing information to identify threatened areas that are still responding to the effects of altered hydrological conditions, and where mortality is likely to be ongoing. These areas do not yet show the high degrees of mortality that make dead stands distinguishable from living flooded forest stands in the radar images. We measured local maximum water levels at 28 known field locations, represented by the high-water marks left on tree trunks during the last flood (before June 2017). We then assigned observed maximum water levels to their respective mapped objects, which we then grouped into four floodplain classes: "high *igapó*", "intermediate *igapó*", "low *igapó*" (high and low referencing terrain height, according to the Junk et al. (2015) classification) and "submerged", this last designation meaning areas that used to be low *igapó* but currently remain permanently flooded. From the images, we extracted backscattering coefficients from different

dates and respective levels to represent each flood pulse phase: dry, low, medium and high water (Figure 6).

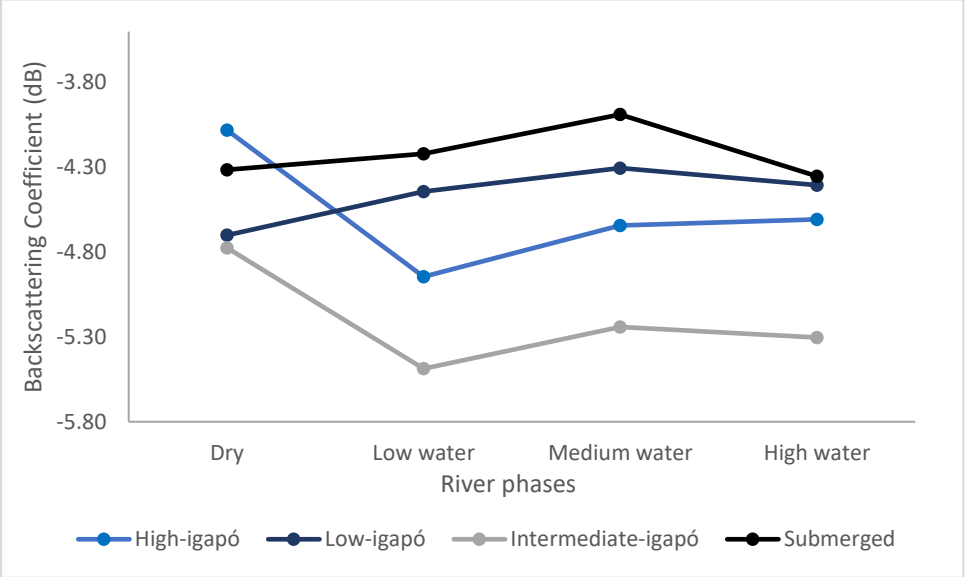

Figure 6 – L-band radar backscatter for different topographical levels of igapó forests at different periods of the flood-pulse regime.

We first analyzed the temporal radiometric behavior of each group of images corresponding to different periods of the hydrological (flood-pulsing) regime for each floodplain class, to determine the best configuration to get good separability of classes based on the backscattered signal. Using an average image (n= 6) of the medium water level images (between 400 and 449 cm at Cachoeira Morena Station), we extracted the backscattering coefficients and applied a threshold to discriminate areas of "high", "intermediate", "low" and "submerged" *igapó*, this last class remaining flooded even during the average low water period. We defined a minimum mean flooding threshold of -4.48 dB to characterize areas that are now continuously flooded, and thereby likely undergoing mortality.

Validation

Classification accuracy was assessed using between 20 and 30 samples per vegetation class, based on high-resolution image interpretation and on observations made in the field in June of 2017, from a boat all along the focal area, using a GPS receiver. We applied the methods developed by Pontius and Millones (2011) and Pontius and Santacruz (2014) to verify the disagreement in class quantity and allocation, the latter subdivided into exchange and shift.

Results

Our classification using the random forests algorithm had an overall accuracy of 87.2% along the entire studied reach (Table S2). We mapped 9,800 km^2 of flooded forest, 135 km^2 of non-forest areas and 13 km^2 of dead stands between the hydroelectric dam and the Uatumã river mouth (Figure 7). Most flooded forest and water areas were located close to or within the confluence of the Uatumã River with the Amazon River. The water and upland classes were the most accurately classified, while the remaining three classes had some degree of confusion. Accuracy assessment showed the highest quantity disagreement errors as 12% for water and 6% for dead stands, respectively, while shift and exchange errors only occurred between flooded forest and non-forest classes, in a small proportion (Figure 8).

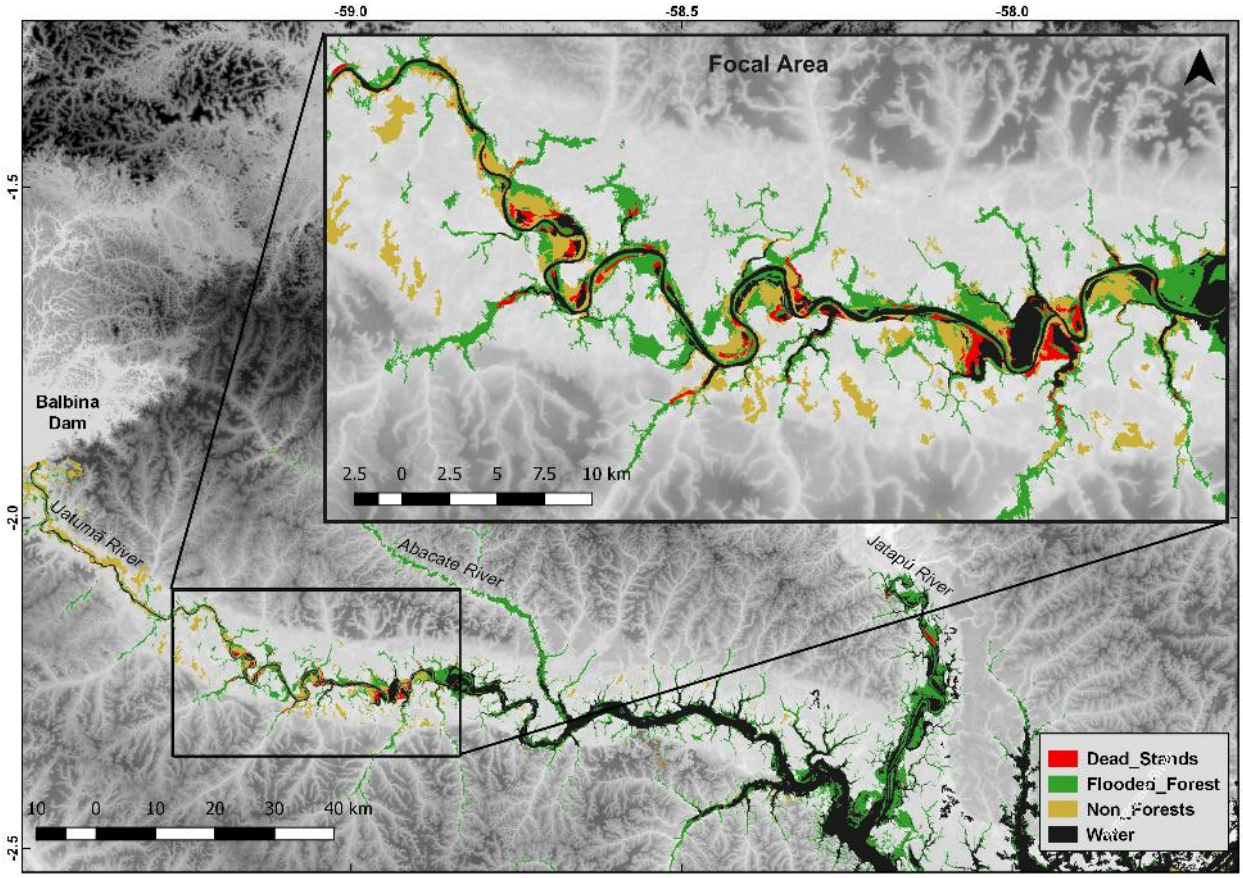

Figure 7 – Classification of the floodplains of the Uatumã River and its major tributaries (Abacate and Jatapú rivers) downstream of the Balbina dam. Dead forests occurred extensively along a stretch of about 80 km (focal area), between 43 and 123 km downstream of the Balbina hydroelectric power plant. Background: shaded relief derived from the SRTM digital elevation model.

After mapping, we identified that along the 300-km reach of the Uatumã River originally studied, massive mortality occurred mostly over a shorter reach, which we denominated the focal area (FA). The FA comprised an 80-km river reach beginning 43 km below the dam and included 90 km^2 of flooded forest and 50 km^2 of non-forest areas. Massive mortality within the FA covered about 11 km^2, corresponding to 12% of the original flooded forest cover. The furthest mapped dead stand was observed at 123 km below the dam, and about 39 km before the confluence with Abacate River.

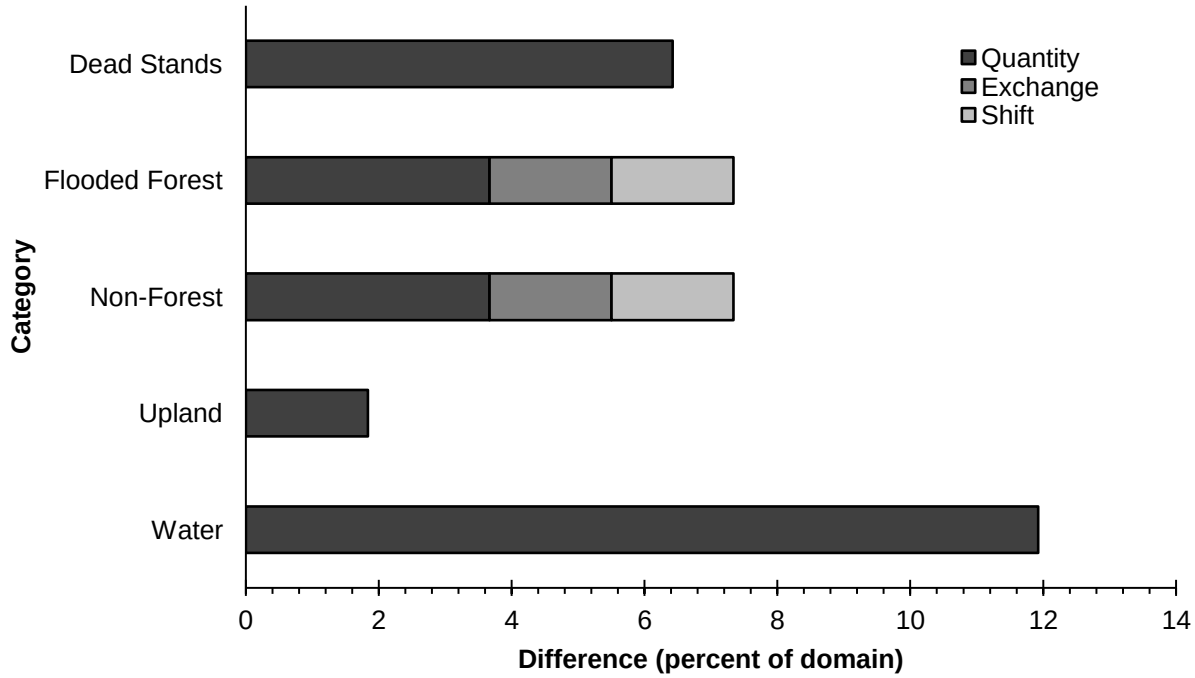

Figure 8 – Per-class disagreement between produced maps and ground-truth observations, following Pontius and Millones (2011) and Pontius and Santacruz (2014).

We mapped an additional 19 km^2 of threatened areas, defined as floodplain forests that are now almost continuously flooded, corresponding to an additional 18% of the original flooded forest cover within the FA. Before the Balbina Dam was built, these areas were flooded for four to eight months, whereas now they are flooded for almost the entire year and are thus very likely to be undergoing slow mortality. If we include the mapped areas of dead stands and threatened areas within the focal area, ca. 29% of the original *igapó* forest along the 80-km long FA of the Uatumã River has been strongly impacted by the Balbina Dam (Figure 9).

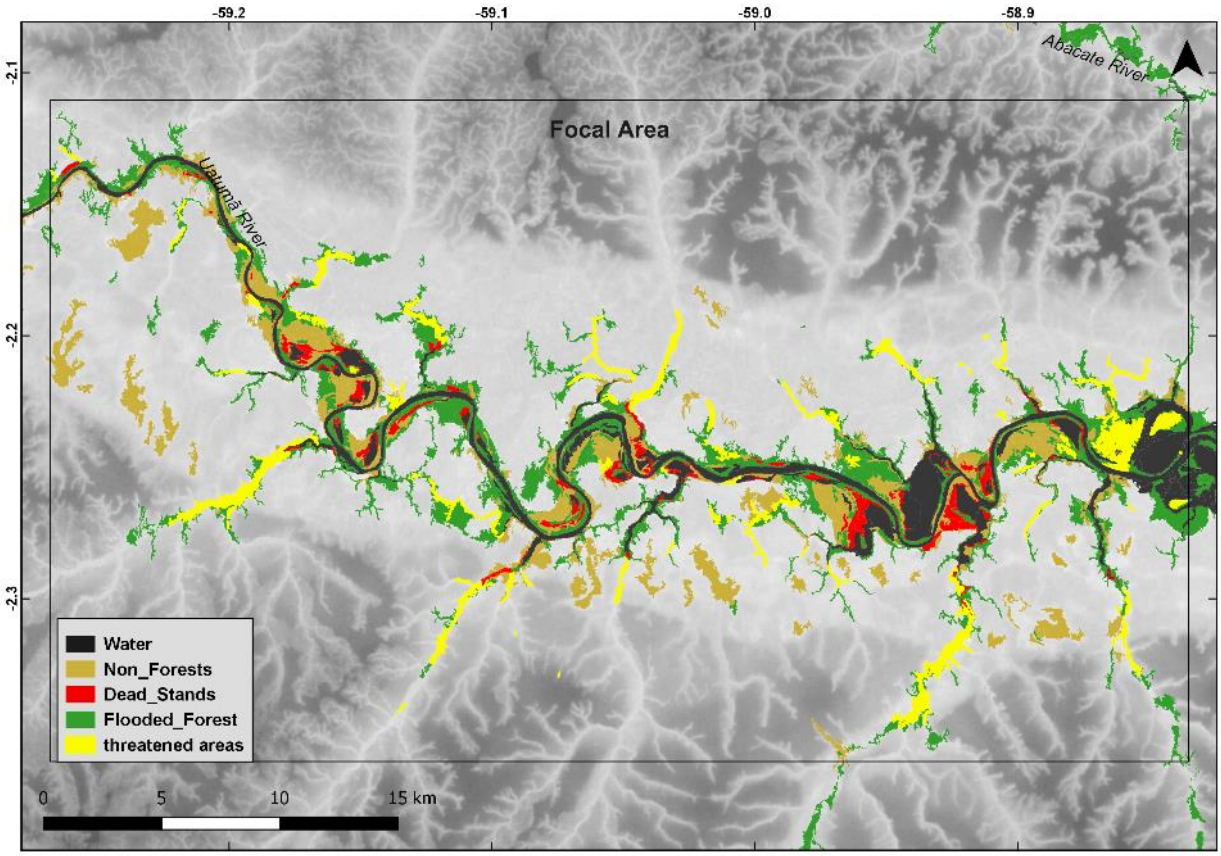

Figure 9 – Map shows potentially threatened areas adjacent to dead stands in the focal area. These areas can spend entire years flooded, depending on the management of river flow by the hydropower facility.

Discussion

Our work shows that (1) there were significant losses of *igapó* forest downstream of the Balbina dam, caused by the changes in the flood pulse, and several areas are still undergoing mortality and may disappear in the near future; and (2) *igapó* forests are highly sensitive to hydrological disturbances linked to loss of flood pulse seasonality; (3) the downstream impacts caused by the dams are not trivial and need to be taken into account in environmental impact assessments and reports; (4) to preserve downstream forests, the maintenance of a flood pulse that is the closest possible to the natural pulse in necessary as a mitigating action for Amazon hydroelectric projects, even if it results in reduced hydroelectric efficiency.

In the first 40 km immediately after the dam (and up to about 10 km downstream of the rapids of Cachoeira Morena), the Uatumã River follows a steep downslope along a narrow channel, where few flooded *igapós* can develop, explaining the absence of mapped floodplain forests and consequently dead stands. In addition, this reach is greatly altered by human

settlements, with different land cover types and little natural vegetation left. The effects of flood pulse changes caused by Balbina are also less evident after 120 km downstream of the dam, where the abnormal discharge caused by damming seems to be attenuated by contributions from the two largest tributary rivers (Abacate and Jatapú rivers) and, at some point, by the Amazon River backwater effect (Meade et al. 1991).

Massive mortality occurred along regions where specific hydrogeomorphological conditions favored the formation of large floodplain forests controlled exclusively by the Uatumã River flood pulse, corresponding to the reach starting 43 km after the dam and ending before the Abacate River mouth. Also, almost all dead stands were located on the insides of channel meanders, further emphasizing the connection between channel morphology and ecological impacts. Our findings corroborate Assahira et al. (2017), who made field observations of dead trees for about 100 km below the Balbina Dam.

It is important to note that our method only detects dead forest stands and potential ongoing mortality areas when they are located below current maximum flooding levels, and thus still exhibit some double-bounce response in the image series. Despite comprising a third of all flooded forest areas, these classes may not represent the entirety of lost *igapó* forests downstream; there are several past floodplain areas which are now topographically above the current maximum flooding heights and are no longer annually flooded, nor do they remain flooded for a predictable time. This change will very likely lead to profound changes in species composition, community structure and ecosystem processes over time, as the forest transitions to upland forest structure and dynamics, and thus represents a yet to be quantified additional amount of *igapó* forest loss (Lobo 2017, Assahira et al. 2017).

High flood tolerance is also not a protection from the effects of flood pulse changes. In black-water *igapó* floodplains, a few tree species have the necessary adaptations to tolerate very long periods of flooding (up to 300 days per year), forming monodominant or even monospecific stands. One of the most frequent tree species in this category is *Eschweilera tenuifolia* (O. Berg) Miers, locally known as *macacarecuia* or *cuieira* (Mori and Prance 1990, Junk et al. 2015). Despite being highly flood-tolerant, we observed several populations of this species suffering massive mortality within the studied area. Massive mortality was also observed for populations of the less frequent species *Macrolobium acaciifolium* within the same or similar areas, at slightly higher elevations of the Uatumã floodplains (Assahira et al. 2017).

Furthermore, a compound effect of the mortality of established adult plants is that changes in the hydrological cycle may create a barrier to seed dispersal and germination, which

are generally synchronized with the flood pulse (Oliveira-Wittmann et al. 2010). Oxygen limitation in soil due to uninterrupted flooding can also lead to high mortality of potentially regenerating soil seeds and young saplings (Yang and Li 2013), as establishment and recruitment occur when the soil is exposed by the receding water levels (Parolin et al. 2010).

In the Central Amazonian floodplains, multiannual extreme wet and dry periods can also have dramatic effects, such as the 1971-75 period when large-scale dieback of shrubs and trees colonizing the lowest elevations of *várzeas* and *igapós* was observed (Piedade et al. 2013). Junk (1989) related this phenomenon to a multiannual period of abnormally high minimum water levels caused by several La Niña events (Schöngart and Junk 2007, Marengo 2009). During strong El Niño events, the black-water *igapós* along the Negro River and other black-water rivers are also especially vulnerable to wildfires (Sombroek 2001, Flores et al. 2014, Resende et al. 2014), as the El Niño-induced rainfall anomalies coincide with the low-water periods of these rivers, with strong implications for plant-water availability (Schöngart et al. 2017b). Large-scale fires were reported for the El Niño-induced droughts in 1925/26 (Williams et al. 2005), 1997/98 (Nelson 2001, Flores et al. 2014) and 2015/16 (Aragão et al. 2018). These climatic vulnerabilities are expected to become more frequent in the future and may further compound the effects of river damming on floodplain forests.

Igapó ecosystems are more susceptible to wildfire than uplands (*terra firme*) or *várzeas*, due to the scarcity of nutrients and the long-term flooding that leads to an accumulation of root mats and litter on the surface, and to a drier microclimate when they are not flooded (Dos Santos and Nelson 2013, Flores et al. 2014, Resende et al. 2014, Almeida et al. 2016). The large amounts of dead biomass resulting from mass mortality induced by hydroelectric damming, associated with the drier microclimate in these forests, could make these ecosystems even more susceptible to wildfires (Kauffman et al. 1988, Cochrane et al. 1999, Resende et al. 2014, Almeida et al. 2016, Flores et al. 2017). Therefore, rising temperatures and increasing drought frequency and intensity (Gloor et al. 2013, 2015, Marengo and Espinoza 2016) combined with land-use changes associated with deforestation and fire (Nobre et al. 2016, Aragão et al. 2018), as well as the implementation of construction of additional hydroelectric dams (Lees et al. 2016, Forsberg et al. 2017), may severely impact the *igapó* ecosystems in the future.

Massive mortality will also have several impacts on the entire ecosystem, such as niche and diversity losses, changes in community structure, facilitation of pests and diseases, and changes in biogeochemical cycles (Franklin et al. 1987, Cherubini et al. 2002). Even edge-related tree mortality on upland forests (Mesquita et al. 1999) can became a problem if the

"buffer" provided by *igapó* forests is broken and adjacent upland forests are exposed. For the lowest-lying *igapós* of the Uatumã River, the carbon stock of aboveground biomass has been estimated at 118±13 Mg C ha^{-1} (Neves 2018). Considering the area of dead forests calculated in the present study as a conservative estimate (10.9 km^2), we can estimate a biomass loss of 129±14 x 10^9 g C. However, as the total mortality process is expected to affect 30 km^2 of forests (29% of the original *igapó*), biomass loss may reach 354 ± 38 x 10^9 g. This would further worsen Balbina's greenhouse gas emissions budget, estimated at 2.5 x 10^{12} g C (CO_2 equivalent emissions) due to increased methane (CH_4) emissions from the reservoir area (Fearnside 1995, Kemenes et al. 2011).

In summary, our study confirms that threats to floodplains downstream of hydropower enterprises are evident, and the environmental effects of existing and proposed hydroelectric dams need to be better understood in Amazonia and other wetlands at risk (Kingsford 2000, Zahar et al. 2008, Ziegler et al. 2013, Junk et al. 2014). Furthermore, this information must be considered when licensing and quantifying the environmental impacts of these enterprises. The legal instrument that assists the Brazilian government in making decisions about large infrastructure projects is the Environmental Impact Assessment (EIA; *Estudo de Impacto Ambiental* in Portuguese), and its accompanying Environmental Impacts Report (RIMA, in Portuguese), which must characterize the environmental conditions of an area prior to the approval of a proposed project, and must indicate all potential impacts, as well as proposing mitigating measures when appropriate (Brasil 1986). However, the Brazilian Amazon EIA/RIMAs are often disregarded during decision making (Cochrane et al. 2017, Ritter et al. 2017). Our suggestion is to improve their diagnostic and predictive power, complementing the impact reports with surveys downstream of affected areas, as well as dynamic projective analyses of changes and predicted flood-pulse pattern after damming.

Although we could map the most fragile areas, it is still difficult to predict the exact duration and extent of the ongoing tree mortality process due to the alteration of the flood pulse. It is likely, however, that it will last for decades to come (Assahira et al. 2017) and that climate change and land-use interactions will probably intensify the deleterious effects caused by dams in the Amazon (Nobre et al. 2016). Fearnside (2016) raised the following question: "Tropical dams: to build or not to build?" Our study adds to previous evidence that the negative environmental and social effects of tropical hydropower dams are enormous and that these effects can reach distant areas, yet they can be overlooked by scientific studies and not

considered in EIA/RIMAs. This framework needs to change, and the available science must be considered to support decision-making.

Acknowledgments

We thank the two anonymous reviewers and Megan F. King who directly contributed to this paper, the National Institute for Amazon Research (INPA), the PELD/MAUA group, and the Ecosystem Dynamics Observatory at the Universidade Estadual Paulista "Júlio de Mesquita Filho" (UNESP Rio Claro) for support and data provision. We also thank the RDS Uatumã and ATTO project for the infrastructure and work support, and the Brazilian Council for Scientific Research (CNPq) for financing the project and the PhD fellowship of AF Resende (MCTI/CNPq/FNDCT nº 68/2013 - Large-Scale Biosphere-Atmosphere Program in the Amazon - LBA), PELD-MAUA project (403792/2012-6 - MCTI/CNPq/FAPs Nº 34/2012 and 441590/2016-0 -CNPq/CAPES/FAPS/BC-Fundo Newton) . We also thank the Alaska Satellite Facility for providing the ALOS/PALSAR images. This work was conducted within the framework of the Kyoto & Carbon Initiative of the Japanese Aerospace Agency (JAXA). AS Streher acknowledges Ph.D. fellowship #2015/17534-3, São Paulo Research Foundation and TSF Silva acknowledges CNPq productivity grant #310144/2015-9.

References

Abad, J.D.; Vizcarra, J.; Paredes, J.; Montoro, H.; Frias, C.; Holguin, C. 2013. Morphodynamics of the upper Peruvian Amazonian rivers , implications into fluvial transportation. *International Conference IDS2013 - Amazonia*: 1–10.

Adeney, J.M.; Christensen, N.L.; Vicentini, A.; Cohn-Haft, M. 2016. White-sand Ecosystems in Amazonia. *Biotropica* 48: 7–23.

Almeida, D.R.A. de; Nelson, B.W.; Schietti, J.; Gorgens, E.B.; Resende, A.F.A.F.A.F.; Stark, S.C.; et al. 2016. Contrasting fire damage and fire susceptibility between seasonally flooded forest and upland forest in the Central Amazon using portable profiling LiDAR. *Remote Sensing of Environment* 184: 153–160.

Anderson, E.P.; Jenkins, C.N.; Heilpern, S.; Maldonado-ocampo, J.A.; Carvajal-vallejos, F.M.; Encalada, A.C.; et al. 2018. Fragmentation of Andes-to-Amazon connectivity by hydropower dams. *Science Advances*: 1–8.

Andreae, M.O.; Acevedo, O.C.; Araùjo, A.; Artaxo, P.; Barbosa, C.G.G.; Barbosa, H.M.J.; et al. 2015. The Amazon Tall Tower Observatory (ATTO): Overview of pilot measurements on ecosystem ecology, meteorology, trace gases, and aerosols. *Atmospheric Chemistry and Physics* 15: 10723–10776.

Aragão, L.E.O.C.; Anderson, L.O.; Fonseca, M.G.; Rosan, T.M.; Vedovato, L.B.; Wagner, F.H.; et al. 2018. 21st Century drought-related fires counteract the decline of Amazon deforestation carbon emissions. *Nature Communications* 9: 1–12.

Arnesen, A.S.; Silva, T.S.F.F.; Hess, L.L.; Novo, E.M.L.M.L.M.; Rudorff, C.M.; Chapman, B.D.; et al. 2013. Monitoring flood extent in the lower Amazon River floodplain using ALOS/PALSAR ScanSAR images. *Remote Sensing of Environment* 130: 51–61.

ASF DAAC. 2015. *ASF DAAC. PALSAR_Radiometric_Terrain_Corrected_high_res*. Includes Material © JAXA/METI 2007. (https://www.asf.alaska.edu/sar-data/palsar). .

Assahira, C.; Resende, A.F. de; Trumbore, S.E.; Wittmann, F.; Cintra, B.B.L.; Batista, E.S.; et al. 2017. Tree mortality of a flood-adapted species in response of hydrographic changes caused by an Amazonian river dam. *Forest Ecology and Management* 396: 113–123.

Benchimol, M.; Peres, C.A. 2015. Edge-mediated compositional and functional decay of tree assemblages in Amazonian forest islands after 26 years of isolation. *Journal of Ecology* 103: 408–420.

Benz, U.C.; Hofmann, P.; Willhauck, G.; Lingenfelder, I.; Heynen, M. 2004. Multi-resolution, object-oriented fuzzy analysis of remote sensing data for GIS-ready information. *ISPRS Journal of Photogrammetry and Remote Sensing* 58: 239–258.

Blaschke, T. 2010. Object based image analysis for remote sensing. *ISPRS Journal of Photogrammetry and Remote Sensing* 65: 2–16.

Brasil. 1986. Resolução CONAMA nº 01, de 23 de janeiro de 1986. *CONAMA - Conselho Nacinal o Meio Ambiente*.

Breiman, L. 2001. Random forests. *Machine Learning* 45: 5–32.

Castello, L.; Macedo, M.N. 2015. Large-scale degradation of Amazonian freshwater ecosystems. *Global Change Biology* 22: 990–1007.

Castello, L.; Mcgrath, D.G.; Hess, L.L.; Coe, M.T.; Lefebvre, P.A.; Petry, P.; et al. 2013. The vulnerability of Amazon freshwater ecosystems. *Conservation Letters* 6: 217–229.

Cherubini, P.; Fontana, G.; Rigling, D.; Dobbertin, M.; Brang, P.; Innes, J.L. 2002. Tree-life history prior to death: two fungal root pathogens affect tree-ring growth differently. *Journal of ecology* 90: 839–850.

Cochrane, M.A.; Alencar, A.; Schulze, M.D.; Jr, C.M.S.; Nepstad, D.C.; Lefebvre, P.; et al. 1999. Positive Feedbacks in the Fire Dynamic of Closed Canopy Tropical Forests. 284: 1832–1835.

Cochrane, S.M.V.; Matricardi, E.A.T.; Numata, I.; Lefebvre, P.A. 2017. Landsat-based analysis of mega dam flooding impacts in the Amazon compared to associated environmental impact assessments: Upper Madeira River example 2006–2015. *Remote Sensing Applications: Society and Environment* 7: 1–8.

Fearnside, P.M. 1995. Hydroelectric Dams in Brazilian Amazonia As. *Environmental Conservation* 22: 7–19.

Fearnside, P.M. 2014. Impacts of Brazil's Madeira River Dams: Unlearned lessons for hydroelectric development in Amazonia. *Environmental Science and Policy* 38: 164–172.

Fearnside, P.M. 2016. Tropical dams: To build or not to build? *Science* 351: 456–457.

Fearnside, P.M.; P.M., F. 1989. Brazil's Balbina Dam: Environment versus the legacy of the pharaohs in Amazonia. *Environmental Management* 13: 401–423.

Ferreira-Ferreira, J.; Silva, T.S.F.; Streher, A.S.; Affonso, A.G.; De Almeida Furtado, L.F.; Forsberg, B.R.; et al. 2014. Combining ALOS/PALSAR derived vegetation structure and inundation patterns to characterize major vegetation types in the Mamirauá Sustainable Development Reserve, Central Amazon floodplain, Brazil. *Wetlands Ecology and Management* 23: 41–59.

Ferreira, L.; Parolin, P. 2011. Effects of flooding duration on plant demography in a black-water floodplain forest in central Amazonia. *Pesqui Bot*: 323–332.

Finer, M.; Jenkins, C.N. 2012. Proliferation of hydroelectric dams in the andean amazon and implications for andes-amazon connectivity. *PLoS ONE* 7: 1–9.

Flores, B.M.; Piedade, M.T.F.; Nelson, B.W. 2014. Fire disturbance in Amazonian blackwater floodplain forests. *Plant Ecology and Diversity* 7: 319–327.

Flores, B.M.; Holmgren, M.; Xu, C.; van Nes, E.H.; Jakovac, C.C.; Mesquita, R.C.G.; et al. 2017. Floodplains as an Achilles' heel of Amazonian forest resilience. *Proceedings of the National Academy of Sciences* 114: 4442–4446.

Foley, J.A.; Botta, A.; Coe, M.T.; Costa, M.H. 2002. El Niño-Southern oscillation and the climate, ecosystems and rivers of Amazonia. *Global Biogeochemical Cycles* 16: 79-1-79–20.

Foote, a. L.; Pandey, S.; Krogman, N.T. 1996. Processes of wetland loss in India. *Environmental Conservation* 23: 45.

Forsberg, B.R.; Melack, J.M.; Dunne, T.; Barthem, R.B.; Goulding, M.; Paiva, R.C.D.; et al. 2017. *The potential impact of new Andean dams on Amazon fluvial ecosystems*. Vol. 12.1–35p.

Franklin, J.F.; Shugart, H.H.; Harmon, M.E. 1987. Tree Death as an Ecological Process. *BioScience* 37: 550–556.

Gloor, M.; Brienen, R.J.W.; Galbraith, D.; Feldpausch, T.R.; Schöngart, J.; Guyot, J.L.; et al. 2013. Intensification of the Amazon hydrological cycle over the last two decades. *Geophysical Research Letters* 40: 1729–1733.

Gloor, M.; Barichivich, J.; Ziv, G.; Brienen, R.; Schöngart, J.; Peylin, P. 2015. Recent Amazon climate as background for possible ongoing Special Section : .

Hess, L.L.; Novo, E.M.L.M.; Slaymaker, D.M.; Holt, J.; Steffen, C.; Valeriano, D.M.; et al. 2002. Geocoded digital videography for validation of land cover mapping in the Amazon basin. *International Journal of Remote Sensing* 23: 1527–1556.

Householder, E.; De Assis, R.L.; Schöngart, J.; Junk, W.J.; Wittmann, F.; Piedade, M.T.F.F.; et al. 2012. Habitat specifity, endemism and the neotropical distribution of Amazonian white-water floodplain trees. *Ecography* 36: 690–707.

IDESAM, I. de C. e D.S. do A. 2009. Série Técnica Planos de Gestão Reserva de Desenvolvimento Sustentável do Uatumã Volumes 1 e 2. 1 and 2: 150.

International Rivers, F.P.; ECOA. 2017. *Dams in Amazonia*. Dams in Amazonia. (http://dams-info.org/en/about/tech/). Accessed on 04 Sep. 2018.

Junk, W.J. 1989. *Flood tolerance and tree distribution in central Amazonian floodplains*. 47–64p.

Junk, W.J.; Mello, J.A.S.N. de. 1990. Impactos ecológicos das represas hidrelétricas na bacia amazônica brasileira. *Estudos Avançados* 4: 126–143.

Junk, W.J.; Bayley, P.B.; Sparks, R.E. 1989. The flood pulse concept in river-floodplain systems. *Proceedings of the International Large River Symposium* 106: 110–127.

Junk, W.J.; Wittmann, F.; Schöngart, J.; Piedade, M.T.F. 2015. A classification of the major habitats of Amazonian black-water river floodplains and a comparison with their white-water counterparts. *Wetlands Ecology and Management* 23: 677–693.

Junk, W.J.; Piedade, M.T.F.; Schöngart, J.; Cohn-Haft, M.; Adeney, J.M.; Wittmann, F. 2011. A classification of major naturally-occurring amazonian lowland wetlands. *Wetlands* 31: 623–640.

Junk, W.J.; Piedade, M.T.F.; Lourival, R.; Wittmann, F.; Kandus, P.; Lacerda, L.D.; et al. 2014.

Brazilian wetlands: Their definition, delineation, and classification for research, sustainable management, and protection. *Aquatic Conservation: Marine and Freshwater Ecosystems* 24: 5–22.

Kahn, J.R.; Freitas, C.E.; Petrere, M. 2014. False shades of green: The case of Brazilian Amazonian hydropower. *Energies* 7: 6063–6082.

Kauffman, J.B.; Uhl, C.; Cummings, D.L. 1988. Fire in the Venezuelan Amazon 1: Fuel Biomass and Fire Chemistry in the Evergreen Rainforest of Venezuela. *Oikos* 53: 167.

Kemenes, A.; Forsberg, B.R.; Melack, J.M. 2007. Methane release below a tropical hydroelectric dam. *Geophysical Research Letters* 34: 1–5.

Kemenes, A.; Forsberg, B.R.; Melack, J.M. 2011. CO2 emissions from a tropical hydroelectric reservoir (Balbina, Brazil). *Journal of Geophysical Research: Biogeosciences* 116.

Kingsford, R.T. 2000. Ecological impacts of dams, water diversions and river management on floodplain wetlands in Australia. *Austral Ecology* 25: 109–127.

Latrubesse, E.M.; Arima, E.Y.; Dunne, T.; Park, E.; Baker, V.R.; D'Horta, F.M.; et al. 2017. Damming the rivers of the Amazon basin. *Nature* 546: 363–369.

Lees, A.C.; Peres, C.A.; Fearnside, P.M.; Schneider, M.; Zuanon, J.A.S. 2016. Hydropower and the future of Amazonian biodiversity. *Biodiversity and Conservation* 25: 451–466.

Lewis, W.M.; Hamilton, S.K.; Lasi, M. a.; Rodríguez, M.; Saunders, J.F. 2000. Ecological Determinism on the Orinoco Floodplain. *BioScience* 50: 681.

Liaw, A.; Wiener, M. 2002. Classification and Regression by randomForest. *R news* 2: 18–22.

Ligon, F.K.; Dietrich, W.E.; Trush, W.J. 1995. Downstream Ecological Effects of Dams. *BioScience* 45: 183–192.

Lobo, G. de S. 2017. *A alteração do regime hidrológico afeta a composição florística e estrutura de florestas de igapó? Um estudo comparativo entre um rio regulado e outro prístino na Reserva de Desenvolvimento Sustentável do Uatumã, Amazônia Central*. 70p.

Manyari, W.V.; de Carvalho, O.A. 2007. Environmental considerations in energy planning for the Amazon region: Downstream effects of dams. *Energy Policy* 35: 6526–6534.

Marengo, J.A. 2009. Long-term trends and cycles in the hydrometeorology of the Amazon basin since the late 1920s. *Hydrological Processes* 23: 3236–3244.

Marengo, J.A.; Espinoza, J.C. 2016. Extreme seasonal droughts and floods in Amazonia: Causes, trends and impacts. *International Journal of Climatology* 36: 1033–1050.

Meade, R.H.; Rayol, J.M.J.M.J.M.; Da Conceic??o, S.C.; Natividade, J.R.G.J.R.G.J.R.G.; Conceicão, S.C.; Natividade, J.R.G.J.R.G.J.R.G. 1991. Backwater Effects in the Amazon

River Basin of Brazil. *Environ Geol Water Sci* 18: 105–114.

Melack, J.M.; Hess, L.L. 2010. Remote sensing of the distribution and extent of wetlands in the Amazon basin. In: *Amazonian Floodplain Forests*, Springer, p.43–59.

Mesquita, R.C.G.; Delamônica, P.; Laurance, W.F. 1999. Effect of surrounding vegetation on edge-related tree mortality in Amazonian forest fragments. *Biological Conservation* 91: 129–134.

Mori, S.A.; Prance, G.T. 1990. *Flora Neotropica Monograph 21 (II) Lecythidaceae - part II. The zygomorphic-flowered New World genera (Couroupita, Corythophora, Bertholletia, Couratari, Eschweilera & Lecythis)*. Vol. 70.1–376p.

Mumba, M.; Thompson, J.R. 2005. Hydrological and ecological impacts of dams on the Kafue Flats floodplain system, southern Zambia. *Physics and Chemistry of the Earth* 30: 442–447.

Nelson, B.W. 2001. Fogo em florestas da Amazônia Central em 1997. *Anais X SBSR*: 1675–1682.

Neves, J.R.D. 2018. *Mudanças na fitofisionomia e estoque e produção de biomassa pelas alterações no ciclo hidrológico em florestas alagáveis de igapó na Amazônia Central*. Instituto Nacional de Pesquisas da Amazônia, 69pp.

Nilsson, christer. 2000. Alterations of riparian ecosystemes caused by river regulation. *Bio Science* 50: 783–792.

Nobre, C.A.; Sampaio, G.; Borma, L.S.; Castilla-Rubio, J.C.; Silva, J.S.; Cardoso, M. 2016. Land-use and climate change risks in the Amazon and the need of a novel sustainable development paradigm. *Proceedings of the National Academy of Sciences* 113: 10759–10768.

Oliveira-Wittmann, A.; Lopes, A.; Conserva, A.D.S.; Wittmann, F.; Piedade, M.T.F. 2010. Seed germination and seedling establishment of Amazonian floodplain trees. In: *Amazonian Floodplain Forests*, Springer, p.259–280.

Parolin, P.; Waldhoff, D.; Piedade, M.T.F. 2010. Fruit and seed chemistry, biomass and dispersal. In: *Amazonian Floodplain Forests*, Springer, p.243–258.

Parolin, P.; De Simone, O.; Haase, K.; Waldhoff, D.; Rottenberger, S.; Kuhn, U.; et al. 2004. Central Amazonian Floodplain Forests: Tree Adaptations in a Pulsing System. *The Botanical Review* 70: 357–380.

Piedade, M.T.F.; Schongart, J.; Wittmann, F.; Parolin, P.; Junk, W.J. 2013. Impactos ecológicos da inundação e seca na vegetação das áreas alagáveis amazônicas. *Eventos climáticos*

extremos na Amazônia: causas e conseqüências: 405–457.

Pontius, R.G.; Millones, M. 2011. Death to Kappa: Birth of quantity disagreement and allocation disagreement for accuracy assessment. *International Journal of Remote Sensing* 32: 4407–4429.

Pontius, R.G.; Santacruz, A. 2014. Quantity, exchange, and shift components of difference in a square contingency table. *International Journal of Remote Sensing* 35: 7543–7554.

Prance, G.T. 1979. Notes on the Vegetation of Amazonia III. The Terminology of Amazonian Forest Types Subject to Inundation. *Brittonia* 31: 26.

R Core Team. 2018. R: A Language and Environment for Statistical Computing. .

Resende, A.F.; Nelson, B.W.; Flores, B.M.; de Almeida, D.R.; de Resende, A.F.; Nelson, B.W.; et al. 2014. Fire damage in seasonally flooded and upland forests of the Central Amazon. *Biotropica* 46: 643–646.

Ritter, C.D.; McCrate, G.; Nilsson, R.H.; Fearnside, P.M.; Palme, U.; Antonelli, A. 2017. Environmental impact assessment in Brazilian Amazonia: Challenges and prospects to assess biodiversity. *Biological Conservation* 206: 161–168.

Dos Santos, A.R.; Nelson, B.W. 2013. Leaf decomposition and fine fuels in floodplain forests of the Rio Negro in the Brazilian Amazon. *Journal of Tropical Ecology* 29: 455–458.

Schlüter, U.B.; Furch, B. 1992. Morphological, anatomical, and physiological investigations on the tolerance to flooding by the tree Macrolobium acaciifolium, characteristic of the white- and blackwater inundation forest near Manaus, Amazonas. 12: 51–69.

Schöngart, J.; Junk, W.J. 2007. Forecasting the flood-pulse in Central Amazonia by ENSO-indices. *Journal of Hydrology* 335: 124–132.

Schöngart, J.; Wittmann, F.; Junk, W.J.; Piedade, M.T.F. 2017. Vulnerability of Amazonian floodplains to wildfires differs according to their typologies impeding generalizations. *Proceedings of the National Academy of Sciences* 114: 201713734.

Schöngart, J.; Piedade, M.T.F.; Ludwigshausen, S.; Horna, V.; Worbes, M.; Schongart, J.; et al. 2002. Phenology and stem-growth periodicity of tree species in Amazonian floodplain forests. *Journal of Tropical Ecology* 18: 581–597.

Schöngart, J.; Piedade, M.T.F.; Wittmann, F.; Junk, W.J.; Worbes, M.; Piedade, T.F. 2005. Wood growth patterns of Macrolobium acaciifolium (Benth.) Benth. (Fabaceae) in Amazonian black-water and white-water floodplain forests. *Oecologia* 145: 454–461.

Shi, Z.; Fung, K.B. 1994. A comparison of digital speckle filters. *Proceedings of IGARSS '94 - 1994 - IEEE International Geoscience and Remote Sensing Symposium* 4: 2129–2133.

Silva, T.S.F.; Costa, M.P.F.; Melack, J.M.; Novo, E.M.L.M. 2008. Remote sensing of aquatic vegetation: theory and applications. *Environmental Monitoring and Assessment* 140: 131–145.

Silva, T.S.F.; Melack, J.; Susin, S.A.; Ferreira-Ferreira, J.; Furtado, L.F. de A. 2015. Capturing the Dynamics of Amazonian Wetlands Using Synthetic Aperture Radar: Lessons Learned and Future Directions. *Remote Sensing of Wetlands*: 455–472.

De Simone, O.; Junk, W.J.; Schmidt, W. 2003. Central Amazon floodplain forests: Root adaptations to prolonged flooding. *Russian Journal of Plant Physiology* 50: 848–855.

Sioli, H. 1984. The Amazon and its main affluents: Hydrography, morphology of the river courses, and river types. : 127–165.

Sombroek, W. 2001. Spatial and Temporal Patterns of Amazon Rainfall. *AMBIO: A Journal of the Human Environment* 30: 388–396.

Targhetta, N.; Kesselmeier, J.; Wittmann, F. 2015. Effects of the hydroedaphic gradient on tree species composition and aboveground wood biomass of oligotrophic forest ecosystems in the central Amazon basin. *Folia Geobotanica* 50: 185–205.

Tilt, B. 2012. Damming china's angry river: Vulnerability in a culturally and biologically diverse watershed. In: *Water, Cultural Diversity, and Global Environmental Change: Emerging Trends, Sustainable Futures?*, p.367–386.

Tilt, B.; Braun, Y.; He, D. 2009. Social impacts of large dam projects: A comparison of international case studies and implications for best practice. *Journal of Environmental Management* 90: S249–S257.

Timpe, K.; Kaplan, D. 2017. The changing hydrology of a dammed Amazon. *Science Advances* 3: 1–14.

Ward, J. V.; Stanford, J.A. 1995. Ecosystems and Its Disruption By Flow Regulation. *Regulated Rivers: Research & Management* II: 105–119.

Williams, E.; Dall'Antonia, A.; Dall'Antonia, V.; Antonia, A.D.; Antonia, V.D.; Almeida, J.M. De; et al. 2005. The drought of the century in the Amazon Basin: an analysis of the regional variation of rainfall in …. *Acta Amazonica* 35: 231–238.

Williams, G.P.; Wolman, M.G. 1984. Downstream effects of dams on alluvial rivers. *U.S. Geol. Surv., Prof. Pap.; (United States); Journal Volume: 1286*: 83.

Wittmann, F.; Junk, W.J. 2017. The Wetland Book. : 1–20.

Wittmann, F.; Schöngart, J.; Montero, J.C.; Motzer, T.; Junk, W.J.; Piedade, M.T.F.F.; et al. 2006. Tree species composition and diversity gradients in white-water forests across the

Amazon Basin. *Journal of Biogeography* 33: 1334–1347.

Wittmann, F.; Marques, M.C.M.; Júnior, G.D.; Budke, J.C.; Piedade, M.T.F.; De Wittmann, A.O.; et al. 2017. The Brazilian freshwater wetscape: Changes in tree community diversity and composition on climatic and geographic gradients. *PLoS ONE* 12: 1–18.

Woodhouse, I.H. 2017. *Introduction to microwave remote sensing*. CRC press, .

Yang, D.; Li, W. 2013. Soil seed bank and aboveground vegetation along a successional gradient on the shores of an oxbow. *Aquatic Botany*.

Zahar, Y.; Ghorbel, A.; Albergel, J. 2008. Impacts of large dams on downstream flow conditions of rivers: Aggradation and reduction of the Medjerda channel capacity downstream of the Sidi Salem dam (Tunisia). *Journal of Hydrology* 351: 318–330.

Ziegler, A.D.; Petney, T.N.; Grundy-Warr, C.; Andrews, R.H.; Baird, I.G.; Wasson, R.J.; et al. 2013. Dams and Disease Triggers on the Lower Mekong River. *PLoS Neglected Tropical Diseases* 7.

Supplementary material

Figure S1 – The photography shows an undisturbed igapó at the Abacate River, one important tributary of the Uatumã River (by Maíra da Rocha).

Table S2 – ALOS PALSAR 1 Image codes, mode, path and frame locations, date of acquisition and its respective river level according to ANA (Brazilian National Water Agency) gage.

Granule Name	*Beam Mode*	*Path Number*	*Frame Number*	*Acquisition date*	*River Level*
ALPSRP080087140	FBD	74	7140	27/7/2007	406.5
ALPSRP081837140	FBD	72	7140	8/8/2007	404
ALPSRP084317140	FBD	73	7140	25/8/2007	327
ALPSRP086067130	FBD	71	7130	6/9/2007	406
ALPSRP100217140	FBS	74	7140	12/12/2007	419.5
ALPSRP101967140	FBS	72	7140	24/12/2007	378
ALPSRP104447140	FBS	73	7140	10/1/2008	361
ALPSRP106197130	FBS	71	7130	22/1/2008	401
ALPSRP113637140	FBS	74	7140	13/3/2008	424.5
ALPSRP115387140	FBS	72	7140	25/3/2008	406
ALPSRP117867140	FBS	73	7140	11/4/2008	450
ALPSRP119617130	FBS	71	7130	23/4/2008	445
ALPSRP120347140	FBD	74	7140	28/4/2008	465
ALPSRP122097140	FBD	72	7140	10/5/2008	491
ALPSRP124577140	FBD	73	7140	27/5/2008	477
ALPSRP126327130	FBD	71	7130	8/6/2008	459
ALPSRP127057140	FBD	74	7140	13/6/2008	459
ALPSRP131287140	FBD	73	7140	12/7/2008	461
ALPSRP133037130	FBD	71	7130	24/7/2008	442
ALPSRP133767140	FBD	74	7140	29/7/2008	443
ALPSRP135517140	FBD	72	7140	10/8/2008	427
ALPSRP137997140	FBD	73	7140	27/8/2008	420
ALPSRP139747130	FBD	71	7130	8/9/2008	449
ALPSRP180737140	FBD	74	7140	16/6/2009	549.5
ALPSRP182487140	FBD	72	7140	28/6/2009	ND
ALPSRP184967140	FBD	73	7140	15/7/2009	ND
ALPSRP186717130	FBD	71	7130	27/7/2009	495
ALPSRP187447140	FBD	74	7140	1/8/2009	474
ALPSRP189197140	FBD	72	7140	13/8/2009	412.5
ALPSRP191677140	FBD	73	7140	30/8/2009	373
ALPSRP193427130	FBD	71	7130	11/9/2009	357
ALPSRP207577140	FBS	74	7140	17/12/2009	342
ALPSRP209327140	FBS	72	7140	29/12/2009	357
ALPSRP211807140	FBS	73	7140	15/1/2010	470
ALPSRP220997140	FBS	74	7140	19/3/2010	376
ALPSRP222747140	FBS	72	7140	31/3/2010	347.5
ALPSRP226977130	FBS	71	7130	29/4/2010	342
ALPSRP229457140	FBD	72	7140	16/5/2010	354

ALPSRP231937140	FBD	73	7140	2/6/2010	345
ALPSRP233687130	FBD	71	7130	14/6/2010	349
ALPSRP234417140	FBD	74	7140	19/6/2010	368
ALPSRP236167140	FBD	72	7140	1/7/2010	350
ALPSRP238647140	FBD	73	7140	18/7/2010	335
ALPSRP240397130	FBD	71	7130	30/7/2010	350
ALPSRP241127140	FBD	74	7140	4/8/2010	387
ALPSRP242877140	FBD	72	7140	16/8/2010	335
ALPSRP245357140	FBD	73	7140	2/9/2010	380
ALPSRP247107130	FBD	71	7130	14/9/2010	387
ALPSRP261257140	FBS	74	7140	20/12/2010	380.5
ALPSRP263007140	FBS	72	7140	1/1/2011	401
ALPSRP265487140	FBS	73	7140	18/1/2011	398
ALPSRP267237130	FBS	71	7130	30/1/2011	430
ALPSRP267967140	FBS	74	7140	4/2/2011	437
ALPSRP269717140	FBS	72	7140	16/2/2011	420
ALPSRP272197140	FBS	73	7140	5/3/2011	419
ALPSRP273947130	FBS	71	7130	17/3/2011	445

Table S3 – Confusion Matrix generated by Random Forest as result of the internal out-of-bag independent validation, showing the percentage of wrong classification in the validation set for each class using one-third of the training set.

	Dead Stands	*Flooded Forest*	*Grassland*	*Upland*	*Water*	*Class. error*
Dead Stands	14	1	2	0	3	0.30
Flooded Forest	1	37	6	1	2	0.21
Grassland	1	9	55	4	4	0.24
Upland	0	1	5	119	0	0.05
Water	2	2	3	0	96	0.07

Capítulo 2

Resende, A. F.; Macedo, M. O., Feitosa, Y O; Pereira, G. A., Trumbore, S. E.; Piedade, M. T. F., Silva, K. F. A., Stahle, D. W., and Schöngart, J. F**lood-pulse disturbances and climate-growth relationships of *Eschweilera tenuifolia* (Lecythidaceae) tree species in Central Amazonian floodplain**. *Dendrochronology* (in preparation)

Flood-pulse disturbances and climate-growth relationships of Eschweilera tenuifolia (Lecythidaceae) tree species in Central Amazonian floodplain

Angélica Faria de Resende, Maíra Oliveira Macedo, Yuri Oliveira Feitosa, Gabriel de Assis Pereira, Susan E. Trumbore, Maria Teresa Fernandez Piedade, Ketlen Fernanda de Almeida Silva, David W. Stahle, Jochen Schöngart

Abstract

Climate and land-use changes are increasing disturbance agents in the Amazon basin. In the Amazonian floodplains the intensification of the hydrological regime triggered by oceanic forcing and the implementation of hydroelectric power plants are increasing threats for these ecosystems. The evergreen tree species *Eschweilera tenuifolia* (O. Berg) Miers (Lecythidaceae) is endemic to the nutrient-poor Central Amazonian floodplain forests (*igapó*) where it forms monodominant stands at the lowest topographies, spending most time of its life inundated. This species intensely depends on the flood-pulse, what depends on the equilibrium of a large- and local-scale climate but can be vastly affected by flow alterations leaded by dams' implementations. We tested in this study the influence of the intensification of the hydrological regime during the last three decades effects on growth, characterized by an increase in the magnitude and frequency of severe floods at the Jaú National Park (JNP, anthropogenically undisturbed) and substantial disturbances of the hydrological regime at the Uatumã Sustainable Development Reserve (USDR) as a consequence of the implementation of the hydroelectric power plant Balbina. We crossdated tree-ring series of *E. tenuifolia* to produce reliable tree-ring chronologies for climate-growth relationships at the JNP and the USDR. Therefore, we correlated the tree-ring chronologies with monthly water level and precipitation data of the study site and sea surface temperature (SST) anomalies from the tropical Atlantic and Pacific oceans breaking the time in periods before and after 1982/1983 when the Balbina dam was implemented but also the intensification of the Amazon climate was starting. At both sites robust tree-ring chronologies were produced with accurate tree-ring statistics (Sample Signal Strength >0.85) for the periods 1927-1999 (JNP) and 1920-2006 (USDR). For the period before the intensification of the hydrological regime (before 1982), tree growth presents negative correlations with monthly water levels and positive correlations with SST in the equatorial sections of the Pacific Ocean. With the intensification of the hydrological regime (after 1983) the population of the JNP shows increasing positive correlations with SST anomalies in the Pacific basin and negative correlations with the tropical Atlantic Ocean. This reflects the mechanism responsible for the intensification of the hydrological cycle caused by a warming of the tropical Atlantic Ocean and simultaneously cooling of the Equatorial Pacific leading to an intensified Walker circulation enhancing

cloud convection and rainfall over the central and northern part of the Amazon basin. At the USDR the construction of the Balbina dam in the 1980s resulted into opposite climate-growth correlations with the hydrological regime and SST signals in the chronology as a consequence of the abrupt and heavy disturbance in macrohabitats dominated by the tree species. The tree species *Eschweilera tenuifolia* responds sensitively to hydroclimatic disturbances and the intensification of these events could turn this species, and consequently the entire macrohabitat it represents, more vulnerable in the future.

Keywords: Igapó, hydroelectric dam, Balbina, ^{14}C-dating, dendrochronology, sea surface temperatures.

Introduction

The flood-pulse is imperative on shaping Amazonian floodplain forests and triggering growth rhythms and life cycles of its biota (Junk et al. 1989, Junk et al. 2011). The downstream flood-pulse loss by river damming is causing massive tree mortality in the lower topographies of black-water *igapó* forests (Assahira et al. 2017, Resende et al. 2019), but the imposed new hydrological stress, together with extreme climate events, may be affecting life and growth of the remaining trees (Resende et al. 2019). The temporal effect of disturbances can be accessed through the secondary growth variation between years, recorded in the tree-rings (D'Arrigo et al. 2011).

The presence of a monomodal and predictable flood-pulse characterizes the floodplain forests covering approximately 750,000 km^2 along the big rivers of the Amazon basin (Wittmann and Junk 2017). The *igapós* are floodplains of black or clear waters with lower fertility compared to the *várzeas* which are influenced by the white-water rivers with a high load of nutrient-rich sediments (Prance 1979, Sioli 1984). Floodplains trees developed combinations of anatomical, morphological, physiological and biochemical adaptations to tolerate high (up to 10 meters) and long-lasting floods (Junk 1989, De Simone et al. 2002, Parolin et al. 2004). The anoxic conditions during the inundation period reduce the cambium activity leading to its dormancy, resulting in the formation of the annual tree rings (Worbes et al. 1992, Schöngart et al. 2002).

Floodplain trees can be bioindicators of hydrological disturbances, mainly the species living at marginal sites under extreme flood conditions, once they are long-living and have secondary growth closely linked to the hydrological cycle and climate (Schöngart et al. 2002,

2004, 2005, 2017a). The tree-ring width is a proxy of the tree performance in a changing environment (Schweingruber 1996). The tree ring is a record of the entire tree life including their reactions to the biotic and abiotic conditions (Fritts 1976). The availability of resources as light, oxygen and water during the growth phase result in the variation of the ring width. This way, the environmental variables, and ecological information are recorded in the annual rings along the entire life-span of a tree (Fichtler and Worbes 2012).

The predictability, frequency, and duration of such seasonality have been recently affected by climate and anthropogenic disturbances. Extreme climate events can prolong droughts in different regions and periods across the Amazon basin (Aragão et al. 2018), leading to very low water levels and increasing the duration of the terrestrial phase in floodplains (Schöngart et al. 2004, Marengo et al. 2011, Piedade et al. 2013, Tomasella et al. 2013). The hydrological cycle can also be intensely altered by extreme floods, which are significantly increasing in frequency and magnitude in Amazonia (Gloor et al. 2013, 2015, Marengo and Espinoza 2016, Barichivich et al. 2018). This increase of severe floods in the Amazon basin in the last three decades is caused by an intensification of the Walker cell due to enhancing sea surface temperatures (SST) in the Tropical Atlantic and simultaneously a cooling of SST in the Equatorial Pacific (Barichivich et al. 2018).

An intensification of the hydrological regime can also occur as a consequence of land-use changes such large-scale deforestation in the catchment area of large rivers (Costa et al. 2013) or the implementation of hydroelectric power plants (Mumba and Thompson 2005, Forsberg et al. 2017, Timpe and Kaplan 2017, Assahira et al. 2017). In the Uatumã River, the operation of the Balbina dam, starting in 1989 resulted into dramatic changes of the hydrological regime by increasing the minimum water levels, decreasing the maximum water levels and alternating the temporal occurrence of floods and droughts (Timpe and Kaplan 2017, Assahira et al. 2017).

Studying the impact of the intensification of the hydrological regime, caused by climate and land-use changes, on tree growth in the floodplains is a major challenge since the performance of dendrochronological studies in these environments (Schöngart et al. 2004, 2005, Batista and Schöngart 2018). By producing tree-ring chronologies and analyzing their correlation to climatic and hydrological variables at different time scales, this study aims to identify which climate and hydrological parameters exert more influence on tree growth of the species *Eschweilera tenuifolia* (O. Berg) Miers (Lecythidaceae). We focus on the following questions: How do hydroclimatic variations influence the growth of *E. tenuifolia* in periods

with and without the influence of the river damming? What local and global hydroclimatic variables influence tree growth of *E. tenuifolia* in periods with and without the influence of the river damming? How did the intensification of the hydrological regime impact tree growth in the Central Amazonian floodplains?

Methods

Study areas and species descriptions

We sampled trees from two sub-basins of the black-water *igapó* system in Central Amazonia, as part of the Ecological Long-Term Monitoring Project (PELD) of the MAUA (Ecology, Monitoring and Sustainable Use of wetlands) group at the National Institute for Amazon Research (INPA). The first site is the Jaú National Park (JNP), a federal conservation unit created in 1980, which represents an undisturbed floodplain forest (Figure 1). The second site is located at the Uatumã Sustainable Development Reserve (USDR), downstream the Balbina dam, which was implemented in the 1980s for hydroelectric power generation, represents a disturbed system (Assahira et al. 2017, Resende et al. 2019). The Uatumã River drains into the Amazon mainstream while the Jaú River flows into the Negro River, a direct affluent of the Amazon River. At both locations occur macrohabitats formed by monodominant populations of the tree species *Eschweilera tenuifolia* occurring at the lowest topographies in the *igapó*, flooded by acid and nutrient-poor black-waters with no sediment load.

Climate conditions are similar at both study sites with mean annual precipitation of 2153 mm at JNP, and 1982 mm at USDR and monthly mean temperature of 26.5 °C (JNP) and 27°C (USDR) (for the period 1901-2015, CRU data plot from the website of World Bank 2019) (Figure S1). A distinct dry season occurs at both study sites from July to September. The seasonality of the rainfall regime and temperature is more pronounced at the USDR with a slightly higher monthly temperature variation and less rainfall during the dry season, especially during the months August-October (<100 mm). A monomodal flood-pulse characterizes the hydrological regime at the JNP with maximum water levels occurring around June and minimum water levels around October/November (FVA and IBAMA 1998). At the USDR the monomodal flood-pulse regime was severely disturbed after the begin of the operation of the Balbina dam in 1989, leading to a reduction of maximum water levels, an increase of the

minimum water levels and further a high variability of the temporal appearance of the maximum and minimum water level (Assahira et al. 2017).

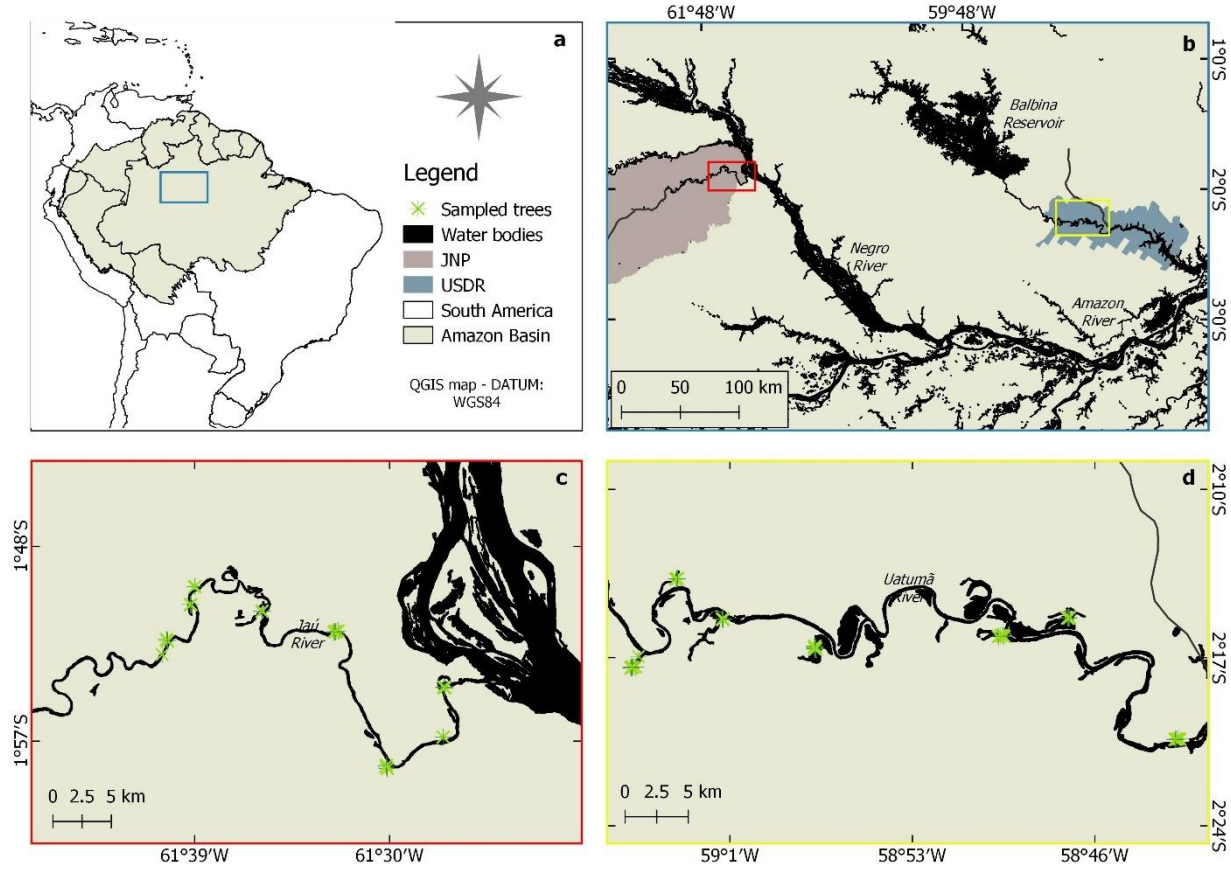

Figure 1- Location of a) the Amazon basin in South America and b) the study regions in the sub-basins of the Jaú and Uatumã rivers in Central Amazonia indicating the sampling sites of Eschweilera tenuifolia at c) the Jaú National Park (JNP) and d) the Uatumã Sustainable Development Reserve (USDR).

The tree species *Eschweilera tenuifolia* is endemic to oligotrophic floodplain environments, commonly forming monodominant stands at the low-lying *igapós* with up to 10 months of flooding (Junk et al. 2015). It is the only tree species able to survive in such marginal environments, and it is easily affected by the river hydrological disturbances since there is a strong dependence of this species on the river flood-pulse (Mori and Prance 1990, Junk et al. 2015). Reticulate parenchyma characterizes the tree rings, typically for Lecythidaceae (Worbes 1989), with a higher percentage of fiber tissue in the earlywood and parenchyma in the latewood (Figure 2).

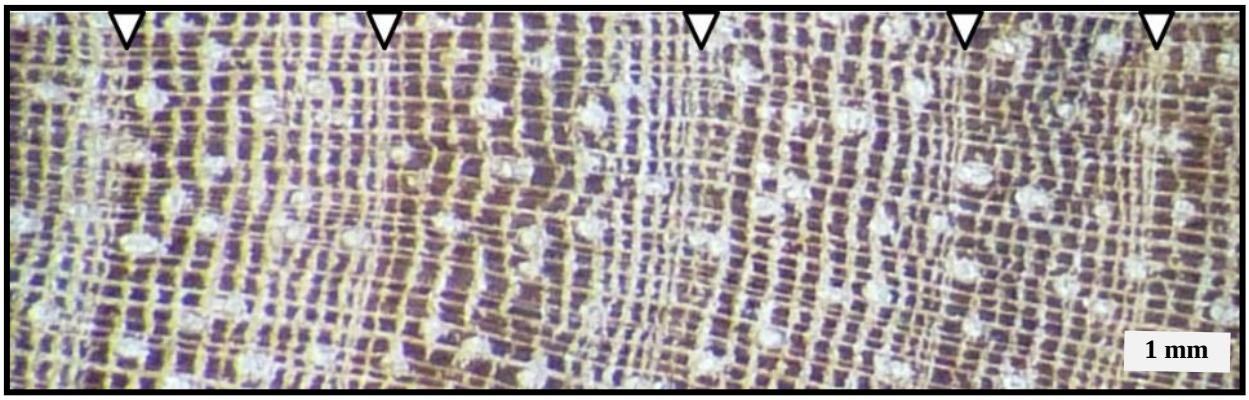

Figure 2 - Macroscopic wood anatomy of tree rings from Eschweilera tenuifolia (Lecythidaceae) characterized by alternating parenchyma and fiber bands with a higher percentage of fiber and parenchyma in the earlywood and latewood section, respectively (reticulate parenchyma).

Experimental delineation, samples preparation, and dendrochronological analysis

At each area, sampling occurred at the same macrohabitats characterized opened monodominant *Eschweilera*-formations in lakes connected to the main channel. At these sites distributed along the main river channel with about 10 km distance between them, we collected in the dry season of 2015 and 2016 two cores with 5 mm increment borers of from 62 living trees at the USDR and 31 individuals at the JNP and a total of 50 dead trees at the USDR (n=29) and JNP (n=21), always sampling trees with different sizes. Additionally, we sampled two entire cross sections in 2018 with a chainsaw from living trees at the USDR (collections under licenses 51133-1/2015 and 61/2015 - 28/2018 from SISBio and DEMUC/SEMA, respectively). From all trees we recorded geographic positions by GPS, the diameter at the breast height (DBH), the flood height printed at the tree trunk and took note of further relevant information (such as if some dead tree were fallen, abnormal branches in one side, healthy state).

All samples were sanded and polished at the Dendroecological Laboratory (INPA/MAUA). The rings were marked under a stereomicroscope (LEICA MS5) and measured using a digital measuring table (LINTAB) supported with TSAP software (RinnTech 2011) for tree-ring measurement and crossdating. The COFECHA software and the dplR R-package were used to perform the individual series quality control (Holmes 1992, Bunn 2008) and poor quality series (those presenting low correlation with a temporary master series) were totally or partially removed from the data set. For crossdating, detrending and building a master chronology for each area, we used the dplR package, implemented in the R software (Bunn 2008, R Core Team 2018). At the first moment, only living trees series were used to build the

first chronology per sampling site. In a second step, we used this chronology as a reference curve to date the dead trees using dendrochronology and radiocarbon dating for those trees who died after the bomb peak. Those series were then implemented in the data set, to improve the replications and data quality of the final master series keeping high-correlated tree-ring series.

Although we had some long individual series with more than 400 tree rings, we focused on building a high-quality master chronology for the period with more samples and reliable dating, once less replicated periods might include trees with missing and false rings which are propagating errors along with the time series. We calculated the basic statistics for each chronology using dplR which comprises the interseries correlation (IC) (mean correlation coefficient based on the relations of each individual tree-ring series and a chronology built from all the other series, same parameter as the series intercorrelation in COFECHA; Holmes and Richard 1983), the average correlation among trees within the common overlap period (Rbar) (Cook and Kairiukstis 1990) and the Sample Signal Strength (SSS) (Wigley et al. 1984). The SSS was used instead of the EPS (Expressed Population Signal) by being more relevant for seeking the sample representativity, as suggested by Bunn (2008) and Buras (2017).

To confirm the annual formation of tree rings from *E. tenuifolia*, we applied radiocarbon (^{14}C) dating of material obtained from different years in the period after the bomb peak of the 1960s (Hua et al. 2013). Therefore, we isolated 14 pre-dated rings from 12 trees (seven from USDR and five from JNP) by simple ring-counting from bark to pith direction (for four samples we had to use three tree-rings to complete the necessary amount of wood sample). As tree-ring formation in the Central Amazonian floodplains starts in the 2nd half of a year and stops in the first half of the following year (Schöngart et al. 2002), we considered the period of latewood formation to associate calendar years to tree rings (for instance, a ring formed during the 2014/15 period is considered 2015). The analysis was done by the Max-Planck-Institute of Biogeochemistry (Jena, Germany) ^{14}C laboratory (Steinhof et al. 2004, 2017, Steinhof 2013) (SISGEN license for transport: Remessa Nº R643423). The results of ^{14}C dating were turned into calendar date using Oxcal v 4.3 (Ramsey 2001, Bronk Ramsey 2016) for southern hemisphere zone SH3 (Hua et al. 2013).

Instrumental climate data and climate analysis

To verify the climate signal for both developed chronologies, we used monthly precipitation, sea surface temperature (SST) anomalies where we chose HadlSST1 from the

Met Office Hadley Centre (Rayner et al. 2003) from the KNMI Climate Explorer website (Trouet and Van Oldenborgh 2013, KNMI 2019) and hydrological data (river level) from the Brazilian National Agency for Waters (ANA 2018). For the USDR, hydrological data are available since 1930. For the JNP we used data from the Port of Manaus at the lower Negro River available since 1903, since the existing local gauge data since 2005 at the JNP is too short to perform reliable analysis. Due to the backwater effect caused by the Solimões River the hydrological regime of the Negro River is very similar along its lower course until its confluence with the Branco River (Meade et al. 1991) and the water level fluctuations at the study sites are highly correlated with those recorded in Manaus (FVA and IBAMA 1998, Junk et al. 2015).

For climate-growth analyses, the chronologies and the climate data were entered in the "treeclim R package" (Zang and Biondi 2015). The correlation analysis was implemented in the Treeclim package following the "Dendroclim2002" original software (Biondi and Waikul 2004). For the analyses, we considered the whole period of available climate data and those stretches of the chronologies with SSS >0.85 (Figure S2). Correlations between the chronology and climate data from both sites were computed for periods of 30 years with offsets every five years. We used this approach to observe changes in the climate-growth relationships starting in the 1980s due to the implementation of the Balbina dam at the USDR (Assahira et al. 2017) and the intensification of the hydrological cycle in the Amazon basin (Gloor et al. 2013, Barichivich et al. 2018). For the analysis with SST anomalies, we computed spatial correlations comprising the entire record using the KNMI Climate Explorer platform (KNMI 2019).

Results

Radiocarbon dating

The ^{14}C-datings of the 14 isolated and pre-dated tree rings from the period after the bomb peak (JNP: n=5; USDR: n=9) indicated contrasting results (Table S1). For six samples the pre-dating by ring-count was confirmed by radiocarbon dating, three samples showed a displacement of one year, while for five samples the displacement was between two and five years. The displacement was positive in three cases, possibly because we counted false rings as being annual tree rings, while for the other five samples the difference was negative, possibly due to the occurrence of missing rings. Almost all problematic samples originated from the

disturbed site at the USDR (only two of seven samples were precisely dated), while samples from the JNP showed a high congruence (only one sample of five showed a one-year displacement).

Tree-ring chronologies

For the JNP we built a tree-ring chronology with 27 series from 24 different trees with a mean Rbar of 0.202 and IC of 0.404 (Figure 3). SSS was higher than 0.85 for the period between 1927 and 1999 (Figure S2). For the USDR dataset, we produced a chronology out of 19 series from 17 trees (Rbar= 0.242, IC = 0.416), indicating for the period 1920-2006 with SSS >0.85 (Figure S2). In both cases, we could include some dead trees (seven cross-sections for JNP and two from USDR, radiocarbon and crossdated) to improve our chronologies. Detrending of the chronologies was performed using a spline with a wavelength cutoff of 0.5 (50%) for both areas (Figure 3).

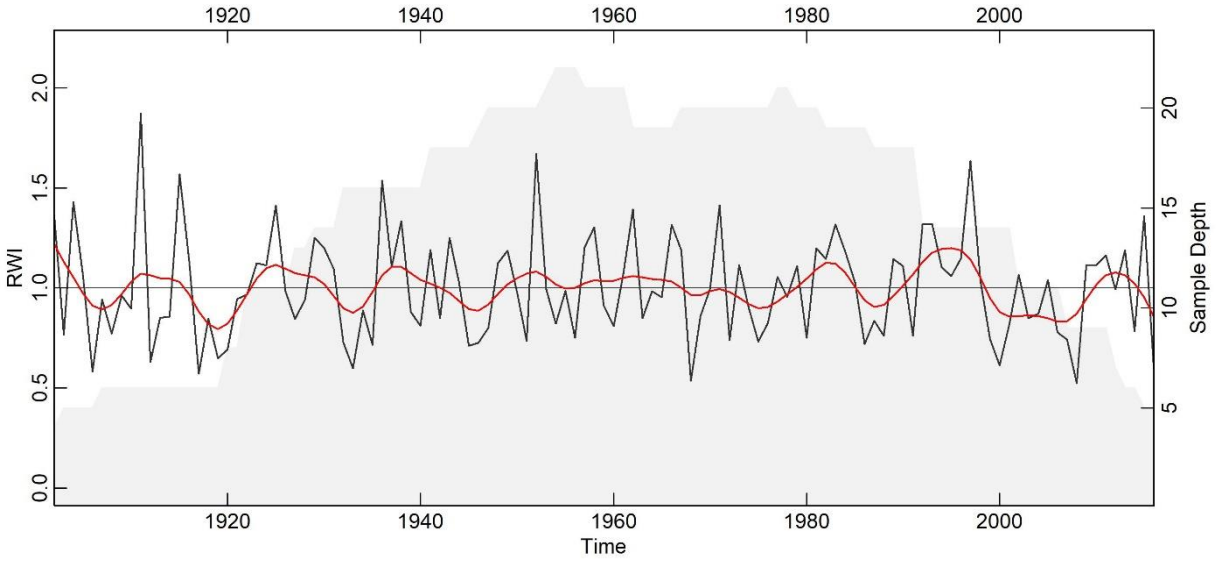

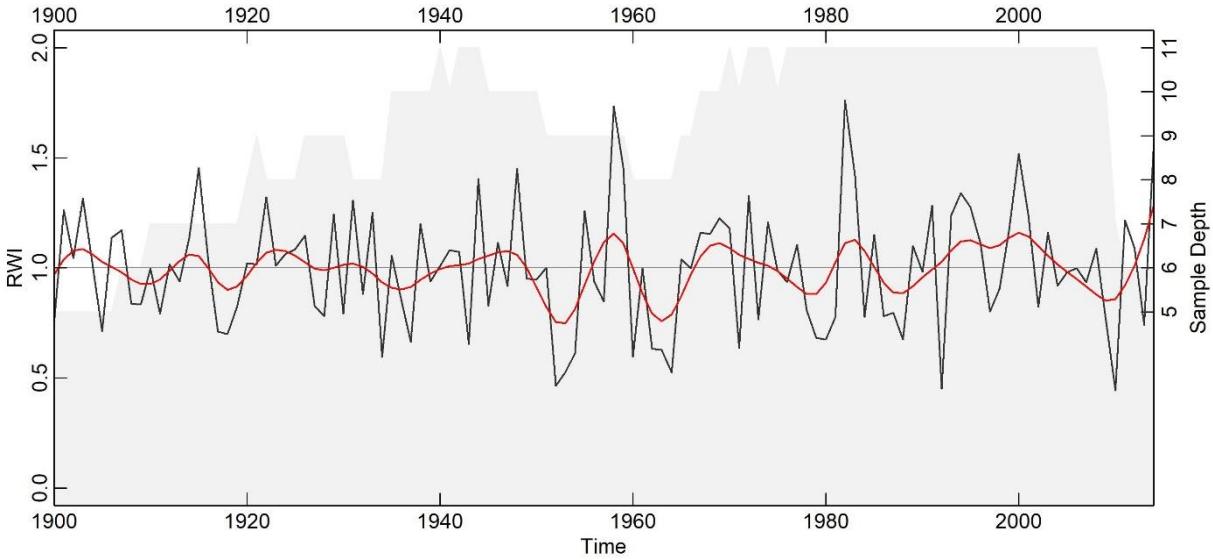

Figure 3 – Tree-ring chronologies (ring-width indices – RWI) of the Jaú National Park (JNP; upper panel) and b) the Uatumã Sustainable Development Reserve (USDR; lower panel). Indicated are the number of replicates (sample depth; grey area) and ten years smoothing spline (red curve).

Climate-growth relationships

The chronologies were correlated to climate variables and water level records only for the periods with the SSS >0.85 (JNP: 1927-1999; USDR: 1920-2006). At the JNP the chronology presented significant negative correlations with monthly river levels, especially in the period of rising water levels (April-May) for the period from 1930-84 (Figure 4). After this period the correlations with monthly water levels are evident for the low-water regime (September-November). The river level at the USDR was negatively correlated to tree growth for the period between 1939 and 1988 mainly for November (low water period) (figure 4). For the following periods, coinciding with the operation of the Balbina dam, we observed an opposite and non-significant relationship with the hydrological regime.

Correlations of tree growth with monthly precipitations did not show a conclusive pattern indicating significant negative relationships for February (rainy season) and July (dry season) in the periods 1930-1964 (JNP) and for September/October (dry season) in the period 1939-1973 and for February (rainy season) in the period 1954-1988 at the USDR. Positive correlations with monthly precipitation were observed for the period 1940-69 at the JNP in the transition from the wet to the dry season (June) and dry season (October) and at the USDR for the dry season (September and October) in the periods 1964-1993 and 1974-2003.

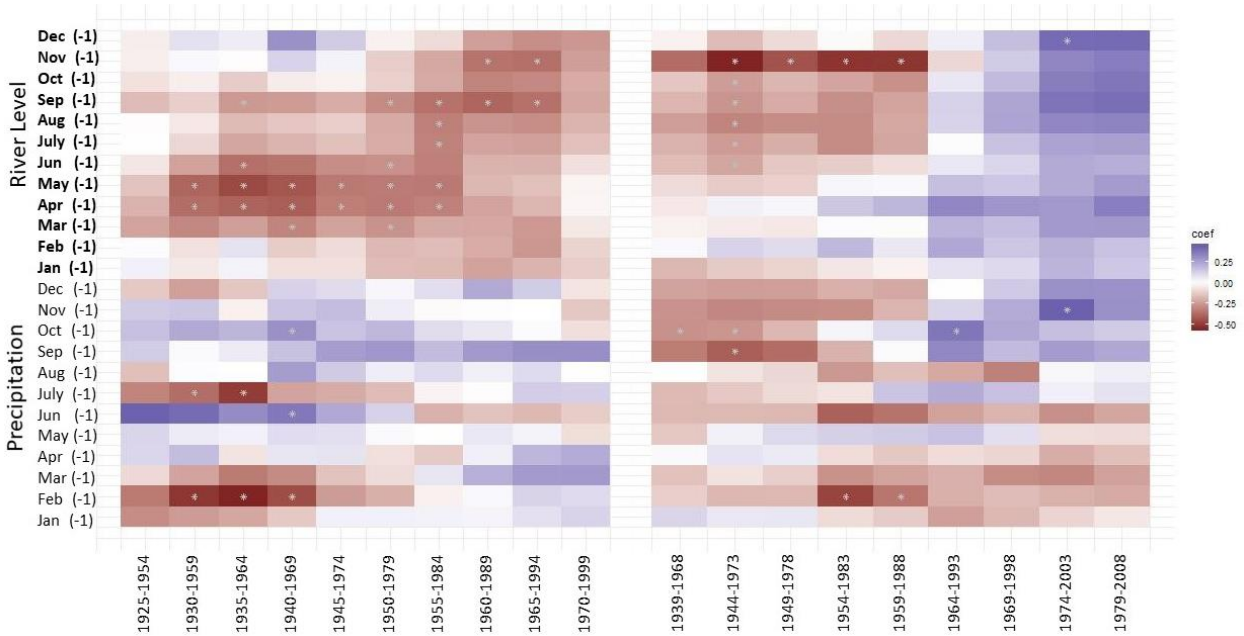

Figure 4 – Climate-growth relationships of Eschweilera tenuifolia (Lecythidaceae) with monthly water levels and precipitation (the (-1) means it corresponds to the previous year) at the Jaú National Park – JNP (left) and Uatumã Sustainable Development Reserve – USDR (right). For climate-growth relationships a period of 30 years was applied which was shifted along the chronology with an offset of five years. Only sections of the chronologies were considered with an SSS >0.85 (JNP: 1927-1999; USDR: 1920-2006; Figure S2).

The correlations with SST anomalies indicate for the JNP positive correlation along the Equatorial Pacific basin for the months November-January (1926-1982) (Figure 5). For the period of an intensified hydrological regime tree growth at the JNP showed powerful correlations with SST anomalies (April-June) of the tropical Atlantic (negative) and across the Pacific basin (positive) for the period 1983-2000. At the USDR the correlations with SST anomalies during the pre-dam period (1920-82) showed negative correlations with SST in the equatorial sections of the Pacific Ocean for the months April-June. This signal changed to the opposite for the post-dam period characterized by a modified hydrological regime as a consequence of the dam operation (1983-2006). During this period trees did only show positive correlations with the SST anomalies of the Equatorial Pacific in the central sections (Figure 5), opposite to the population growing at the JNP.

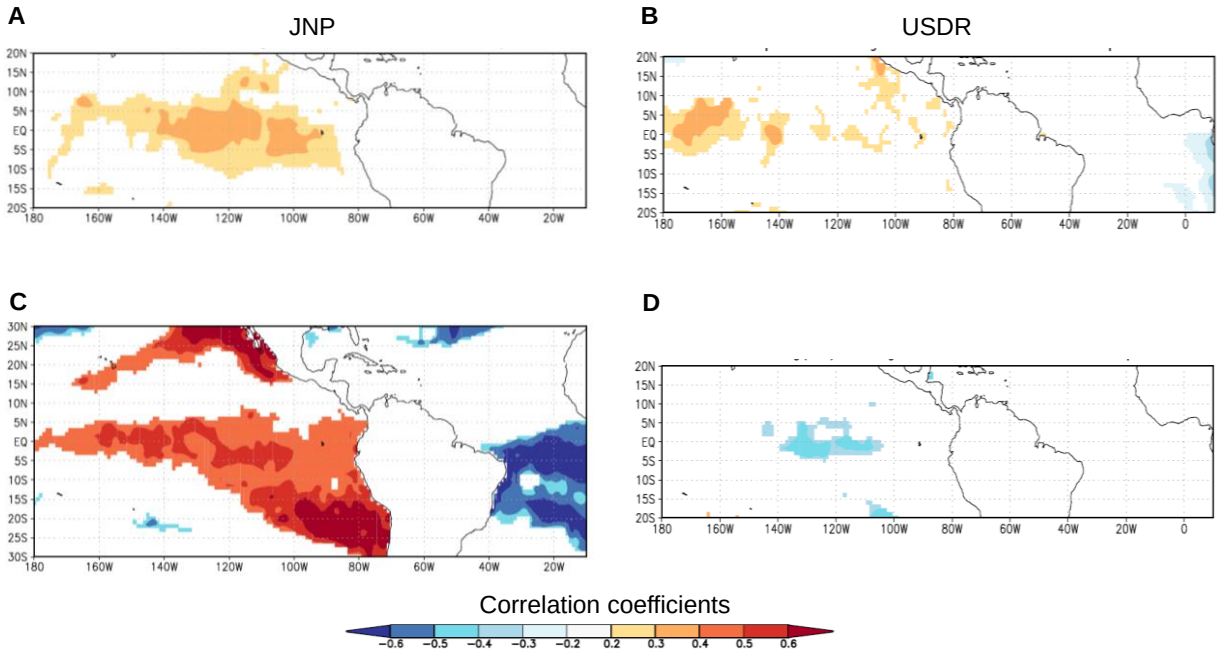

Figure 5 – Relationships of Eschweilera tenuifolia (Lecythidaceae) from the Jaú National Park – JNP (left panels) and Uatumã Sustainable Development Reserve – USDR (right panels) with sea surface temperature (SST) anomalies before the period of an intensified hydrological cycle: a) correlation map with SST anomalies from November (last year) to January for the period 1920-82 for the JNP chronology. And b) correlation map with SST anomalies from April to June for the period 1920-82 for the USDR chronology, and during the period of an intensified hydrological cycle for c) SST anomalies from April to June for the period 1983-2000 for the JNP chronology and b) SST anomalies from June to August for the period 1983-2006 for the USDR chronology.

Discussion

The radiocarbon analysis together with the evident climate signal, in the two robust chronologies, evidence that *E. tenuifolia* rings are certainly annual, however with frequently missing and false rings, common for tropical tree species (Brienen et al. 2016, Schöngart et al. 2017a). This makes it challenging to produce reliable, well-replicated and exactly dated tree-ring chronologies. Many samples are needed, and one may preferentially obtain some good quality stem discs to build a consistent chronology (Stahle 1999). Although we had more wood samples from the USDR, just 17 trees could be used (18% of the total) to build a chronology, but it was only possible because of two entire stem discs obtained from living trees where we could follow each ring across the transversal surface, identifying missing rings and excluding false ones. The crossdating of these two specimens was essential to start building up the tree-ring chronology for the USDR-site. For the JNP dataset, we could use more trees (46%) to build a chronology, although we had no stem discs of living trees. The difficulty of cross-dating tree-

ring series at the USDR is probably associated with the substantial disturbance of the hydrological regime which caused during consecutive years permanent flooding conditions and also altered the temporal occurrence of floods and droughts (Assahira et al. 2017). These observations corroborate with the results of radiocarbon dating, showing that dating of the USDR samples was more problematic (accuracy of 29%) than that of the JNP samples (accuracy of 80%).

The few studies already published in Southern America tropical forests found in general higher Rbars between 0.22 and 0.52 (Locosselli et al. 2016, López and Villalba 2016, Pereira et al. 2018, Granato-Souza et al. 2019) compared to this study. Most of these studies apply the EPS to evaluate the suitability and robustness of chronologies for climate correlations and reconstructions. We chose the SSS instead, once the functionality and the 0.85 thresholds, was originally proposed for this parameter by the same authors (Wigley et al. 1984) and the SSS was meant to show the predictive power at the subsample level (Buras 2017). Although we have a comparable low sample depth in our tree-ring chronologies of *E. tenuifolia,* the tree-ring statistics indicate that it is a reliable time series allowing the analysis of climate-growth relationships.

Climate-growth relationships of *E. tenuifolia* indicate a negative correlation with water levels (Figure 4). This climate-growth relationship is consistent with many other floodplain trees showing a negative correlation to the water level under the regular flood-pulse regime (Schöngart et al. 2002). The abrupt changes in the signal observed in the UDSR site is possibly related to the different disturbances which occurred during the construction (Neves et al. 2019) and operation (Assahira et al. 2017) of the Balbina hydroelectric power plant. During the period when the Uatumã River was first dammed for fill the lake, the water discharge in the sections downstream of the dam were heavily reduced (Fearnside 1990) and possibly tree growth of *E. tenuifolia* was favored by sporadic inundations that increased the water availability in the floodplains especially in the dry season, which is the growing season of floodplain trees (Worbes 1989, Schöngart et al. 2002). During the operation of the Balbina dam, starting in 1989, however, the increase of minimum water levels, especially in the period after the year 2000 (Assahira et al. 2017) caused the extinction of the terrestrial phase at macrohabitats dominated by *E. tenuifolia* species at the lowest topographies (Junk et al. 2015, Resende et al. 2019). This probably resulted in a loss of the climate-growth relationships with the hydrological regime, as trees of *E. tenuifolia* were subjected to long-lasting anoxic conditions.

The response of tree growth to the intensified hydrological regime is even more evident with the indicated spatial correlations with SST of the Pacific and Atlantic oceans. In the period before the intensification of the hydrological regimes, both chronologies show positive correlations with SST in the Equatorial Pacific indicating an enhanced tree growth during warm ENSO phases (El Niño conditions), as it was also shown for the floodplain species *Piranhea trifoliata* (Picrodendraceae) (Schöngart et al. 2004) and *Macrolobium acaciifolium* (Fabaceae) (Schöngart et al. 2005) in the Central Amazonian floodplains. With the intensification of the hydrological regime in the Amazon basin, trees growing in the undisturbed igapó site (JNP) indicate a much stronger relationship to SST in the Pacific basin (positive correlations) and also with the tropical Atlantic (negative correlations), which was not evident for the period before. This pattern reflects exactly the mechanisms leading to the enhanced frequency and magnitude of severe floods in the Central Amazon basin, caused by an intensified Walker circulation over the Amazon basin as a result of a warming tropical Atlantic and a simultaneously cooling of the Equatorial Pacific during the last three decades (Barichivich et al. 2018).

The intensification of the hydrological regime at the USDR, characterized by a steady decrease in the river flow during the Balbina dam construction (Fearnside 1990, Neves et al. 2019) and an increase of the annual minimum water levels during the operation period (especially after the year 2000) (Assahira et al. 2017, Resende et al. 2019) resulted into a weakening of the climate-growth relationships and to an even opposite signal, exposing the trees to a long-lasting terrestrial phases and afterward to even permanent flooding and consequently anoxic conditions. This dramatic change in the hydrological regime possibly created inverted growth conditions for *E. tenuifolia* enhancing the tree growth during the period of the Balbina dam construction and afterwards to a dramatic decline (chapter 3) as a consequence of the permanent flooding conditions resulting consequently into the observed mass mortality of this species (Resende et al. 2019).

Acknowledgments

We thank the Jaú National Park, the RDS Uatumã and ATTO project for the infrastructure and work support. The Brazilian Council for Scientific Research (CNPq) for financing the project and the PhD fellowship of AF Resende (MCTI/CNPq/FNDCT nº 68/2013 – Large-Scale Biosphere-Atmosphere Program in the Amazon – LBA), PELD-MAUA project

(403792/2012-6 – MCTI/CNPq/FAPs Nº 34/2012 and 441590/2016-0 – CNPq/CAPES/FAPS/BC-Fundo Newton). We must also thank for the support from IBAMA, SISbio, SISgen, ICMBio and DEMUC/SEMA, for the licenses for collecting and transporting samples. We also thank field work help of Reginaldo from Jaú, Victor Lery, Eduardo Rios, Alberto Peixoto, Josué from USDR, Sr. Domingos from USDR, Celso Rabelo, Jekiston (also for the samples), Anderson Reis, and Gildo Feitoza.

References

ANA, A.N. de Á. 2018. *HIDROWEB - Sistema de Informações Hidrológicas*. (http://www.snirh.gov.br/hidroweb/publico/medicoes_historicas_abas.jsf). Accessed on 10 May 2019.

Aragão, L.E.O.C.; Anderson, L.O.; Fonseca, M.G.; Rosan, T.M.; Vedovato, L.B.; Wagner, F.H.; et al. 2018. 21st Century drought-related fires counteract the decline of Amazon deforestation carbon emissions. *Nature Communications* 9: 1–12.

Assahira, C.; Resende, A.F. de; Trumbore, S.E.; Wittmann, F.; Cintra, B.B.L.; Batista, E.S.; et al. 2017. Tree mortality of a flood-adapted species in response of hydrographic changes caused by an Amazonian river dam. *Forest Ecology and Management* 396: 113–123.

Barichivich, J.; Gloor, E.; Peylin, P.; Brienen, R.J.W.; Schöngart, J.; Espinoza, J.C.; et al. 2018. Recent intensification of Amazon flooding extremes driven by strengthened Walker circulation. *Science Advances* 4: eaat8785.

Batista, E.S.; Schöngart, J. 2018. Dendroecology of Macrolobium acaciifolium (Fabaceae) in Central Amazonian floodplain forests. *Acta Amazonica* 48: 311–320.

Biondi, F.; Waikul, K. 2004. DENDROCLIM2002: A C++ program for statistical calibration of climate signals in tree-ring chronologies. *Computers and Geosciences*.

Brienen, R.J.W.; Schöngart, J.; Zuidema, P.A. 2016. Tree Rings in the Tropics: Insights into the Ecology and Climate Sensitivity of Tropical Trees. In: Springer, Cham, p.439–461.

Bronk Ramsey, C. 2016. Radiocarbon Calibration and Analysis of Stratigraphy: The OxCal Program. *Radiocarbon*.

Bunn, A.G. 2008. A dendrochronology program library in R (dplR). *Dendrochronologia* 26: 115–124.

Buras, A. 2017. A comment on the expressed population signal. *Dendrochronologia* 44: 130–132.

Cook, E.; Kairiukstis, L. 1990. *Methods of dendrochronology*. In: Cook, E.R.; Kairiukstis, L.A. (Eds.) Springer Netherlands, Dordrecht, .

Costa, M.H.; Coe, M.T.; Loup Guyot, J. 2013. Effects of Climatic Variability and Deforestation on Surface Water Regimes. *Amazonia and Global Change*: 543–553.

D'Arrigo, R.; Abram, N.; Ummenhofer, C.; Palmer, J.; Mudelsee, M. 2011. Reconstructed streamflow for Citarum River, Java, Indonesia: Linkages to tropical climate dynamics. *Climate Dynamics* 36: 451–462.

Fearnside, P.M. 1990. Balbina licoes tragicas na Amazonia. *Ciência Hoje*: 34–40.

Fichtler, E.; Worbes, M. 2012. Wood anatomical variables in tropical trees and their relation to site conditions and individual tree morphology. *IAWA Journal* 33: 119–140.

Forsberg, B.R.; Melack, J.M.; Dunne, T.; Barthem, R.B.; Goulding, M.; Paiva, R.C.D.; et al. 2017. *The potential impact of new Andean dams on Amazon fluvial ecosystems*. Vol. 12.1–35p.

Fritts, H.C. 1976. *Tree Rings and Climate.* .

FVA; IBAMA. 1998. Plano de Manejo do Parque Nacional do Jaú. : 258.

Gloor, M.; Brienen, R.J.W.; Galbraith, D.; Feldpausch, T.R.; Schöngart, J.; Guyot, J.L.; et al. 2013. Intensification of the Amazon hydrological cycle over the last two decades. *Geophysical Research Letters* 40: 1729–1733.

Gloor, M.; Barichivich, J.; Ziv, G.; Brienen, R.; Schöngart, J.; Peylin, P. 2015. Recent Amazon climate as background for possible ongoing Special Section : .

Granato-Souza, D.; Stahle, D.W.; Barbosa, A.C.; Feng, S.; Torbenson, M.C.A.; de Assis Pereira, G.; et al. 2018. Tree rings and rainfall in the equatorial Amazon. *Climate Dynamics* 0: 1–13.

Holmes, Richard, L. 1983. Computer-assisted Quality Control in Tree-ring Dating and Measurement. *Tree-Ring Bulletin* 43: 69–78.

Holmes, R.L. 1992. Program COFECHA: Version 3. *The University of Arizona, Tucson*.

Hua, Q.; Barbetti, M.; Rakowski, A.Z. 2013. Atmospheric Radiocarbon for the Period 1950–2010. *Radiocarbon* 55: 2059–2072.

Junk, W.J. 1989. *Flood tolerance and tree distribution in central Amazonian floodplains*. 47–64p.

Junk, W.J.; Wittmann, F.; Schöngart, J.; Piedade, M.T.F. 2015. A classification of the major habitats of Amazonian black-water river floodplains and a comparison with their white-water counterparts. *Wetlands Ecology and Management* 23: 677–693.

Junk, W.J.; Piedade, M.T.F.; Schöngart, J.; Cohn-Haft, M.; Adeney, J.M.; Wittmann, F. 2011. A classification of major naturally-occurring amazonian lowland wetlands. *Wetlands* 31: 623–640.

KNMI, C.E. 2019. *Climate Explorer: Starting point*. (https://climexp.knmi.nl/start.cgi). Accessed on 07 May 2019.

Locosselli, G.M.; Schöngart, J.; Ceccantini, G. 2016. Climate/growth relations and teleconnections for a Hymenaea courbaril (Leguminosae) population inhabiting the dry forest on karst. *Trees - Structure and Function* 30: 1127–1136.

López, L.; Villalba, R. 2016. An assessment of Schinopsis brasiliensis Engler (Anacardiacea) for dendroclimatological applications in the tropical Cerrado and Chaco forests, Bolivia. *Dendrochronologia* 40: 85–92.

Marengo, J.A.; Espinoza, J.C. 2016. Extreme seasonal droughts and floods in Amazonia: Causes, trends and impacts. *International Journal of Climatology* 36: 1033–1050.

Marengo, J.A.; Tomasella, J.; Alves, L.M.; Soares, W.R.; Rodriguez, D.A. 2011. The drought of 2010 in the context of historical droughts in the Amazon region. *Geophysical Research Letters* 38: 1–5.

Meade, R.H.; Rayol, J.M.J.M.J.M.; Da Conceic??o, S.C.; Natividade, J.R.G.J.R.G.J.R.G.; Conceicão, S.C.; Natividade, J.R.G.J.R.G.J.R.G. 1991. Backwater Effects in the Amazon River Basin of Brazil. *Environ Geol Water Sci* 18: 105–114.

Mori, S.A.; Prance, G.T. 1990. *Flora Neotropica Monograph 21 (II) Lecythidaceae - part II. The zygomorphic-flowered New World genera (Couroupita, Corythophora, Bertholletia, Couratari, Eschweilera & Lecythis)*. Vol. 70.1–376p.

Mumba, M.; Thompson, J.R. 2005. Hydrological and ecological impacts of dams on the Kafue Flats floodplain system, southern Zambia. *Physics and Chemistry of the Earth* 30: 442–447.

Neves, J.R.D.; Piedade, M.T.F.; Resende, A.F. de; Feitosa, Y.O.; Schöngart, J. 2019. Impact of climatic and hydrological disturbances on black-water floodplain forests in Central Amazonia Juliana. *Biotropica*.

Parolin, P.; De Simone, O.; Haase, K.; Waldhoff, D.; Rottenberger, S.; Kuhn, U.; et al. 2004. Central Amazonian Floodplain Forests: Tree Adaptations in a Pulsing System. *The Botanical Review* 70: 357–380.

Pereira, G. de A.; Barbosa, A.C.M.C.; Torbenson, M.C.A.; Stahle, D.W.W.W.W.W.; Souza, D.G. de; Santos, R.M. Dos; et al. 2018. The Climate Response of Cedrela Fissilis Annual

Ring Width in the Rio São Francisco Basin, Brazil . *Tree-Ring Research* 74: 162–171.

Piedade, M.T.F.; Schongart, J.; Wittmann, F.; Parolin, P.; Junk, W.J. 2013. Impactos ecológicos da inundação e seca na vegetação das áreas alagáveis amazônicas. *Eventos climáticos extremos na Amazônia: causas e conseqüências*: 405–457.

Prance, G.T. 1979. Notes on the Vegetation of Amazonia III. The Terminology of Amazonian Forest Types Subject to Inundation. *Brittonia* 31: 26.

R Core Team. 2018. R: A Language and Environment for Statistical Computing. .

Ramsey, C.B. 2001. Development of the Radiocarbon Calibration Program\. *Radiocarbon* 43: 355–363.

Rayner, N.A.; Parker, D.E.; Horton, E.B.; Folland, C.K.; Alexander, L. V.; Rowell, D.P. 2003. Global analyses of sea surface temperature, sea ice, and night marine air temperature since the late nineteenth century. *Journal of Geophysical Research* 108: 4407.

Resende, A.F. de; Schöngart, J.; Streher, A.S.; Ferreira-Ferreira, J.; Piedade, M.T.F.; Silva, T.S.F.; et al. 2019. Massive tree mortality from flood pulse disturbances in Amazonian floodplain forests: The collateral effects of hydropower production. *Science of The Total Environment* 659: 587–598.

RinnTech. 2011. TSAP-WIN 4.64. .

Schöngart, J.; Bräuning, A.; Barbosa, A.C.M.C.; Lisi, C.S.; de Oliveira, J.M. 2017. Dendroecological studies in the neotropics: history, status and future challenges. In: *Dendroecology*, Springer, p.35–73.

Schöngart, J.; Piedade, M.T.F.; Ludwigshausen, S.; Horna, V.; Worbes, M.; Schongart, J.; et al. 2002. Phenology and stem-growth periodicity of tree species in Amazonian floodplain forests. *Journal of Tropical Ecology* 18: 581–597.

Schöngart, J.; Junk, W.J.; Piedade, M.T.F.; Ayres, J.M.; Hüttermann, A.; Worbes, M. 2004. Teleconnection between tree growth in the Amazonian floodplains and the El Niño-Southern Oscillation effect. *Global Change Biology* 10: 683–692.

Schöngart, J.; Piedade, M.T.F.; Wittmann, F.; Junk, W.J.; Worbes, M.; Piedade, T.F. 2005. Wood growth patterns of Macrolobium acaciifolium (Benth.) Benth. (Fabaceae) in Amazonian black-water and white-water floodplain forests. *Oecologia* 145: 454–461.

Schweingruber, F.H. 1996. Principles of Dendrochronology. .

De Simone, O.; Müller, E.; Junk, W.J.; Schmidt, W. 2002. Adaptations of Central Amazon tree species to prolonged flooding: Root morphology and leaf longevity. *Plant Biology* 4: 515–522.

Sioli, H. 1984. The Amazon and its main affluents: Hydrography, morphology of the river courses, and river types. : 127–165.

Stahle, D.W. 1999. Useful strategies for the development of tropical tree-ring chronologies. *IAWA Journal* 20: 249–253.

Steinhof, A. 2013. Data Analysis at the jena 14C Laboratory. *Proceedings of the 21st International Radiocarbon Conference* 55: 282–293.

Steinhof, A.; Altenburg, M.; Machts, H. 2017. Sample Preparation at the Jena 14C Laboratory. *Radiocarbon* 59: 815–830.

Steinhof, A.; Adamiec, G.; Gleixner, G.; Klinken, J. van; Wagner, T. 2004. THE NEW 14C ANALYSIS LABORATORY IN JENA, GERMANY. *Arizona Board of Regents on behalf of the University of Arizona* 46: 51–58.

Timpe, K.; Kaplan, D. 2017. The changing hydrology of a dammed Amazon. *Science Advances* 3: 1–14.

Tomasella, J.; Pinho, P.F.; Borma, L.S.; Marengo, J.A.; Nobre, C.A.; Bittencourt, O.R.F.O.; et al. 2013. The droughts of 1997 and 2005 in Amazonia: Floodplain hydrology and its potential ecological and human impacts. *Climatic Change* 116: 723–746.

Trouet, V.; Van Oldenborgh, G.J. 2013. KNMI Climate Explorer: A Web-Based Research Tool for High-Resolution Paleoclimatology. *Tree-Ring Research* 69: 3–13.

Wigley, T.M.L.; Briffa, K.R.; Jones, P.D. 1984. On the Average Value of Correlated Time Series, with Applications in Dendroclimatology and Hydrometeorology. *Journal of Climate and Applied Meteorology* 23: 201–213.

Wittmann, F.; Junk, W.J. 2017. The Wetland Book. : 1–20.

Worbes, M. 1989. Growth Rings, Increment and Age of Trees in Inundation Forests, Savannas and a Mountain Forest in the Neotropics. *IAWA Journal* 10: 109–122.

Worbes, M.; Klinge, H.; Revilla, J.D.J.D.; Martius, C. 1992. On the dynamics, floristic subdivision and geographical distribution of várzea forests in Central Amazonia. *Journal of Vegetation Science* 3: 553–564.

World Bank, C.C. 2019. *World Bank Climate Change Knowledge Portal | for global climate data and information!*. (https://climateknowledgeportal.worldbank.org/
country/brazil/climate-data-historical). Accessed on 07 May 2019.

Zang, C.; Biondi, F. 2015. Treeclim: An R package for the numerical calibration of proxy-climate relationships. *Ecography* 38: 431–436.

Supplementary material

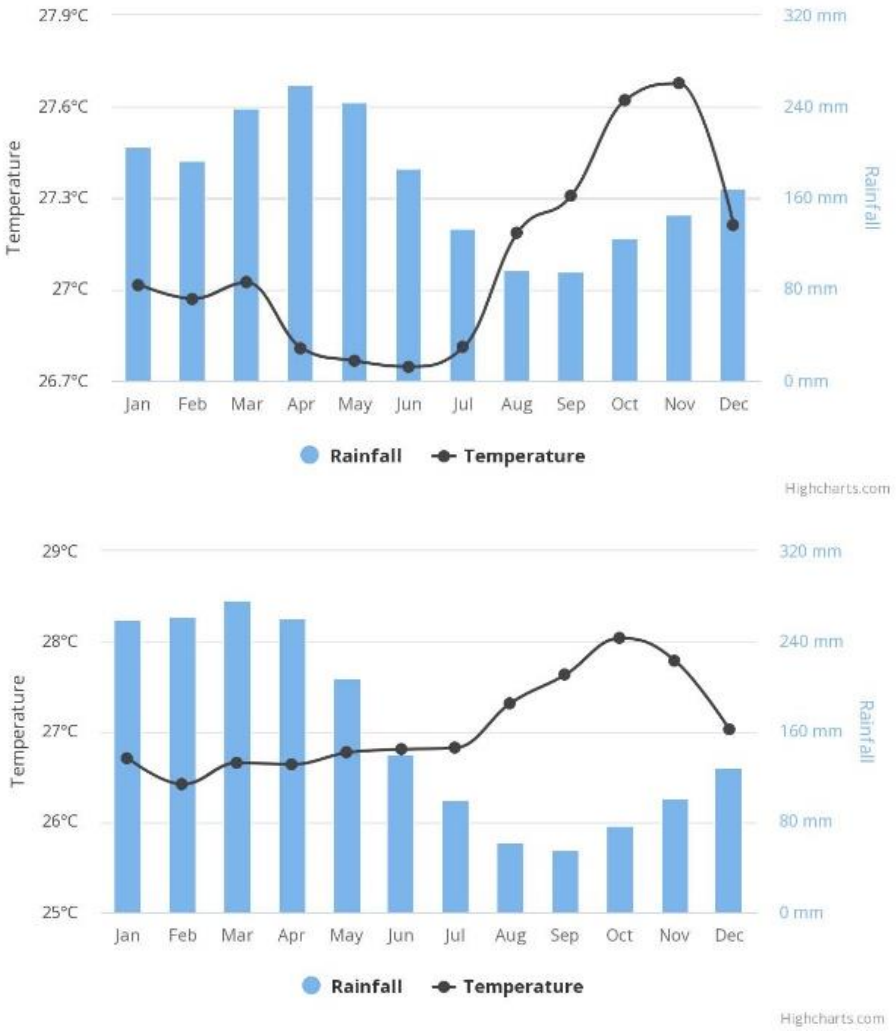

Figure S1 – Monthly temperature and precipitation (1901-2016) at the Jaú National Park (top) and Uatumã Sustainable Development Reserve (bottom) (data: (World Bank 2019)*).*

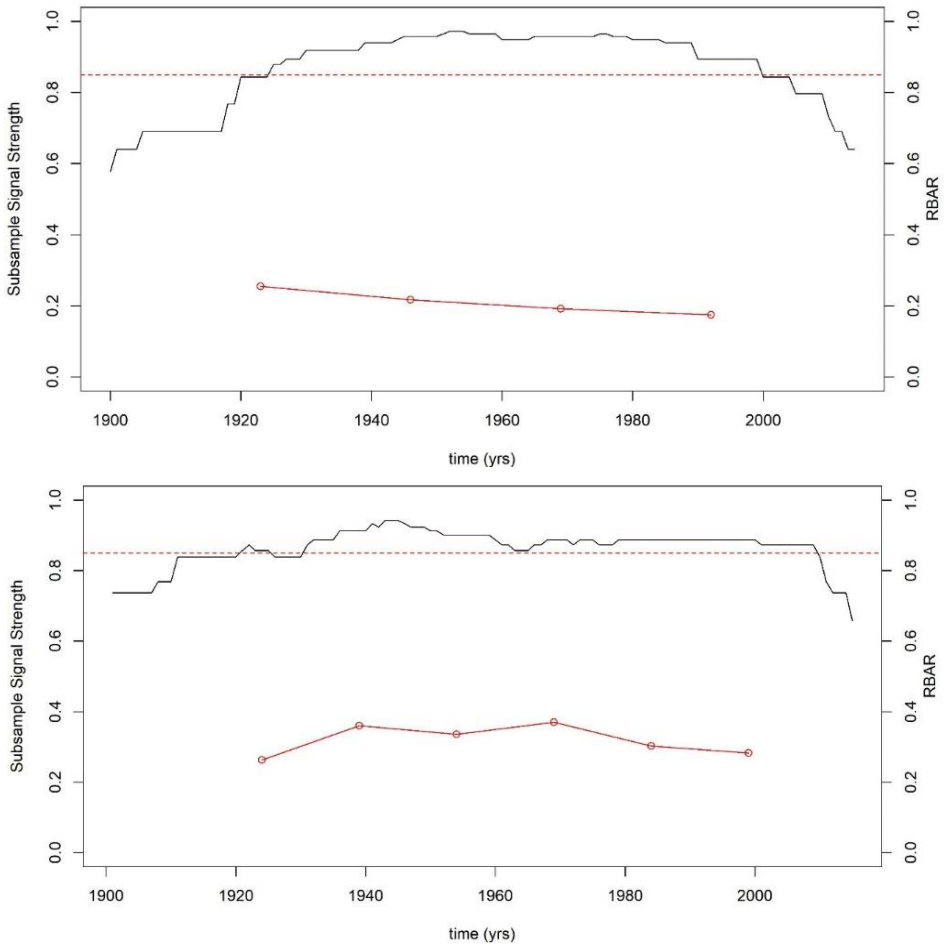

Figure S2 – Running SSS (black line) and Rbar (red line) for the tree-ring chronologies from Eschweilera tenuifolia trees from the Jaú National Park (JNP) and Uatumã Sustainable Development reserve (USDR) (bottom).

Table S1 – Tree ring ^{14}C dating results from Eschweilera tenuifolia trees from the Jaú National Park (JNP) and Uatumã Sustainable Development reserve (USDR). Calendar dating using Oxcal v3.4 (Bomb 13 SH 3).

Study Area	*Sample code*	*Postulated period*	*^{14}C cal. date*	*Prob. (%)*	*Min. Difference*
JNP	61A	1972	1971-1972	89.7	0
JNP	50A	2008-2010	2004-2008	90.1	0
JNP	53A	2008	2007-2011	93.2	0
JNP	49A	2007	2007-2011	93.5	0
JNP	46A	2010	2007-2009	85.4	-1
USDR	130A	1984	1988-1991	76.8	4
USDR	151A	1987	1983-1985	72.4	-2
USDR	130A2	1974	1973-1974	84.5	0
USDR	132A	1978-1980	1973-1975	88.5	-3
USDR	150B	1992	1976-1978	91.9	-4
SDR	151B	1978-1980	1977-1979	95.4	0
USDR	170B	1981	1977-1980	93.6	-1
USDR	165A	1971-1975	1980-1982	69.8	5
USDR	162B	1989	1990-1992	95.4	1

Capítulo 3

Resende, A. F.; Feitosa, Y. O.; Andrade, V. H. F.; Piedade, M. T. F.; Trumbore, S. E.; Durgante, F. M. and Schöngart, J. **Flood-pulse disturbances as a threat for long-living Amazonian trees**. *Global Change Biology* (in preparation)

Flood-pulse disturbances as a threat for long-living Amazonian trees

Angélica Faria de Resende, Yuri Oliveira Feitosa, Victor Hugo Ferreira Andrade, Maria Teresa Fernandez Piedade, Susan Trumbore, Flávia Machado Durgante and Jochen Schöngart

Abstract

The long-living tree species *Eschweilera tenuifolia* (O. Berg) Miers (Lecythidaceae) was chosen to study the impact caused by natural and anthropogenic hydrological disturbances. This species is endemic to oligotrophic floodplain forests (*igapó*), occurring preferentially in high-flooded areas, where it forms monodominant stands. *E. tenuifolia* is among the best-adapted tree species in this nutrient-poor and stressful environment where it tolerates inundation periods of over ten months per year. We aimed to understand why populations of *E. tenuifolia* had died in disturbed *igapó* forests at the Uatumã Sustainable Development Reserve (USDR) due to the Balbina hydroelectric power plant, implemented in the 1980s, causing hydrological disturbances downstream of the dam. In a second study area without anthropogenic (land-use) changes, the Jaú National Park (JNP), we studied growth and mortality patterns in *igapó* forests. We analyzed a total of 91 individuals (62 living and 29 dead) at the USDR and 52 trees (31 living and 21 dead) at the JNP. Structural (diameter at breast height - DBH, flood height) and ecological variables (age, mean annual diameter increment - MDI) were sampled to understand their characteristics during the species' lifespan. Therefore, we analyzed age-diameter relationships. mean passage time through 5-cm diameter classes, growth change patterns, growth ratios, MDI clustering and ratios among the living and dead trees. We also dated the death of each individual using ^{14}C dating, and cautiously examined the cause of death for each one by considering growth decay just before the death year and relating the causes to climatic or anthropogenic disturbances. Our results showed similar structural parameters for both studied populations. The MDI was 2.04 ± 0.39 mm at JNP and 2.28 ± 0.69 mm at USDR with estimated maximum ages of 466 years (JNP) and 498 years (USDR), except for one single tree of 175 cm in DBH at the USDR with an estimated age of 820 yrs. Living trees from JNP showed distinct growth changes after 1975, an exceptional hydrological event with several consecutive

years of flooding as a consequence of high annual minimum water levels. At the USDR the distinctness of changing growth patterns was observed after 1983, the exact year when the Balbina dam construction began. The cause of death for individuals from the USDR was the hydrological disturbance caused by the installation of the Balbina power plant, with 93% of mortality occurring after the beginning of the dam cooperation, mainly between 1990 and 2000. At the JNP trees died in different periods, probably due to different extreme hydrological events or even natural senescence. The flood-adapted tree species *Eschweilera tenuifolia* is highly sensitive to both, long-lasting dry and wet periods caused by climatic or anthropogenic extreme events. The flood-pulse alteration, even more than 30 years after the disturbance continues interfering in both mortality and growth of the species which can potentially cause regional extinction of this well-adapted and endemic species, especially at the disturbed site.

Key-words: *Eschweilera tenuifolia*, ^{14}C dating, hydrological disturbance, extreme climatic events, hydroelectric dam, Balbina.

Introduction

The flood-pulse function of many rivers from the biggest hydro basin in the world is threatened by a combination of an increase in the occurrence and frequency of extreme climate events (Barichivich et al. 2018), and a growing occupation pressure over the Amazon Forest (Davidson et al. 2012, Nobre et al. 2016). Unprecedented land-use changes in the Brazilian Amazon inevitably brings the need for more hydroelectric power plants, which directly affects the water regime. Big Amazonian rivers have associated floodplain forests that depend on the flood-pulse equilibrium. For accessing the relation of the flood-pulse disturbances and the growth and death of floodplain trees, we used dendroecological tools and radiocarbon dating to study the species *Eschweilera tenuifolia* growing at the same macrohabitat under natural and disturbed igapós.

The black-water *igapós*, are acidic, sediment-poor Amazonian forested floodplains, which occur along rivers and comprise over 140,000 km^2 of the Amazon basin (Melack and Hess 2010, Junk et al. 2015). *Igapó* forests are older and geomorphologically more stable environments than the dynamic *várzea* along the sediment-loaded white-water rivers (Prance 1980, Sioli 1984, Furch 1997), as well as being more defiant for trees to overcome the imposed nutrient deficit. Both floodplain types are subject to the flood-pulse (Junk et al. 1989), the annual river levels oscillation, that can last from a couple of days to more than ten months, depending on the topographic level of each floodplain macrohabitat. Monodominant and opened stands of *Eschweilera tenuifolia* with a low inter-tree competition establish on clayish substrates of the low-lying positions of the topography, the most inundated environment colonized by trees in these floodplains (Junk et al. 2015, 2018).

To tolerate the monomodal flood-pulse, floodplain tree species have developed specific anatomical, morphological, physiological and biochemical adaptations that allow them to survive low oxygen availability (Parolin et al. 2004, Parolin 2009, Piedade et al. 2010). A set of different adaptations can be found usually acting in combination, among them the production of phytohormones such as ethylene, directly linked to root elongation, aerenchyma and lenticels formation, stem hypertrophy and adventitious root expansion (Jackson 1990, Armstrong and Drew 2002, Voesenek et al. 2003, Crawford and Braendle 2007, Parolin 2009, Sauter 2013). The adaptations are due to the evolutionary pressure triggered by the flood-pulse over millions of years (Junk 1989).

The anoxic conditions induced by the annual flood-pulse lead to a decrease in diameter increment and a cambial dormancy during the high-water period resulting in the formation of annual tree rings (Worbes 1989, Schöngart et al. 2002). Dendroclimatological studies indicate that ring width is correlated with the duration of the non-flooded period (Schöngart et al. 2004, 2005, Batista and Schöngart 2018). However, *igapó* species growth slower than *várzea* species because of the oligotrophic conditions of soil and water (Worbes 1997, Schöngart et al. 2005, Da Fonseca Júnior et al. 2009, Rosa et al. 2017). By using tree-rings analysis, it is possible to understand the ecology of trees as well as to detect disturbance events in the past, such as extreme temperatures, rainfall, fires, insect attacks, severe droughts, floods, among others factors (Cook and Kairiukstis 1990, Schweingruber 1996, Baker et al. 2005, Speer 2009)

In the Amazon region, severe droughts and floods are not a recent phenomenon, they have also been registered in the past (Marengo et al. 2016, Granato-Souza et al. 2019). During the last three recent decades, however, an intensification of extreme hydroclimatic events has been observed, especially of extreme flood events (Gloor et al. 2013, Marengo and Espinoza 2016, Barichivich et al. 2018). The causes for hydroclimatic extreme events (droughts and floods) are the El Niño-Southern Oscillation (ENSO) originating from the Equatorial Pacific and the Meridional Mode across the tropical Atlantic ocean determining the position of the Intertropical Convergence Zone (ITCZ) (Nobre et al. 2013). Since climate and hydrology are the foremost drivers of wetlands formation, the recent intensification of both parameters is probably affecting the floodplain forests, especially the most flood-adapted tree species *E. tenuifolia.*

Also, anthropic pressures from governments, multinational companies, and even big landowners, who consider this region "not well-developed" are a growing vector of disturbances in the Amazon basin. Hydroelectric power plants, mining, deforestation for livestock, and soy production are occupying or threatening large areas and interfering in the hydrological cycle as well as in the carbon balance (Fearnside 2005, 2015a, Malhi et al. 2008, Davidson et al. 2012, Castello et al. 2013, Nobre et al. 2016, Lovejoy and Nobre 2018, Artaxo 2019). With respect to hydroelectric power plants, the flood-pulse loss by damming affects the riparian ecosystems downstream of the dam (Ligon et al. 1995, Lobo et al. 2019, Neves et al. 2019), and causes massive tree mortality (Assahira et al. 2017, Resende et al. 2019) and destruction of other environmental components such as the aquatic fauna (Lees et al. 2016). The many extant and more than 280 planned hydroelectric dams in Amazonia (Castello and Macedo 2015b, Forsberg et al. 2017, Latrubesse et al. 2017, Timpe and Kaplan 2017, Anderson

et al. 2018) pose a severe threat, depleting the ecosystems upstream and causing downstream disturbances over long distances in floodplain forests, leading to losses of macrohabitats and ecosystem services (Junk et al. 2018, Resende et al. 2019).

Eschweilera tenuifolia is highly dependent on a regular flood-pulse, and therefore it is prone to suffer from both anthropogenic and climatic disturbances (Junk et al. 2015, Resende et al. 2019) especially at the edge of forest establishment. We selected *E. tenuifolia* to analyze growth patterns and then elucidate the mechanisms leading to different levels of mortality of this key species. To do so we analyzed the effects of different magnitudes of hydrological alterations in the species' growth and survival by comparing an *igapó* site without anthropogenic impacts (Jaú River at the Jaú National Park - JNP), and another along the *igapós* of the Uatumã Sustainable Development Reserve (USDR) suffering strong downstream disturbances caused by the hydroelectric power plant Balbina established in the Uatumã River in the 1980s (Assahira et al. 2017). The main questions of this study are: (1) How are diameter growth rates of *E. tenuifolia* under undisturbed conditions? (2) How varies the secondary growth of this species under disturbance regimes? (3) When, how and why trees from both areas died? Moreover, for the USDR area: (4) Is the regularity of the flood-pulse loss still affecting living trees even more than 30 years after the dam implementation? (5) Is the tree growth dissimilar in comparison with the period before the dam? Furthermore, for the JNP area: (6) is it possible to notice differences in the secondary growth for the period after the intensification of the Amazonian hydrological cycle?

Methods

The study species Eschweilera tenuifolia (O. Berg) Miers

Eschweilera tenuifolia belongs to the nut family Lecythidaceae and is commonly known as *macacarecuia* (*macaco* means monkey while *cuia* means gourd, in Brazilian Portuguese) or *cuieira*. The genus *Eschweilera* is biggest among the Lecythidaceae family, occurring in the most diverse tropical environments. The species *E. tenuifolia* is the only one in the section *Jugastrum* (*E. parvifolia* clade) (Huang et al. 2015) because despite having a standard flower typical of *Eschweilera* it lacks a flower pedicel, has unique wedge-shaped seeds, the aril is absent, there is a corky seed coat, and seed germination is lateral. The fruit is bowl-shaped

(*cuia*), and mature trees are about 15 to 20 meters tall with diameters of up to two meters (Mori and Prance 1990, Huang et al. 2015). Despite the hard-shelled fruits, the seeds are consumed mainly by birds and fishes during the aquatic phase (Maia and Piedade 2000) and birds, monkeys, and other terrestrial animals in the terrestrial phase, when is possible to access the trees by land (Barnett et al. 2002, 2005, 2013). Leaves and flowers are also consumed when fruits and seeds are scarce (Barnett et al. 2013). The fruits and seeds present sophisticated dispersion adaptations, such as a porous layer and water-repellency that make them buoyant (Kubitzki and Ziburski 1994). Peak leaf abscission is during the high water and insolation period, from June to August, while the peak production of new leaves is between August and September (Maia and Piedade 2000) when the water level is decreasing and the growing period starts for floodplain trees (Schöngart et al. 2002). Flowers and fruits are produced after the new leaves, as it has been described for trees along the Tarumã-mirim River in Central Amazonia (Maia and Piedade 2000), a Negro River sub-basin where the flooding pattern is similar to our study areas.

Another relevant observation is that *E. tenuifolia* also occurs in macrohabitats characterized by mixed forests with high interspecific competition for resources at low topographies in the *igapó* (main river tributaries) (Figure S1). However, it is common to find *E. tenuifolia* as a monodominant or even monospecific species spread along with the lowest level of the floodplain (up to 10 months of flooding), mainly in lakes (Ferreira and Prance 1998, Junk et al. 2015) with low inter-tree competition (Schöngart et al. 2017*a*) (Figure S2). Trees of this species are well adapted to these harsh environment (Junk et al. 2015). This species is very abundant throughout the entire Amazon and Orinoco basins (Mori and Prance 1990, Ferreira and Prance 1998) and forms monodominant stands in lakes and also occurs along the main river and its tributaries (Ferreira and Stohlgren 1999, Junk et al. 2015). The wood of the species is dense (0.77 g cm^3) (Parolin and Ferreira 1998, Parolin and Worbes 2015) and larger individuals always present hollows, degraded tree crowns, longitudinally twisted stems and bark-covered knots which is typical for ancient trees (Schöngart et al. 2017*a*). Therefore *E. tenuifolia* is an interesting bioindicator to be used to indicate environmental disasters that occurred in the past by means of dendrochronological studies.

Study areas

Jaú National Park

The Jaú National Park (JNP) was created in 1980 to promote the preservation of existing ecosystems. It is currently considered as a World Natural Heritage Site and Biosphere Reserve by the United Nations Educational, Scientific and Cultural Organization - UNESCO (Figure 1). Today it is managed by the Chico Mendes Institute for Biodiversity Conservation - ICMBio. The 2,272,000 ha park is in the state of Amazonas and has an annual average temperature about 26.5º C, and the average annual rainfall varies around 2,153 mm (for the period 1901-2015, CRU data from World Bank?? 2019).

The Jaú River is one of the main tributaries of the Negro River and is characterized by blackish, acidic and nutrient-poor water which seasonally floods the *igapós* (Ferreira 2000b). The Jaú annual river level oscillation is mostly affected by the backwater effect of the Negro River. In addition to the *igapós*, the conservation unit also consists of upland forests (*terra firme*), white-sand forest ecosystems (*campinarana*) and poorly-drained permanently flooded areas (*chavascais*), forming a mosaic of landscapes due to its varied geological composition and soil drainage (FVA and IBAMA 1998). The JNP is not considered to have been impacted by anthropic activities, since the few groups of residents that live inside the conservation unit use its resources only for subsistence, without causing significant impacts to the local ecosystem (FVA and IBAMA 1998).

Uatumã Sustainable Development Reserve

The Uatumã Sustainable Development Reserve (USDR) was created in 2004, comprises 424,430 ha and is located in Amazonas State about 150 km northeast from its capital Manaus (IDESAM 2009), downstream of the Balbina Hydroelectric Power Plant (2º14 'S, 58º29' W) (Figure 1). The Uatumã River had its hydrological cycle altered by the installation of the Balbina dam since 1983 (Assahira et al., 2017). There are different forest ecosystems in this conservation unit such as upland forests (*terra firme*), floodplain forests (*igapó*) as well as opened (*campina*) and closed (*campinarana*) white-sand ecosystems. The average annual temperature is around 27º C, and the mean total rainfall is 1,982 mm (for the period 1901-2015, CRU data from World Bank?? 2019).

The USDR represents an environment that has been modified by human activities, and this is characterized by the damming of the Uatumã River by the implementation of the Balbina dam (1983-87). The regime of opening and closing of the floodgates according to power generation needs means that the annual flood-pulse that occurred there naturally no longer exists in a regular and predictable pattern. The change in annual maximum and minimum levels has resulted in a decrease in annual amplitude and caused an increase in the duration of the aquatic phase and the flooding of low floodplain topographies for consecutive years, causing the mortality of adapted tree species such as *Macrolobium acaciifolium* (Assahira et al. 2017) and *E. tenuifolia* (Resende et al. 2019).

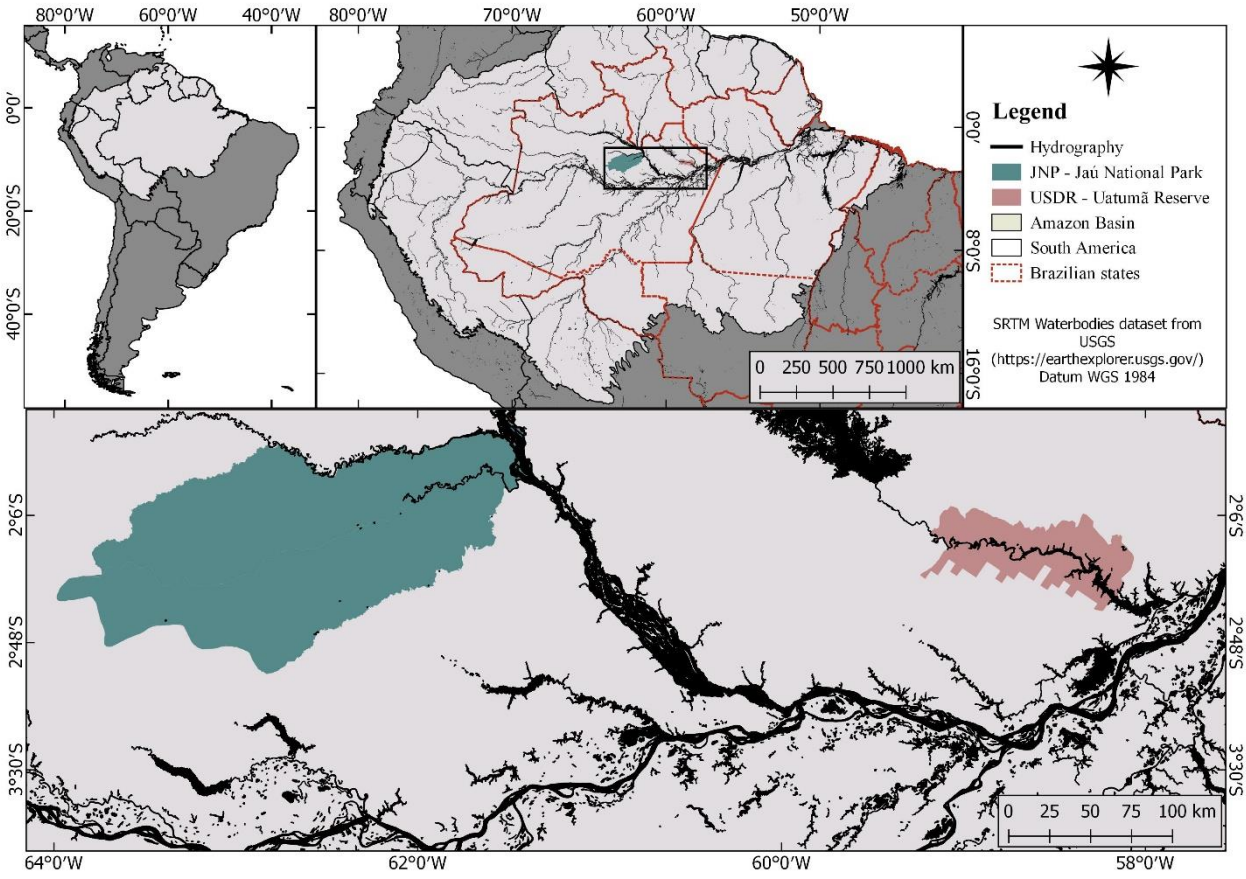

Figure 1 - Map showing the location of both study areas in the Jaú National Park (JNP; green) and the Uatumã Sustainable Development Reserve (USDR; pink).

Data collection in the field

A total of 93 living trees (31 at JNP and 62 at USDR) were sampled along the Jaú and Uatumã rivers, respectively, with different diameters at breast height (DBH) (from 10 to 120

cm, except for one individual with 175 cm at USDR) to consider possible ontogenetic effects on tree growth (Bowman et al. 2013) (licenses 51133-1/2015 and 61/2015 - 28/2018 from SISBio and DEMUC/SEMA, respectively). The inundation level and environmental data were also collected for the lakes and/or tributaries, and the GPS points for each tree. Two cores were sampled per individual (total of 240 cores) using an increment borer of 5 mm internal diameter (except for additional stem discs from two trees of the USDR). Additionally, we sampled cross sections from 21 dead trees in JNP and 29 in USDR using a chainsaw. Almost all the samples were collected with the cambium present (the bark of this species is easily detached and lost because of its fibrous inner bark, locally named *envira*) or at least with sapwood to ensure the preservation of the last ring (or close to it). Only two dead trees were collected with bark (JNP). The same set of data was collected for the dead and living trees. Most of our samples came from lakes; no dead trees were sampled along tributaries, only some living ones (13 from JNP and 12 from USDR). Most of the sampling occurred during the terrestrial phase (September to December) of 2015, some dead trees were sampled at the USDR in 2016 and two stem discs of living trees in 2018 (USDR).

The samples were deposited at the Dendroecological Laboratory of the National Institute for Amazon Research (INPA), where they were carefully glued on appropriate wooden supports and sanded with 1200 grit sandpaper to enable the microscopical analysis of the growth rings, characterized by an alternation of fiber and parenchyma bands. The first step of this analysis comprised the delimitation of growth rings under a LEICA MS5 microscope, when all the tree rings were marked using an extra fine-tip pencil. In a second step, ring width was measured to the nearest 0.01 mm using a with HD camera coupled to a digital measuring device (LINTAB) connected to a computer-supported with the software Time Series Analyzes and Presentation (TSAP-Win) which creates ring-width time series simultaneously to its measurement. Since the formation of growth rings in the Central Amazonian floodplains occurs during the growing season initiating in the second half of the year and finishing during the first half of the following year (Schöngart et al. 2002), we conventionally attribute the calendar year of latewood formation to the tree ring (for example, the growth ring formed in the period 1982/83 is associated to the calendar year 1983).

Dendroecological analyses

Diameter growth models and age estimates of hollow trees

Many of the *E. tenuifolia* trees presented hollows which age cannot be inferred by dating techniques. Therefore we estimate the age of hollow trees by age-diameter relationships of non-hollow trees. First, we estimated the diameter of the hollow by the difference between the DBH measured in the field and length of the analyzed cores. In the second step we used non-linear growth models based on the site-specific population trajectory. Based on this relationship we interfered the age of the hollow part of the tree by its diameter (Figure S3). We found the sigmoidal as the best-adjusted model (Schöngart 2008), having well-distributed residuals (Beissner et al. 2002, R Core Team 2018). After adjusting the model, we used the three generated coefficients in the following model:

$$DBH = a/ (1+ (b/age)^{c}) \quad \text{Eq. 1}$$

Where DBH is the cumulative diameter for the given year, age the respective age at the given year and *a*, *b*, and *c* are the model parameters.

For living non-hollow trees, the field DBH was maintained, and for those without bark, we added to the field DBH the value of 2.35 cm (SD = 1.21 cm), which was the mean bark thickness calculated using trees with bark and pith (no hollow); the value was fixed, because there was no correlation between DBH and bark thickness. No trunks with large deformations or buttresses were observed at 1.3 m height of the sampled individuals. Therefore, it was not necessary to correct the DBH. Differences due to eccentricity of the pith were reduced using the average of two to four rays for each individual (Figure S3). Only for one individual from USDR, we were not able to model the hollow DBH, because of its large DBH of 175 cm from which 145 cm were hollow, and we had no other individual with the DBH larger than 93 cm for the site. For this single tree, we just used linear modeling passing through the pith to estimate its age (model DBH = Age*x).

The tree rings were measured in order to calculate the mean annual diameter increment (MDI) per individual. Average and standard deviation of MDI, DBH, and age for each area were calculated to observe the differences (*t*-test significance levels) between the same species

growing in natural and disturbed environments. Those measurements were obtained directly from the samples while the age had to be estimated for several individuals.

Mean passage time of diameter growth rates

To understand growth patterns over the life-span, we defined 5-cm diameter classes for the growth rate modeling. Deriving from the individual cumulative diameter growth curve we calculated mean and standard deviation of the mean passage time for each 5-cm size class. To avoid underestimates of the time per class, incomplete 5-cm classes were discounted. For instance, if a tree was hollow and the hollow DBH is 2.3 cm, and the tree's external DHB is 17.4 cm, there will be just two complete classes of 5-10 cm and 10-15 cm (Figure S4).

Suppression and liberation events and the growth decay before death

We analyzed every individual growth trajectory by using the growth change approach (Brienen and Zuidema 2006, Brienen et al. 2010). This method has been proposed for studying canopy attainment or light limitations in competitive environments such as tropical upland forests. We searched for past liberation and suppression patterns in *E. tenuifolia* trees in both macrohabitats, the open monodominant formation and closed mixed forests, where the principal causes of suppression and release events could be associated to pluriannual severe hydroclimatic events (monodominant formation on lowest topographies in lakes) and/or competition for lights (closed forests on low topographies along small tributaries). Especially in the USDR, we expected distinct changes in tree growth due to the massive disturbance of the hydrological cycle caused by the operation of the hydroelectric dam (Assahira et al. 2017). Growth change analysis is performed for each individual tree transforming the raw tree-ring data into growth changes (expressed in percentage; *%GCi*) based on the difference between the mean increment of the subsequent ten years (*M2*) and the previous ten years (*M1* which includes the central year *i*), divided again by the mean of the last ten years (*M1*), as suggested by Nowacki and Abrams (1997):

$$\%GCi = [(M2-M1)/M1] \times 100 \qquad \text{Eq. 2}$$

To define release and suppression events, we established thresholds of $\%GC \geq 100\%$ and ≤-50% over at least five consecutive years, respectively (Brienen et al. 2010, Schöngart et al. 2015). The number of trees presenting liberation and suppression events were calculated for each area, considering the tree status (living or dead) and macrohabitat (lake or tributary).

To understand the "*causa mortis*" of the dead trees, we examined the last formed tree rings to account for the "in decay" years. The decay was calculated based on the methodology proposed by Cailleret et al. (2017), where the growth ratio (g_r) between the increment in a given year for a dead and the mean increment of living trees of the population at the same DBH is obtained. A value of $g_r \leq 1$ is considered a mortality pattern when it occurred immediately before death. The duration of the decay pattern is obtained based on the number of consecutive years before death with $g_r \leq 1$.

Periodical diameter growth performance

The general dissimilarity coefficient of Gower (Gower 1971) was used to calculate the dissimilarity between the years using raw tree-ring widths per area. The dissimilarity index of Gower allows the use of missing values, proper for tree-ring widths analysis, once there are samples with different lengths (number of rings). Based on the dissimilarity matrix a restricted hierarchical grouping (Constrained Incremental Sums of Squares - CONISS) was performed with restricted clusters in order of the years (Gordon and Birks 1972).

To access the diameter increment changes over time, we broke the data into three periods of same lengths (33 years) for each area, two before (P1: 1917-1949 and P2: 1950-1982) and one after (P3: 1983-2015) the Balbina Dam construction which started in 1983 for trees from USDR. P3 corresponds also to the period of the start of intensification of the hydrological cycle in the Amazon basin (Brienen et al. 2013, Barichivich et al. 2018) and we verified its influence on tree growth and mortality for the trees from the JNP.

For comparing the MDI between equal periods within each area and between study sites, we first performed Shapiro-Wilk normality tests to proceed with the Wilcoxon rank-sum test for non-parametric datasets or t-tests for parametric ones.

Determining the year of death using ^{14}C-dating

Tree rings close to the cambium was dated by ^{14}C to estimate the year of death for 41

trees (only the ones with non-degraded last rings), 13 from JNP e 28 from USDR. The α-cellulose of that rings was extracted following the Jayme-Vise methodology (Green 1963, Steinhoff et al. 2013) while the graphitization and the combustion of samples follow Steinhoff et al. (2017). Radiocarbon analysis was performed at the accelerator mass spectrometer - AMS from the Max-Planck-Institute of Biogeochemistry in Jena, Germany. The AMS analyzed the three carbon isotopes (^{12}C, ^{13}C, and ^{14}C) and all results were corrected for $\delta^{13}C$ fractionation. The precision for modern samples is about 1-3 ‰ based on the long-term reproducibility of secondary standards.

Fraction modern (FM) data were converted to calendar years for ring formation using the OxCal online software v4.3 (Ramsey 2001; Ramsey 2009) and considering the concentration of radioactive carbon in the modern standard (post-1950 period /SA zone) (Hua et al. 2013). We consider only the ^{14}C signatures after bomb-peak (Hua et al. 2013) to date the death with high accuracy (1-4 years). Rings dated in years before bomb-peak with FM between 0.96 and 1.0 was not considered because of high uncertainties caused by the SUESS-effect (Worbes 2002). In that case, the dated of death were determined using just the dendrochronology dating (Assahira et al. 2017). For the deaths after the bomb-peak, in many cases, the given result was a period, for those we also used dendrochronology to reach the exact year in that period. These dates were associated with anthropic (for the USDR trees) and hydroclimatic events (both areas) to understand the causes of their death.

Results

The mean flood level measured for the trees sampled at JNP was 7.8 m ± 0.7 m (6.5 m to 9 m), corresponding to a flood duration from six to ten months induced by a regular flood-pulse. At the USDR the mean flood level was with 7.7 ± 0.6 m (6 to 8 m) similar to the population at the JNP. The flood duration at this site corresponds to the JNP for the pre-dam period, however, was different in the post-dam period due to massive changes in the hydrological regime (Assahira et al. 2017).

The mean DBH and age were similar for both areas, being 43.9 cm (min-max: 16.5-116 cm) for the JNP trees and 45.9 cm (12.1-175.07 cm) at the USDR site, while the mean age was 210 yrs (60-466 yrs) for JNP and 213 yrs (30-498 yrs) for USDR trees. The hollows ages and sizes for JNP trees were smaller for JNP trees (77 yrs with 17.19 cm) than USDR (104 yrs with

22.35 cm). The MDI values were similar (2.04 cm in JNP and 2.28 cm in USDR), but still showed a significant difference between areas (p = 0.01, t-test) (Table 1).

Table 1- Quantitative results for both study areas (JNP: Jaú National Park; USDR: Uatumã Sustainable Development Reserve) (SD: Standard deviation).

	Area	DBH (cm)	Hollow (cm)	HolAge (yr)	Total Age (yrs)	MDI (mm)
Num. Ind.	JNP	52	38	38	52	52
	USDR	91	57	57	90	91
Mean ± SD	JNP	43.9 ± 21.7	17.19 ± 13.82	77 ± 61	210 ± 103	2.04 ± 0.39*
	USDR	45.9 ± 24.6	22.35 ± 23.01	104 ± 76	213 ± 103	2.28 ± 0.69*
Min.	JNP	16.5	2.27	17	60	1.29
	USDR	12.1	4.03	24	30	1.10
Max.	JNP	116	63.2	287	466	2.97
	USDR	93.6 (175.1**)	60.0	272	498 (820**)	4.88

** There was a significant difference between areas (p = 0.01, t-test).*

***: for the individual with the biggest DBH (175.1 cm) the age of the hollow part could not be estimated as its diameter was larger than the maximum DBH (93.6 cm) considered in the age-diameter model. The age of this large individual was estimated dividing the DBH by the MDI of the population.*

The age-DBH model for living and dead, hollow and non-hollow trees demonstrated that the growth trajectory was similar in both areas despite the occurrence of the slow-growing individuals within the USDR (Figure 2). There is consistent growth in both areas, although the USDR trees pattern is more variable between trees. The cumulative DBH is highly correlated to the total ages (r=0.97 for JNP and r=0.96 for USDR).

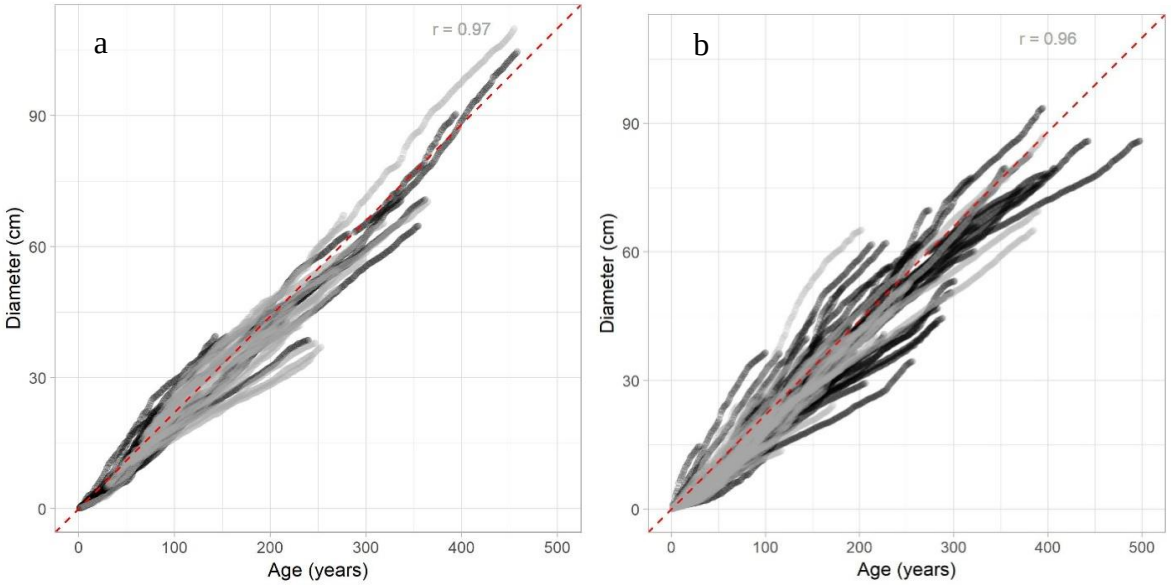

Figure 2 – DBH x Age models for (a) JNP and (b) USDR. The dead individuals are represented in grey while living ones in black. The red dashed line is an imaginary reference representing the same inclination for both to allow comparison.

The mean passage time through 5 cm-DBH classes was 26 years for the JNP and 22 for USRD and was significantly different (p = 0.0003). In both systems the species spent more time to reach 5 cm in DBH than in the subsequent classes, spending 29 years (median) in the JNP, and even more time (32 years) in the USDR. Up to 15 cm, trees in the USDR presented higher median passage times compared to the PNJ and in the subsequent 5-cm classes until 65 cm DBH the opposite pattern was observed. In the following diameter classes, the patterns are indistinct due to the low number of individuals represented in these size classes (Figure 3).

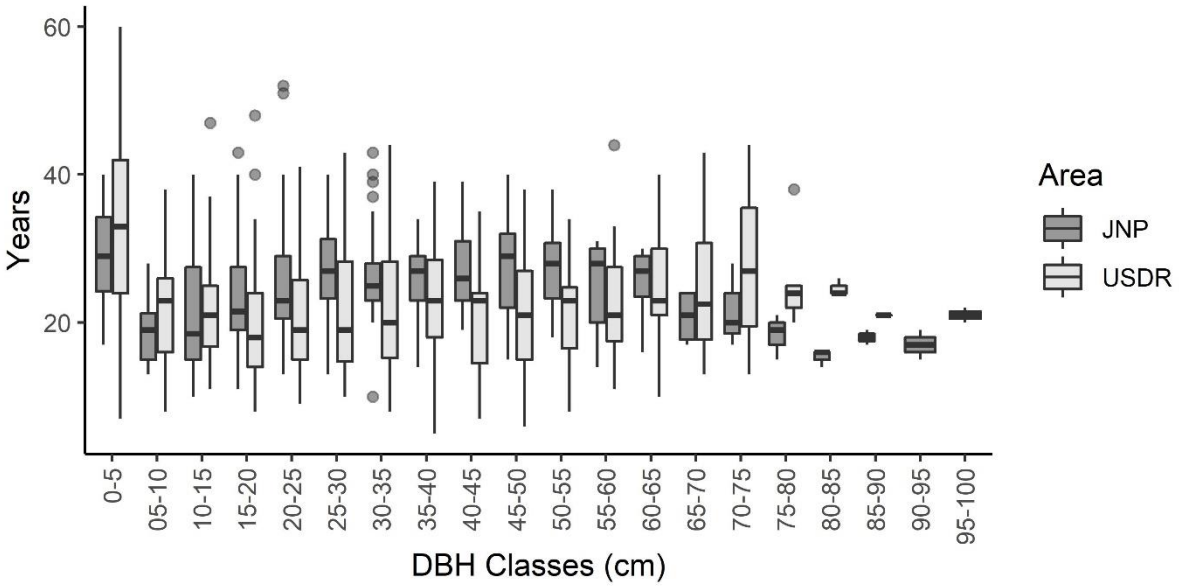

Figure 3 – Median passage time through 5-cm diameter (DBH) classes for the Jaú National Park (JNP; (dark grey) and Uatumã Sustainable Development Reserve (USDR; light grey). Indicated are the median, 25th, and 75th percentiles, as well as outliers (dots).

The lifetime growth analysis showed that only 11% or six trees (four living and two dead) of all the 52 individuals from de JNP showed release or suppression events. Three individuals had one suppression, two others presented only one release, and another one had one suppression and one release event (Figure 4). Interestingly all these trees grew along tributaries in closed *igapó* forests and not in the opened monodominant formation. As the release and suppression events are temporarily not synchronized, they probably are associated with endogenous disturbances (competition). At the USDR site, 17 individuals (18% of all trees) showed such events of release and suppressions. Ten trees were living individuals from which three showed both, suppression and release events, six with just one growth suppression and one with one growth release. Moreover, in eight of these 10 living trees from the USDR, the growth suppression was synchronized and occurred in the period after damming (after 1983) indicating exogenous disturbances (Figure 4).

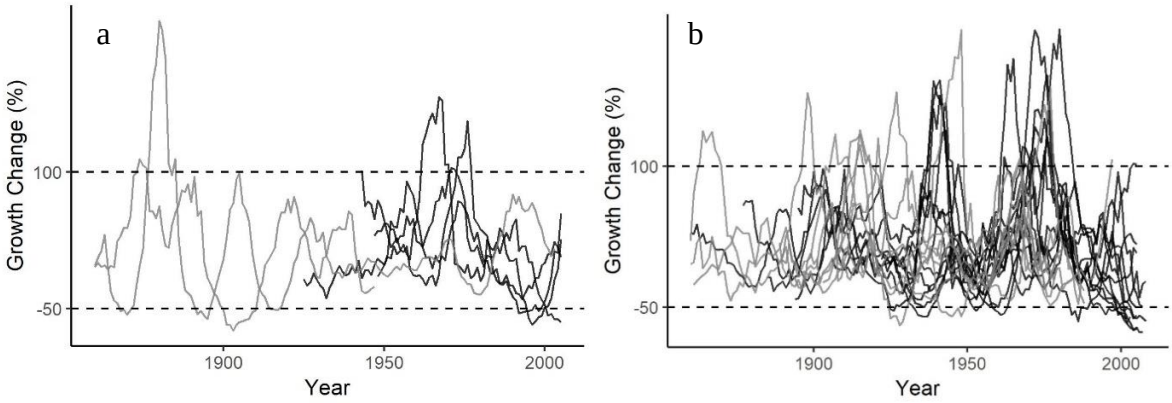

Figure 4 – Dimeter growth changes (%) of trees presenting abnormal growth pattern at (a) the Jaú National Park (JNP) and (b) Uatumã Sustainable Development Reserve (USDR). Dead trees are indicated in black and living ones in grey. The dashed lines indicate the threshold for suppression (<-50) and release (>100) events.

Analyzing the growth ratio (g_r) before the death of each individual, we identified 13 of 21 (62%) of JNP individuals showing at least one year with g_r <1.0 before death. At the USDR 15 of 29 (52%) showed this pattern. This means that the other 38% of the JNP and 48% of the USDR died abruptly. The number of consecutive years with g_r <1.0 varied between both study sites (examples in Figure 5, Figure S5). At the JNP they spent the five-fold time to die in comparison to the USDR. However, at each area, one individual spent up to 28 years (JNP, year of death: 2004) and 29 years (USDR, year of death: 1975) with g_r <1.0 before death.

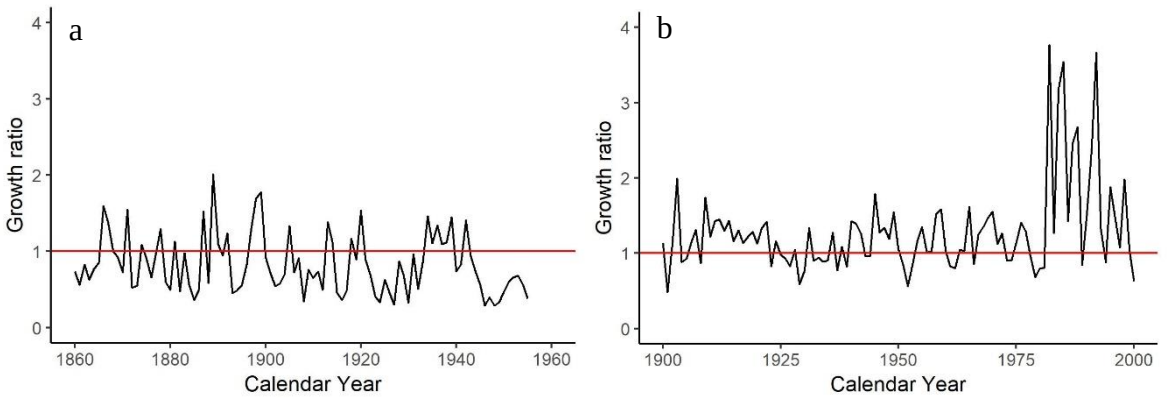

Figure 5– The growth ratio (g_r) for one individual from (a) Jaú National Park (JNP) and (b) Uatumã Sustainable Development Reserve (USDR). The red line shows the threshold of 1.

Using cluster analysis, the JNP living trees were split into two main blocks (Figure 6a), separated by the period 1975/76. At the USDR, living trees were grouped into two distinct

clusters (Figure 6b), separated by the years of 1981-82. In each block, subdivisions can be noticed.

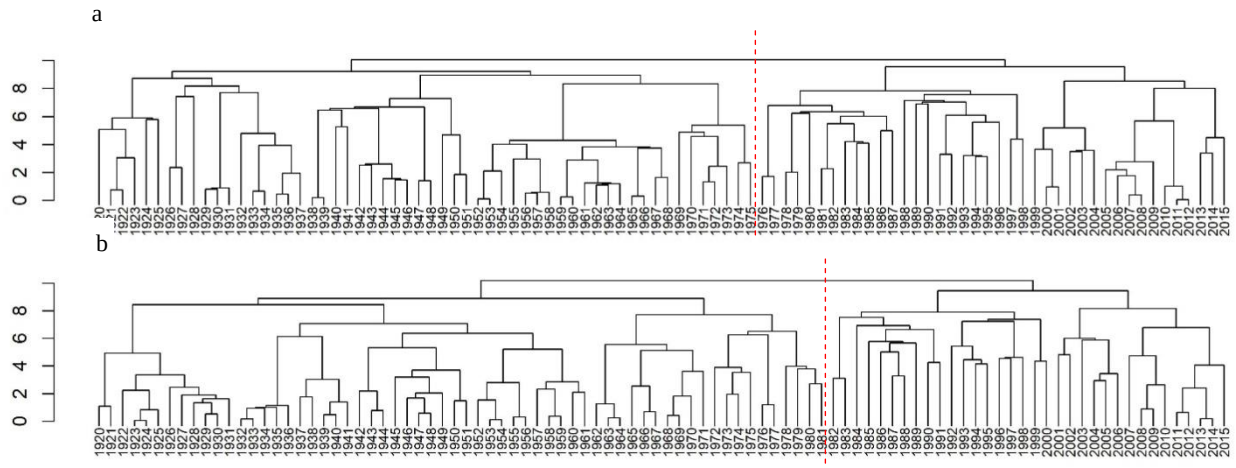

Figure 6 – Cluster analysis for (a) Jaú National Park (JNP) and (b) Uatumã Sustainable Development Reserve (USDR). The dashed red line is showing the moment were the data split.

Comparing for each study site the MDI for equal intervals of 33 years, considering two periods before (P1: 1919-1950; P2: 1951-1982) and after 1983 (P3: 1983-2015), we found no differences between any periods at PNJ. At the USDR the MDIs of the periods P1 and P2 did not differ significantly, however, the MDI of the post-dam period P3 differed significantly from P1 and P2. Between the sites, no significant difference in population growth was detected for P2, however, for the period of intensified changes in the flood-pulse regime (P3) at both sites a significant difference exists (Figure 7, Table S2). For dead trees, the modern radiocarbon analysis showed that mortality occurred during different periods at the JNP without a clear pattern, while 87% of the mortality at the USDR occurred after the begin of the operation of the Balbina dam (Figure 7).

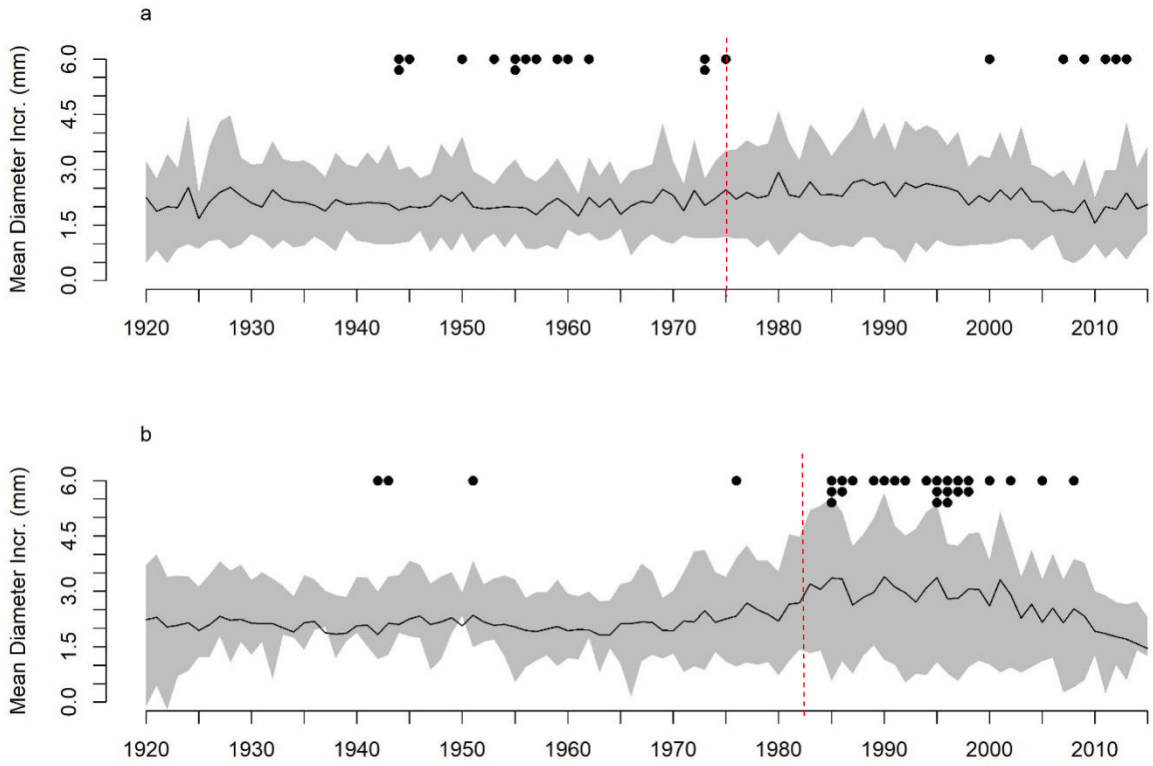

Figure 7 - Mean diameter increment (black line) of all living trees at a) Jaú National Park (JNP) and (b) Uatumã Sustainable Development Reserve (USDR) (grey background indicates the standard deviation). Black dots indicate mortality years. The dashed red lines are showing the critical years for each area by the cluster analysis.

To show the differences in population between both sites we calculated the growth ratio between the analyzed populations of both areas (USDR/JNP; values >1 indicate higher diameter growth at the USDR and vice versa) (Figure 8). Tree growth was considerably lower at the USDR in the period from 1960-65. After 1985 the population of the USDR had a sustained higher diameter increment compared to the JNP which abruptly changed around 2002 resulting into pronounced decline attaining a ratio below 0.9 after 2012 (Figure 8).

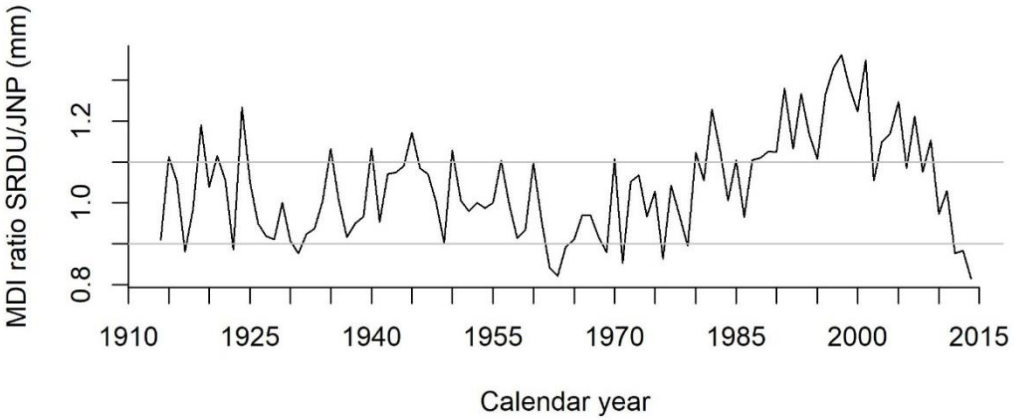

Figure 8 - Mean diameter increment (MDI) ratio between Uatumã Sustainable Development Reserve (USDR) and Jaú National Park (JNP); the ratio is showing how much diameter growth of the population at the USDR was higher (>1) or lower (,1) compared to the JNP. The grey lines are showing 10% thresholds.

Discussion

The age-DBH modeling demonstrated similar trends in growth rates for both studied areas. However, when analyzing each graph in detail, while the population of the JNP showed similar growth rates, they differed more among the analyzed individuals of the USDR. The oldest tree of JNP was 466 years old with a DBH of 116 cm; at the USDR the oldest tree reached 498 years (DBH of 86 cm), indicating for that specific tree a slow growth compared to the whole population. The biggest tree was found at USDR (DBH = 175 cm), but its age could not be modeled by the same method because there were no other trees comparable in size to estimate the age of the hollow part of the trunk. Considering its MDI of 2.15 mm and extrapolating it linearly to the DBH, its age was estimated to be 820 years. We believe that larger *E. tenuifolia* individuals with slower growths can reach a thousand years (Junk et al. 2015), but it is unlikely to find a non-hollow individual at such size. The oldest tree registered for Amazonian floodplains so far using dendrochronological methods was 502 years for a *Macrolobium acaciifolium* individual from the *igapó* forest at the Amanã SDR, Central Amazonia, using linear estimative to fill the hollow (Schöngart et al. 2005).

The MDI for JNP (2.04 ± 0.39 mm) was lower and less variable than for USDR (2.28 ± 0.69 mm), mean ages were quite similar, for JNP 210 ± 103 yrs, and 213 ± 103 yrs for USDR. However, the DBH of trees from USDR was slightly higher (45.9 cm) compared to the JNP (43.9), as well as the hollows DBH and ages (22.35 cm and 104 years against 17.19 cm and 77

years for JNP trees) (table 1). Comparing the MDI with other seven published works, were more than 45 species from blackwater *igapó* forests were evaluated, we can notice the MDI varying between 1.6 to 7.78 mm/year (Worbes 1997, Schöngart et al. 2005, Da Fonseca Júnior et al. 2009, Scabin et al. 2012, Rosa et al. 2017, Neves et al. 2019).

Both *E. tenuifolia* populations had a similar diameter growth until climatic and anthropogenic changes in the hydrological regime get manifested. At the JNP the intensification of the hydrological cycle resulted in an increase in the magnitude and frequency of maximum water levels (Barichivich et al. 2018), while at the USDR the operation of the Balbina dam caused an increase of the minimum water level and an extinction of the terrestrial phase (Assahira et al. 2017). At the USDR we observed a distinct change in growth and mortality of the *Eschweilera*-population with a considerable increase of the MDI after 1982. During this period the construction of the Balbina dam started and as the Uatumã River was dammed, and consequently the water discharge was strongly reduced (Fearnside 1990), increasing the terrestrial phase in the *igapó* forests downstream of the dam, especially at the medium and low topographies (Neves et al. 2019).

The prolonged terrestrial phase might have favored tree growth, and the proximity of the main river allowed the trees to access groundwater, so they hardly may have experienced water deficiency (Schöngart et al. 2004, Piedade et al. 2013). With the begin of the Balbina dam operation in 1989, the scenario changed dramatically leading to a strong decline in the MDI especially in the period after 2002. This significant decrease in population diameter growth was probably caused by the permanent flooding conditions starting around this period (Assahira et al. 2017) (Figure 10). A total of 87% of the sampled dead trees died after the begin of the construction of Balbina dam (Figure 9b). Nowadays, the dead stands comprise 12% of the area of floodplain forests dominated by *E. tenuifolia* of that region (Resende et al. 2019). Based on our results, we can suggest that a significant part of the still-living *E. tenuifolia* trees from USDR will not overcome this massive disturbance and will also die in the next future, as postulated by Resende et al. (2019). At the USDR, the flood-pulse disturbance is still affecting living trees of *E. tenuifolia* even more than 30 years after the begin of the operation of the hydroelectric power plant.

The JNP tree mortalities occurred during different periods, possibly as a consequence of natural senescence or extreme hydro-climatic events like severe droughts associated with El Niño and the Tropical Atlantic Dipole. Although the period 1971-75 was a critical period resulting into an extinction of the terrestrial phase for floodplain trees growing at the low

topographies in Central Amazonia for several years (Piedade et al. 2013), these changes caused growth differences but were not severe enough to cause a massive mortality of the population, although three trees died during this specific period at the JNP (Figure 9a). Also in JNP, the differentiation in the secondary growth for the period after the intensifying of the Amazonian hydrological cycle does not seem to have changed, although some trees died recently in periods of severe floods (2009, 2012-2015) (Barichivich et al. 2018).

The occurrence of a sustained decrease in the growth rate just before death (based on each dead tree MDI and the mean MDI of living ones) is 62% of JNP trees and 52% in USDR and an unexpected result since this pattern is not commonly found for angiosperms once they present a less conservative water usage, low, although this difference is not well comprehended, some explanations for it would be the less conservative hydraulic usage, higher stomatal conductance capacity, among others (Cailleret et al. 2017). It reinforces how unique this species is, being able not just to overcome the short terrestrial phase, but to resist to stressful conditions for years, even though the high mortality in the USDR evidences that long-lasting disturbances attained the tipping point resulting into mass mortality of this population (Resende et al. 2019).

Taking into account the different disturbances that can lead to tree death, only a few studies have shown the effects of river damming and fires on *igapó* forests (Nelson 2001, Flores et al. 2014, 2017, Resende et al. 2014, 2019, Assahira et al. 2017, Schöngart et al. 2017b). In comparison, many studies highlight the effects of different disturbances in upland (*terra firme*) Amazonian environments. Natural tree mortality (de Toledo et al. 2012), extreme climatic events such as windstorms (Negrón-Juárez et al. 2010), droughts (Phillips et al. 2009, Aleixo et al. 2019), fires (Barlow and Peres 2008, Monteiro et al. 2014) and other causes of death related to anthropogenic factors such as forest fragmentation (Williamson et al. 2000) are disturbance factors leading to increased tree mortality. Additionally, the complex environmental interactions in an area that culminate in the mortality of trees over time is one of the less-studied processes in ecology (Franklin et al. 1987, Villalba and Veblen 1998), even though it is of fundamental importance for the understanding of forest ecology and dynamics (Veblen 1986, Johnson and Fryer 1989, Oliver and Larson 1996). The physiological explanation of mortality mechanisms can be linked to hydraulic failure or depletion in carbon reserves (Cailleret et al. 2017), but the trigger behind the depletion of carbon in healthy trees are poorly understood (Bucci et al. 2016). We would still need to differentiate death during a period of extreme drought and during extreme floods (anoxia) for this species.

While the few existing studies on downstream impacts in the igapó floodplain have focused on the dynamics of low (Assahira et al. 2017), medium (Lobo et al. 2019) and high (Lobo et al. 2019) topographies, our study focuses on the macrohabitats at the lowest topographies (up to 10 months of flooding under natural conditions). This is a sparsely studied environment dominated by *E. tenuifolia*, which represents more than 98% of all trees of this environment (Aguiar 2015). Therefore, the species is highly dependent on the river flood pulse, being one of the first living organisms to be affected by disturbances on the hydrology. Since it forms monodominant stands in undisturbed environments and the crowns of neighboring trees do not shade each other, the cause of variations in growth may be due to the river level oscillations (exogenous disturbance) and not light availability (endogenous disturbance) (Figure S2). However, while species such as *E. tenuifolia* and *M. acaciifolium* are losing their niches, other species may be benefit from the hydrological changes in other macrohabitats. In fact, at the low and medium topographies of the *igapó* along the Uatumã River downstream of the Balbina dam, cohorts of newly grown trees from the 1980's (Neves et al. 2019), mainly composed by *Pouteria elegans* (Sapotaceae) at the low topographies (Lobo et al. 2019) and *Nectandra amazonum* Nees (Lauraceae) at the medium levels (Neves et al. 2019), are dominating. Nevertheless, in the most flooded and lower parts of the *igapós* of the USDR, the massive loss of *E. tenuifolia* trees is probably irreplaceable leading to losses of very singular macrohabitats and ecosystem services (Junk et al. 2018).

The extensive loss of low-lying monodominant floodplain forests can lead this macrohabitat to an entire regional collapse affecting all the associated ecosystem services. The growth of the same tree species is no longer similar between altered and pristine areas because it is has changed due to the manipulation of the flood-pulse. The highly-adapted floodplain tree species *Eschweilera tenuifolia* is extremely sensitive and vulnerable to both long- and short-lasting abnormal flooding periods with consequent changes in phase duration, caused by extreme climatic or anthropogenic events. The flood-pulse alteration, even 35 years after the disturbance, continues to cause mortality and abnormal growth anomalies.

Acknowledgments

We want to thank the National Institute of Amazonian Research (INPA), the Laboratory of Dendroecology (Casa 20), the PELD/MAUA group, INCT ADAPTA, and the Botany Post-graduation Program for the structural support. We also thank the staff and coordinators from

the Jaú National Park (ICMBio), the Uatumã Sustainable Development Reserve (SEMA/DEMUC) and ATTO (Amazon Tall Tower Observatory) project for the infrastructure and technical support. The Brazilian Council for Scientific Research (CNPq) for financing the project and the PhD fellowship for A.F. Resende (MCTI/CNPq/FNDCT nº 68/2013 – Large-Scale Biosphere-Atmosphere Program in the Amazon – LBA), PELD-MAUA project (403792/2012-6 – MCTI/CNPq/FAPs Nº 34/2012 and 441590/2016-0 – CNPq/CAPES/FAPS/BC-Fundo Newton). We thank also for the support from IBAMA, SISBIO, SISgen, ICMBio and DEMUC/SEMA, for the licenses for collecting and transporting the wood samples. We thank Tim Vincent for the English revision. We also thank Reginaldo from JNP, Victor Lery, Eduardo Rios, Jaime, Alberto Peixoto, Josué from USDR, Sr. Domingos from USDR, Celso Rabelo, Jekiston (also for the samples), Ketlen Fernanda, Anderson Reis, and Gildo Feitoza for their support during fieldwork or samples preparations.

References

Aguiar, D.P.P. 2015. Influência dos fatores hidro-edáficos na diversidade, composição florística e estrutua da comunidade arbórea de igapó no Parque Nacional do Jaú, Amazônia Central. : 64.

Aleixo, I.; Norris, D.; Hemerik, L.; Barbosa, A.; Prata, E.; Costa, F.; et al. 2019. Amazonian rainforest tree mortality driven by climate and functional traits. *Nature Climate Change*.

Anderson, E.P.; Jenkins, C.N.; Heilpern, S.; Maldonado-ocampo, J.A.; Carvajal-vallejos, F.M.; Encalada, A.C.; et al. 2018. Fragmentation of Andes-to-Amazon connectivity by hydropower dams. *Science Advances*: 1–8.

Armstrong, W.; Drew, M.C. 2002. Root growth and metabolism under oxygen deficiency. *Plant Roots: The Hidden Half*: 729–761.

Artaxo, P. 2019. Working together for Amazonia. *Science* 363: 323–323.

Assahira, C.; Resende, A.F. de; Trumbore, S.E.; Wittmann, F.; Cintra, B.B.L.; Batista, E.S.; et al. 2017. Tree mortality of a flood-adapted species in response of hydrographic changes caused by an Amazonian river dam. *Forest Ecology and Management* 396: 113–123.

Baker, P.J.; Bunyavejchewin, S.; Oliver, C.D.; Ashton, P.S. 2005. Disturbance history and historical stand dynamics of a seasonal tropical forest in western Thailand. *Ecological Monographs* 75: 317–343.

Barichivich, J.; Gloor, E.; Peylin, P.; Brienen, R.J.W.; Schöngart, J.; Espinoza, J.C.; et al. 2018. Recent intensification of Amazon flooding extremes driven by strengthened Walker circulation. *Science Advances* 4: eaat8785.

Barlow, J.; Peres, C.A. 2008. Fire-mediated dieback and compositional cascade in an Amazonian forest Fire-mediated dieback and compositional cascade in an Amazonian forest. .

Barnett, A.A.; Borges, S.H.; Shapley, R.L. 2002. Primates of the Jaú National Park, Amazonas, Brazil. .

Barnett, A.A.; Castilho, C.V. De; Shapley, R.L.; Anic, A. 2005. Diet , Habitat Selection and Natural History of Cacajao melanocephalus ouakary in Ja u ´ National Park , Brazil. 26: 949–969.

Barnett, A.A.; Bowler, M.; Bezerra, B.M.; Defler, T.R. 2013. Ecology and behavior of uacaris (genus Cacajao). : 151–172.

Batista, E.S.; Schöngart, J. 2018. Dendroecology of Macrolobium acaciifolium (Fabaceae) in Central Amazonian floodplain forests. *Acta Amazonica* 48: 311–320.

Beissner, A.; Genske, R.; Prall, M.; Weinholz, P. 2002. Xact Version 7.22b - SciLab GmbH. .

Bowman, D.M.J.S.; Brienen, R.J.W.; Gloor, E.; Phillips, O.L.; Prior, L.D. 2013. Detecting trends in tree growth: not so simple. *Trends in Plant Science* 18: 11–17.

Brienen, R.J.W.; Zuidema, P.A. 2006. Lifetime growth patterns and ages of Bolivian rain forest trees obtained by tree ring analysis. *Journal of Ecology* 94: 481–493.

Brienen, R.J.W.; Zuidema, P.A.; Martínez-Ramos, M. 2010. Attaining the canopy in dry and moist tropical forests: Strong differences in tree growth trajectories reflect variation in growing conditions. *Oecologia* 163: 485–496.

Brienen, R.J.W.; Hietz, P.; Wanek, W.; Gloor, M. 2013. Oxygen isotopes in tree rings record variation in precipitation δ18O and amount effects in the south of Mexico. *Journal of Geophysical Research: Biogeosciences* 118: 1604–1615.

Bucci, S.J.; Goldstein, G.; Scholz, F.G.; Meinzer, F.C. 2016. Physiological Significance of Hydraulic Segmentation, Nocturnal Transpiration and Capacitance in Tropical Trees: Paradigms Revisited. In: Springer, Cham, p.205–225.

Cailleret, M.; Jansen, S.; Robert, E.M.R.; Desoto, L.; Aakala, T.; Antos, J.A.; et al. 2017. A synthesis of radial growth patterns preceding tree mortality. *Global Change Biology* 23.

Castello, L.; Macedo, M.N. 2015. Large-scale degradation of Amazonian freshwater ecosystems Large-scale degradation of Amazonian freshwater ecosystems. *Global Change*

Biology.

Castello, L.; Mcgrath, D.G.; Hess, L.L.; Coe, M.T.; Lefebvre, P.A.; Petry, P.; et al. 2013. The vulnerability of Amazon freshwater ecosystems. *Conservation Letters* 6: 217–229.

Cook, E.; Kairiukstis, L. 1990. *Methods of dendrochronology*. In: Cook, E.R.; Kairiukstis, L.A. (Eds.) Springer Netherlands, Dordrecht, .

Crawford, R.M.M.; Braendle, R. 2007. Oxygen deprivation stress in a changing environment. *Journal of Experimental Botany* 47: 145–159.

Davidson, E.A.; De Araüjo, A.C.; Artaxo, P.; Balch, J.K.; Brown, I.F.; Mercedes, M.M.; et al. 2012. The Amazon basin in transition. *Nature* 481: 321–328.

Fearnside, P.M. 1990. Balbina licoes tragicas na Amazonia. *Ciência Hoje*: 34–40.

Fearnside, P.M. 2005. Deforestation in Brazilian Amazonia: History, rates, and consequences. *Conservation Biology* 19: 680–688.

Fearnside, P.M. 2015. Environmental Destruction in the Brazilian Amazon. *The Future of Amazonia*: 179–225.

Ferreira, L.; Prance, G.T. 1998. Structure and species richness of low-diversity floodplain forest on the Rio Tapajós, Eastern Amazonia, Brazil. *Biodiversity and Conservation* 7: 585–596.

Ferreira, L.V. 2000. Effects of flooding duration on species richness, floristic composition and forest structure in river margin habitat in Amazonian blackwater floodplain forests: Implications for future design of protected areas. *Biodiversity and Conservation* 9: 1–14.

Ferreira, L.V.; Stohlgren, T.J. 1999. Effects of river level fluctuation on plant species richness, diversity, and distribution in a floodplain forest in Central Amazonia. *Oecologia* 120: 582–587.

Flores, B.M.; Piedade, M.T.F.; Nelson, B.W. 2014. Fire disturbance in Amazonian blackwater floodplain forests. *Plant Ecology and Diversity* 7: 319–327.

Flores, B.M.; Holmgren, M.; Xu, C.; van Nes, E.H.; Jakovac, C.C.; Mesquita, R.C.G.; et al. 2017. Floodplains as an Achilles' heel of Amazonian forest resilience. *Proceedings of the National Academy of Sciences* 114: 4442–4446.

Da Fonseca Júnior, S.F.; Piedade, M.T.F.; Schöngart, J. 2009. Wood growth of Tabebuia barbata (E. Mey.) Sandwith (Bignoniaceae) and Vatairea guianensis Aubl. (Fabaceae) in Central Amazonian black-water (igapó) and white-water (várzea) floodplain forests. *Trees - Structure and Function* 23: 127–134.

Forsberg, B.R.; Melack, J.M.; Dunne, T.; Barthem, R.B.; Goulding, M.; Paiva, R.C.D.; et al. 2017. *The potential impact of new Andean dams on Amazon fluvial ecosystems*. Vol. 12.1–

35p.

Franklin, J.F.; Shugart, H.H.; Harmon, M.E. 1987. Tree Death as an Ecological Process. *BioScience* 37: 550–556.

Furch, K. 1997. Chemistry of várzea and igapó soils and nutrient inventory of their floodplain forests. In: *The Central Amazon Floodplain: Ecology of a Pulsing System*, p.47–67.

FVA; IBAMA. 1998. Plano de Manejo do Parque Nacional do Jaú. : 258.

Gloor, M.; Brienen, R.J.W.; Galbraith, D.; Feldpausch, T.R.; Schöngart, J.; Guyot, J.L.; et al. 2013. Intensification of the Amazon hydrological cycle over the last two decades. *Geophysical Research Letters* 40: 1729–1733.

Gordon, N, A.D.; Birks, H.J.B. 1972. Numerical methods in Quaternary palaeoecology I. Zonation of pollen diagrams. *New Phytologist*.

Gower, J.C. 1971. A General Coefficient of Similarity and Some of Its Properties. *Biometrics*.

Granato-Souza, D.; Barbosa, A.C.M.C.; Ferreira Chaves, H. 2019. Drivers of growth variability of Hymenaea stigonocarpa, a widely distributed tree species in the Brazilian Cerrado. *Dendrochronologia* 53: 73–81.

Hua, Q.; Barbetti, M.; Rakowski, A.Z. 2013. Atmospheric Radiocarbon for the Period 1950–2010. *Radiocarbon* 55: 2059–2072.

Huang, Y.; Mori, S.A.; Kelly, L.M. 2015. Toward a phylogenetic-based Generic Classification of Neotropical Lecythidaceae — I. Status of Bertholletia, Corythophora, Eschweilera and Lecythis. 203: 85–121.

IDESAM, I. de C. e D.S. do A. 2009. Série Técnica Planos de Gestão Reserva de Desenvolvimento Sustentável do Uatumã Volumes 1 e 2. 1 and 2: 150.

Jackson, M.B. 1990. Hormones and developmental change in plants subjected to submergence or soil waterlogging. *Aquatic Botany* 38: 49–72.

Johnson, E.A.; Fryer, G.I. 1989. Population dynamics in lodgepole pine-Engelmann spruce forests. *Ecology*.

Junk, W.J. 1989. *Flood tolerance and tree distribution in central Amazonian floodplains*. 47–64p.

Junk, W.J.; Bayley, P.B.; Sparks, R.E. 1989. The flood pulse concept in river-floodplain systems. *Proceedings of the International Large River Symposium* 106: 110–127.

Junk, W.J.; Wittmann, F.; Schöngart, J.; Piedade, M.T.F. 2015. A classification of the major habitats of Amazonian black-water river floodplains and a comparison with their white-water counterparts. *Wetlands Ecology and Management* 23: 677–693.

Junk, W.J.; Piedade, M.T.F.; Cunha, C.N. da; Wittmann, F.; Schöngart, J. 2018. Macrohabitat studies in large Brazilian floodplains to support sustainable development in the face of climate change. *Ecohydrology and Hydrobiology* 18: 334–344.

Kubitzki, K.; Ziburski, A. 1994. Seed Dispersal in Flood Plain Forests of Amazonia. *Biotropica* 26: 30–43.

Latrubesse, E.M.; Arima, E.Y.; Dunne, T.; Park, E.; Baker, V.R.; D'Horta, F.M.; et al. 2017. Damming the rivers of the Amazon basin. *Nature* 546: 363–369.

Lees, A.C.; Peres, C.A.; Fearnside, P.M.; Schneider, M.; Zuanon, J.A.S. 2016. Hydropower and the future of Amazonian biodiversity. *Biodiversity and Conservation* 25: 451–466.

Ligon, F.K.; Dietrich, W.E.; Trush, W.J. 1995. Downstream Ecological Effects of Dams. *BioScience* 45: 183–192.

Lobo, G. de S.; Wittmann, F.; Piedade, M.T.F. 2019. Response of black-water floodplain (igapó) forests to flood pulse regulation in a dammed Amazonian river. *Forest Ecology and Management* 434: 110–118.

Lovejoy, T.E.; Nobre, C. 2018. Amazon Tipping Point. *Science Advances*.

Maia, L.; Piedade, M.T.F. 2000. Phenology of Eschweilera tenuifolia (Lecythidaceae) in Flooded Forest of the Central Amazonia - Brazil. .

Malhi, Y.; Roberts, J.T.; Betts, R. a; Killeen, T.J.; Li, W.; Nobre, C. a. 2008. the Fate of the Amazon. *Science* 319: 169–172.

Marengo, J.A.; Espinoza, J.C. 2016. Extreme seasonal droughts and floods in Amazonia: Causes, trends and impacts. *International Journal of Climatology* 36: 1033–1050.

Marengo, J.A.; Aragão, L.E.O.C.; Cox, P.M.; Betts, R.; Costa, D.; Kaye, N.; et al. 2016. Impacts of climate extremes in Brazil the development of a web platform for understanding long-term sustainability of ecosystems and human health in amazonia (pulse-Brazil). *Bulletin of the American Meteorological Society* 97: 1341–1346.

Melack, J.M.; Hess, L.L. 2010. Remote sensing of the distribution and extent of wetlands in the Amazon basin. In: *Amazonian Floodplain Forests*, Springer, p.43–59.

Monteiro, P.; Balch, J.K.; Nepstad, D.C.; Morton, D.C.; Putz, F.E. 2014. Abrupt increases in Amazonian tree mortality due to drought – fire interactions. .

Mori, S.A.; Prance, G.T. 1990. *Flora Neotropica Monograph 21 (II) Lecythidaceae - part II. The zygomorphic-flowered New World genera (Couroupita, Corythophora, Bertholletia, Couratari, Eschweilera & Lecythis)*. Vol. 70.1–376p.

Negrón-Juárez, R.I.; Chambers, J.Q.; Guimaraes, G.; Zeng, H.; Raupp, C.F.M.; Marra, D.M.;

et al. 2010. Widespread Amazon forest tree mortality from a single cross-basin squall line event. *Geophysical Research Letters* 37: 1–5.

Nelson, B.W. 2001. Fogo em florestas da Amazônia Central em 1997. *Anais X SBSR*: 1675–1682.

Neves, J.R.D.; Piedade, M.T.F.; Resende, A.F. de; Feitosa, Y.O.; Schöngart, J. 2019. Impact of climatic and hydrological disturbances on black-water floodplain forests in Central Amazonia Juliana. *Biotropica*.

Nobre, C.A.; Obregón, G.O.; Marengo, J.A.; Fu, R.; Poveda, G. 2013. Characteristics of Amazonian Climate: Main Features. In: *Amazonia and Global Change*, p.149–162.

Nobre, C.A.; Sampaio, G.; Borma, L.S.; Castilla-Rubio, J.C.; Silva, J.S.; Cardoso, M. 2016. Land-use and climate change risks in the Amazon and the need of a novel sustainable development paradigm. *Proceedings of the National Academy of Sciences* 113: 10759–10768.

Nowacki, G.J.; Abrams, M.D. 1997. Radial-Growth Averaging Criteria for Reconstruction Disturbance Histories from presettlement-origin oaks. 67: 225–249.

Oliver, C.D.; Larson, B.C. 1996. Forest stand dynamics: updated edition. *Forest stand dynamics*: 520.

Parolin, P. 2009. Submerged in darkness: Adaptations to prolonged submergence by woody species of the Amazonian floodplains. *Annals of Botany* 103: 359–376.

Parolin, P.; Ferreira, L. 1998. Are there differences in specific wood gravities between trees in várzea and igapó (Central Amazonia). *Ecotropica* 4: 25–32.

Parolin, P.; Worbes, M. 2015. Wood density of trees in black water floodplains of Rio Jaú National Park, Amazonia, Brazil. *Acta Amazonica* 30: 441–441.

Parolin, P.; De Simone, O.; Haase, K.; Waldhoff, D.; Rottenberger, S.; Kuhn, U.; et al. 2004. Central Amazonian Floodplain Forests: Tree Adaptations in a Pulsing System. *The Botanical Review* 70: 357–380.

Phillips, O.L.; Aragão, L.E.O.C.O.C.; Lewis, S.L.; Fisher, J.B.; Lloyd, J.; López-González, G.; et al. 2009. Drought Sensitivity of the Amazon Rainforest. *Science* 323: 1344–1347.

Piedade, M.T.F.; Schongart, J.; Wittmann, F.; Parolin, P.; Junk, W.J. 2013. Impactos ecológicos da inundação e seca na vegetação das áreas alagáveis amazônicas. *Eventos climáticos extremos na Amazônia: causas e conseqüências*: 405–457.

Piedade, M.T.F.F.; Ferreira, C.S.; Wittmann, A. de O.; Buckeridge, M.S.; Parolin, P.; Oliveira-Wittmann, A.; et al. 2010. Biochemistry of Amazonian floodplain trees. In: *Amazonian*

Floodplain Forests: Ecophysiology, Biodiversity and Sustainable Management, Springer, Dordrecht, p.127–140.

Prance, G.T. 1980. A terminologia dos tipos de florestas amazônicas sujeitas a inundação. *Acta Amazonica* 10: 495–504.

R Core Team. 2018. R: A Language and Environment for Statistical Computing. .

Ramsey, C.B. 2001. Development of the Radiocarbon Calibration Program\. *Radiocarbon* 43: 355–363.

Ramsey, C.B. 2009. Bayesian Analysis of Radiocarbon Dates. *Radiocarbon*.

Resende, A.F.; Nelson, B.W.; Flores, B.M.; de Almeida, D.R.; de Resende, A.F.; Nelson, B.W.; et al. 2014. Fire damage in seasonally flooded and upland forests of the Central Amazon. *Biotropica* 46: 643–646.

Resende, A.F. de; Schöngart, J.; Streher, A.S.; Ferreira-Ferreira, J.; Piedade, M.T.F.; Silva, T.S.F.; et al. 2019. Massive tree mortality from flood pulse disturbances in Amazonian floodplain forests: The collateral effects of hydropower production. *Science of The Total Environment* 659: 587–598.

Rosa, S.A.; Barbosa, A.C.M.C.; Junk, W.J.; da Cunha, C.N.; Piedade, M.T.F.; Scabin, A.B.; et al. 2017. Growth models based on tree-ring data for the Neotropical tree species Calophyllum brasiliense across different Brazilian wetlands: implications for conservation and management. *Trees - Structure and Function* 31: 729–742.

Sauter, M. 2013. Root responses to flooding. *Current Opinion in Plant Biology* 16: 282–286.

Scabin, A.B.; Costa, F.R.C.; Schöngart, J. 2012. The spatial distribution of illegal logging in the Anavilhanas archipelago (Central Amazonia) and logging impacts on species. *Environmental Conservation* 39: 111–121.

Schöngart, J.; Wittmann, F.; Junk, W.J.; Piedade, M.T.F. 2017. Vulnerability of Amazonian floodplains to wildfires differs according to their typologies impeding generalizations. *Proceedings of the National Academy of Sciences* 114: 201713734.

Schöngart, J.; Piedade, M.T.F.; Ludwigshausen, S.; Horna, V.; Worbes, M.; Schongart, J.; et al. 2002. Phenology and stem-growth periodicity of tree species in Amazonian floodplain forests. *Journal of Tropical Ecology* 18: 581–597.

Schöngart, J.; Junk, W.J.; Piedade, M.T.F.; Ayres, J.M.; Hüttermann, A.; Worbes, M. 2004. Teleconnection between tree growth in the Amazonian floodplains and the El Niño-Southern Oscillation effect. *Global Change Biology* 10: 683–692.

Schöngart, J.; Piedade, M.T.F.; Wittmann, F.; Junk, W.J.; Worbes, M.; Piedade, T.F. 2005.

Wood growth patterns of Macrolobium acaciifolium (Benth.) Benth. (Fabaceae) in Amazonian black-water and white-water floodplain forests. *Oecologia* 145: 454–461.

Schöngart, J.; Gribel, R.; Ferreira da Fonseca-Junior, S.; Haugaasen, T.; Group, P.P.; Cient, D.D.P.; et al. 2015. Age and Growth Patterns of Brazil Nut Trees (*Bertholletia excelsa* Bonpl.) in Amazonia, Brazil. *Biotropica* 47: 550–558.

Schweingruber, F.H. 1996. Principles of Dendrochronology. .

Sioli, H. 1984. The Amazon and its main affluents: Hydrography, morphology of the river courses, and river types. : 127–165.

Speer, J.H. 2009. *Fundamentals of Tree-Ring Research*. 521p.

Timpe, K.; Kaplan, D. 2017. The changing hydrology of a dammed Amazon. *Science Advances* 3: 1–14.

de Toledo, J.J.; Magnusson, W.E.; Castilho, C. V; Nascimento, H.E.M. 2012. Tree mode of death in Central Amazonia: Effects of soil and topography on tree mortality associated with storm disturbances. *Forest Ecology and Management* 263: 253–261.

Veblen, T.T. 1986. Age and Size Structure of Subalpine Forests in the Colorado Front Range. *Bulletin of the Torrey Botanical Club* 113: 225–240.

Villalba, R.; Veblen, T.T. 1998. Influences of Large-Scale Climatic Variability on Episodic Tree Mortality in Northern Patagonia. *Ecology* 79: 2624–2640.

Voesenek, L.A.C.J.; Benschop, J.J.; Bou, J.; Cox, M.C.H.; Groeneveld, H.W.; Millenaar, F.F.; et al. 2003. Interactions between plant hormones regulate submergence-induced shoot elongation in the flooding-tolerant dicot Rumex palustris. *Annals of Botany* 91: 205–211.

Williamson, G.B.; Laurance, W.F.; Oliveira, A.A.; Delamônica, P.; Gascon, C.; Lovejoy, T.E.; et al. 2000. Amazonian tree mortality during the 1997 El Nino drought. *Conservation Biology* 14: 1538–1542.

Worbes, M. 1989. Growth Rings, Increment and Age of Trees in Inundation Forests, Savannas and a Mountain Forest in the Neotropics. *IAWA Journal* 10: 109–122.

Worbes, M. 1997. The Forest Ecosystem of the Floodplains. *Ecological Studies* 126: 22.

Worbes, M. 2002. One hundred years of tree-ring research in the tropics-a brief history and an outlook to future challenges. *Dendrochronologia* 20: 217–231.

Worbes, M.; Klinge, H.; Revilla, J.D.J.D.; Martius, C. 1992. On the dynamics, floristic subdivision and geographical distribution of várzea forests in Central Amazonia. *Journal of Vegetation Science* 3: 553–564.

World Bank, C.C. 2019. *World Bank Climate Change Knowledge Portal | for global climate*

data and information!. (https://climateknowledgeportal.worldbank.org/country/brazil/climate-data-historical). Accessed on 07 May 2019.

Supplementary material

Figure S1 - Living Eschweilera tenuifolia trees (yellow dots) at a tributary of the Jaú National Park. The crowns are closer to other tree crowns from different species.

Figure S2 – Monodominant formation of Eschweilera tenuifolia trees, all the visible crowns are living individuals of E. tenuifolia, at a lake island at the Uatumã River.

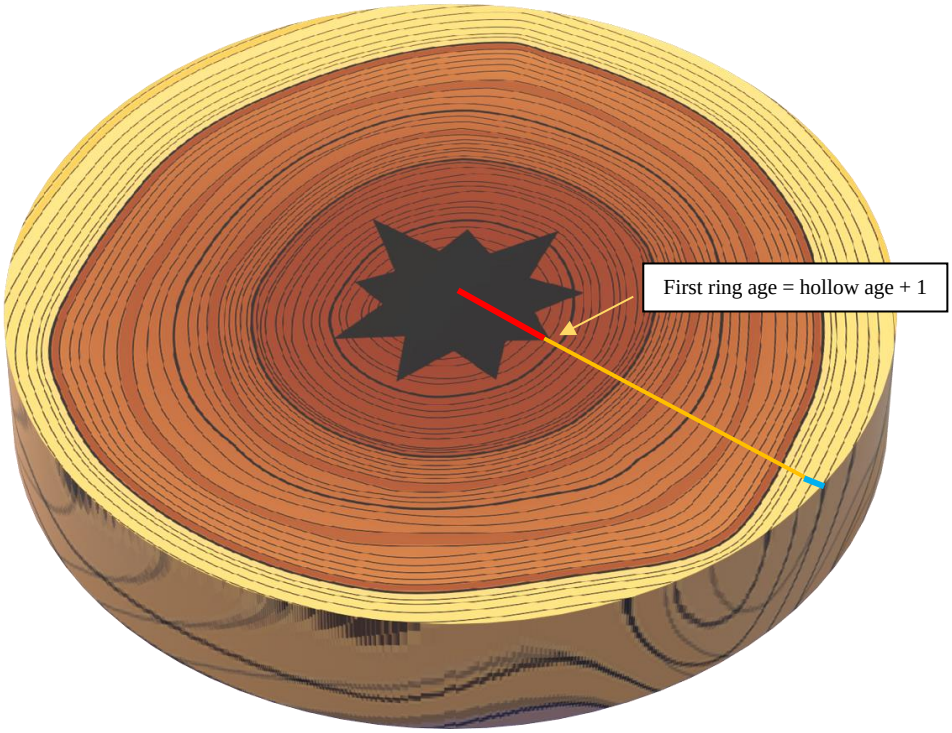

Figure S3 - Tree stem disc representing a hollow tree, the line in blue represents the bark thickness, the line in yellow the core radius and the red line the radius in the hollow section. To estimate the age of hollow trees we used the age-DBH modeling (red line), from the results we assigned to the first ring of remaining wood (yellow line) the estimated age plus one. For instance, when a hollow is estimated in 20 yrs old, the age of the remaining wood at the first ring is 21 yrs.

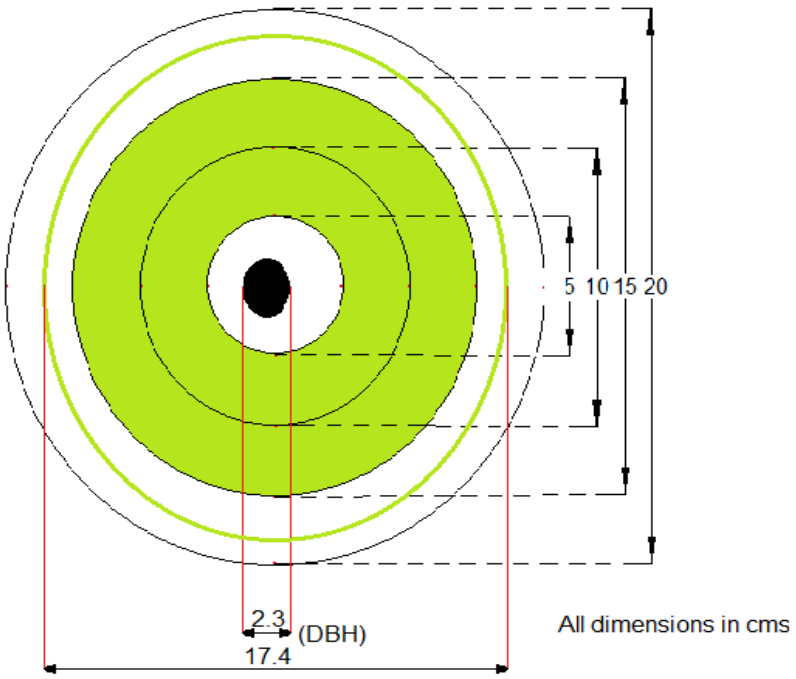

Figure S4 - Example of how the DBH classes are calculated, just whole 5 cm classes are counted.

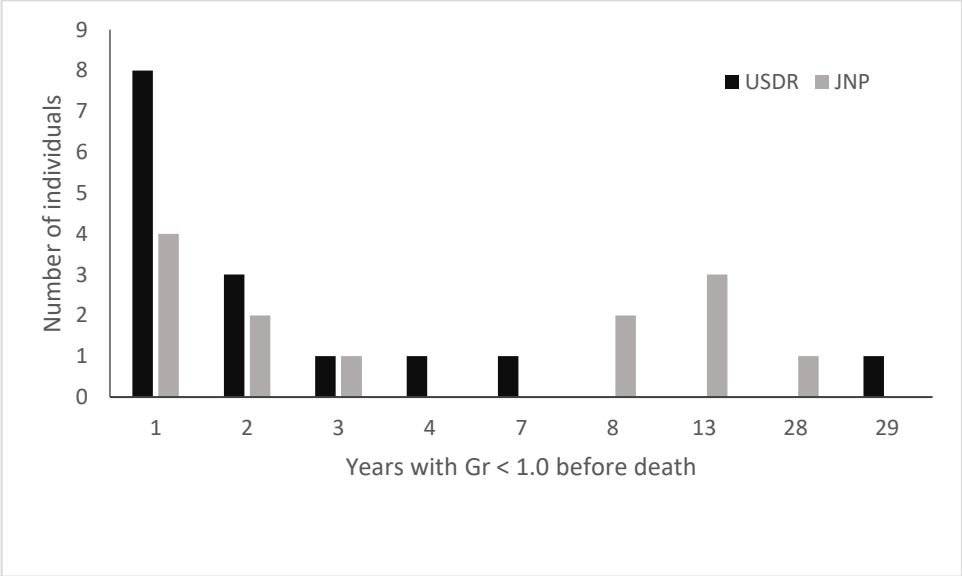

Figure S5 – Graph showing the distribution of years with growth decrease in relation to the population of living trees for dead individuals from both areas with growth ratio (USDR/JNP) gr <1.0, were black bars represents the Uatumã Sustainable Development Reserve (USDR) and grey bars the Jaú National Park (JNP).

Table S1 - Suppression, release or both events per area (Jaú National Park-JNP; Uatumã Sustainable Development Reserve-USDR), considering living and dead trees. Number of individuals (percentage).

Area	*Event*	*Living*	*Dead*
USDR	Release	1 (1.6%)	5 (17.2%)
	Suppression	6 (9.7%)	-
	Both	3 (4.8%)	2 (6.9%)
JNP	Release	1 (3.2%)	1 (4.8%)
	Suppression	2 (6.5%)	1 (4.8%)
	Both	1 (3.2%)	-

Table S2 – The tested differences between key time periods (not all) and study sites (Jaú National Park-JNP; Uatumã Sustainable Development Reserve-USDR). Values in red are significantly different.

Area/Periods of time	*JNP_P1 (1917-1949)*	*JNP_P2 (1950-1982)*	*JNP_P3 (1983-2015)*	*USDR_P1 (1917-1949)*	*USDR_P2 (1950-1982)*	*USDR_P3 (1983-2015)*
JNP_P1	---	*t = -0.76846, df = 57.555, p- = 0.4454*	---	---	---	---
JNP_P2	*t = -0.76846, df = 57.555, p- = 0.4454*	---	*t = -1.5294, df = 61.076, p- = 0.1313*	---	*W = 499, p- = 0.8676*	---
JNP_P3	---	*t = -1.5294, df = 61.076, p- = 0.1313*	---	---	---	*W = 743, p- = 0.00165*
USDR_P1	---	---	---	---	*W = 477, p-value = 0.6454*	---
USDR_P2	---	*W = 499, p- = 0.8676*	---	*W = 477, p-= 0.6454*	---	*W = 267, p-e = 0.0008*
USDR_P3	---	---	*W = 743, p- = 0.00165*		*W = 267, p- = 0.0008*	---

Table S3 – Radiocarbon dating results for death Eschweilera tenuifolia trees from the Jaú National Park (JNP) and Uatumã Sustainable Development reserve (USDR). Calendar dating using Oxcal v3.4 (SH 3 zone).

Study Area	*Sample code*	*Postulated period*	*14C cal. Date*	*Prob. (%)*
UAT	UAT125	1985	1982-1985	91.5
UAT	UAT135	1989	1987-1990	63.2
UAT	UAT136	1995	1990-1994	81.8
UAT	UAT137	1995	1994-1996	81.7
UAT	UAT138	1984	1980-1982	90.6
UAT	UAT139	1999	1998-2000	92
UAT	UAT140	1994	1993-1995	85.3
UAT	UAT141	2004	2003-2005	87.6
UAT	UAT144	1996	1997-2000	92.5
UAT	UAT207	1986	1984-1986	74.3
UAT	UAT212	1994	1993-1995	83.6
UAT	UAT213	1997	1993-1995	83.4
UAT	UAT214	1994	1993-1996	83.8
UAT	UAT216	1984	1984-1985	61.4
UAT	UAT217	1988	1987-1990	73.3
UAT	UAT218	2007	1990-1994	83.3
UAT	UAT219	1990	1989-1992	69.2
UAT	UAT221	1995	1994-1996	83.8
UAT	UAT238	1996	1995-1998	88
UAT	UAT239	2001	1995-1999	90.8
UAT	UAT240	1984	1982-1984	95.4
UAT	UAT241	1993	1993-1996	83.2
UAT	UAT242	1985	1985-1987	75.2
UAT	UAT243	1997	1996-1999	87.9
UAT	UAT244	1991	1989-1995	84.8
UAT	UAT246	1975	1974-1976	91.9
JAU	JAU082	2012	2009-2014	92.2
JAU	JAU088	2011	2007-2013	88.8
JAU	JAU092	2006	2010-2014	60.9
JAU	JAU101	1974	1975-1976	77.3
JAU	JAU108	2008	1998-2001	88.8
JAU	JAU109	1999	1997-1999	90.5
JAU	JAU115	1972	1972-1974	95.4
JAU	JAU116	2010	2008-2011	90.3
JAU	JAU121	1972	1977-1980	95.4

Síntese

O presente trabalho visou estudar o efeito da alteração no pulso de inundação, devido ao barramento do Rio Uatumã pela instalação da hidrelétrica de Balbina, no crescimento e mortalidade de árvores no igapó. Para isso localizamos as áreas de igapó existentes a jusante da barragem e quantificamos as áreas com alta mortalidade arbórea e áreas que ainda são muito afetadas pela alteração do pulso de inundação, onde as árvores vivas estão provavelmente em processo de mortalidade. Uma vez que a parte mais afetada foram as cotas mais baixas de inundação, onde ocorre a espécie *Eschweilera tenuifolia*, escolhemos coletar indivíduos vivos e mortos dessa espécie a jusante da barragem de Balbina, para testar se o crescimento foi afetado após 1983 com a construção e operação da barragem e verificar quando e porque a mortalidade massiva de árvores ocorreu. Para fins comparativos realizamos estudos nos mesmos macro-habitats do Parque Nacional do Jaú onde não há maiores interferências antrópicas resultando na alteração do pulso de inundação.

No primeiro capítulo observamos que a aplicação de métodos de análise de imagem baseada em objetos (OBIA) e o algoritmo Random Forests de classificação supervisionada geraram uma precisão geral de 87,2%. Um total de 9.800 km^2 de florestas de igapó foram mapeados ao longo de todo o rio a jusante da barragem. No trecho denominado área focal que se inicia 43 km após a barragem e se estende por mais 80 km, um total de 12% da floresta de igapó morreu. Essas áreas de mortalidade perfazem majoritariamente os igapós de nível topográfico muito baixo, onde ocorrem poucas espécies arbóreas, sendo dominado majoritariamente por *Eschweilera tenuifolia*. Também detectamos que quase 18% do igapó remanescente pode estar atualmente sofrendo mortalidade por conta do distúrbio hidrológico persistente imposto pela barragem, o que somando aos 12% já afetados poderá chegar a 29%. Além disso, essa grande perda não inclui a totalidade das florestas de igapó perdidas a jusante da barragem, pois as áreas que estão agora acima das atuais altitudes máximas de inundação não são mais inundáveis e não puderam ser mapeadas neste trabalho pela falta de imagens de radar no período anterior à barragem.

Para os igapós mais baixos do Rio Uatumã, o estoque de carbono da biomassa acima do solo foi estimado em 118 ± 12,8 Mg C ha^{-1} (Neves 2018).Considerando a área de florestas

mortas calculada no presente estudo como uma estimativa conservadora (10,9 km^2), podemos estimar uma perda de biomassa de 129 ± 14 x 10^9 g C. No entanto, como o processo de mortalidade total deverá afetar 30 km^2 de florestas (29% do igapó original), a perda de biomassa pode chegar a 354 ± 38 x 10^9 g. Isso agravaria ainda mais o balanço de emissões de gases de efeito estufa de Balbina, estimado em 2,5 x 10^{12} g C (emissões equivalentes de CO_2) devido ao aumento das emissões de metano (CH_4) da área do reservatório (Fearnside 1995, Kemenes et al. 2011). O metano já produzido por florestas alagáveis (Rosenqvist et al. 2002, Pangala et al. 2017) e as emissões dos reservatórios a montante e a jusante são amplamente conhecidos, uma vez que as condições anaeróbicas geram CH_4 (Kemenes et al. 2007, 2016). No entanto, uma vez que a mortalidade massiva de árvores também está ocorrendo em planícies de inundação fluvial a jusante de reservatórios, isso constitui uma fonte adicional de emissões de gases de efeito estufa que deveriam ser contabilizados em áreas a jusante e integradas no balanço da produção de metano por usinas hidrelétricas na Amazônia (Fearnside et al. 2006, Fearnside 2013, 2015b).

No segundo capítulo analisamos como as relações entre crescimento arbóreo e fatores climáticos mudaram com a intensificação do ciclo hidrológico em ambientes naturais (Parque Nacional do Jaú - PNJ) e perturbados (Reserva de Desenvolvimento Sustentável do Uatumã - RDSU). Para isso foram construídas cronologias de anéis de crescimento em cada sítio de estudo que apresentam estatísticas robustas (Rbar > 0,2 e SSS > 0,85) para os períodos 1927-1999 (PNJ) e 1920-2006 (RDSU). As cronologias foram relacionadas com parâmetros regionais de hidrologia (cota mensal média) e clima (precipitação total mensal) e com anomalias de temperaturas superficiais do mar (TSM) do Oceano Pacífico Equatorial e Atlântico Tropical. Os resultados sugerem fortes mudanças nas respostas das árvores de *Eschweilera tenuifolia* à intensificação do ciclo hidrológico, caracterizado pelo aumento da frequência e magnitude de cheias severas no sistema natural (PNJ) e pelo aumento do nível mínimo da água durante o período da operação da barragem de Balbina (RDSU). No PNJ as árvores indicam um aumento nas respostas às anomalias de TSM dos dois oceanos, o que reflete os mecanismos descritos e resulta na intensificação do ciclo hidrológico, causada pelo aquecimento do Atlântico Tropical e o simultâneo esfriamento do Pacífico Equatorial resultando numa intensificação da circulação de Walker, forte convecção de nuvens e aumento de precipitação nas secções norte e central da Bacia Amazônica. Na RDSU, os impactos das mudanças do regime hidrológico induzidas pela barragem de Balbina resultaram em respostas opostas das árvores em comparação com o período pré-barragem.

No terceiro capítulo, o incremento diamétrico médio (IMD) e a idade média para árvores do Rio Jaú foram calculados em 2,04 ± 0,39 mm e 201 ± 103 anos respectivamente, enquanto para árvores do Rio Uatumã o IMD foi 2,28 ± 0,69 mm e a idade média 213 ± 103 anos. Embora a trajetória de crescimento acumulado seja similar ao considerarmos um período de 500 anos de modelagem do crescimento, a análise do IMD por períodos indica que o crescimento das árvores não diferia entre Jaú e Uatumã no período anterior a construção da hidrelétrica de Balbina. Da mesma forma, o IMD no Rio Jaú não apresentou diferença entre os períodos antes e depois a construção. Em contraste, a manipulação do pulso de inundação ocasionada pela operação da barragem resultou na diferenciação do crescimento entre as duas áreas e entre os períodos no Rio Uatumã. As árvores mortas do Rio Uatumã morreram cerca de dez anos após o início da construção da barragem enquanto as do Rio Jaú não apresentaram uma tendência clara ao longo da cronologia avaliada. As árvores vivas do Rio Uatumã apresentaram um aumento no incremento entre 1982 e 2000 e um declínio de crescimento após o ano 2000, que perdura até hoje, caracterizando um padrão de supressão e provável mortalidade.

Enquanto os poucos estudos em florestas de igapó estão focando apenas na dinâmica de níveis baixos a altos, nosso trabalho se concentrou no nível muito baixo, um ambiente quase desconhecido, colonizado por pouco mais do que uma única espécie. A *E. tenuifolia* é uma das primeiras espécies arbóreas a ser afetada por distúrbios hidrológicos fluviais, uma vez que há uma forte dependência desta espécie ao pulso de inundação do rio. Enquanto em níveis com menor inundação, muitas espécies como *Macrolobium acaciifolium* podem estar perdendo seu espaço em igapós da RDSU, outras espécies podem se beneficiar disso, como ocorre no baixo e médio igapó, onde o coorte de árvores nascidas durante os anos de 1970 e 1980 na mesma área é dominada por *Pouteria elegans* (Sapotaceae) (Assahira et al. 2017, Lobo et al. 2019, Neves et al. 2019), mas no nível ainda mais inundado, onde ocorre *E. tenuifolia*, nem mesmo outras espécies deverão colonizar, uma vez que não são capazes de suportar maiores inundações (Junk et al. 2015).

Nosso estudo confirma que as ameaças aos igapós a jusante de empreendimentos hidrelétricos são evidentes, e os efeitos ambientais das barragens hidrelétricas existentes e propostas precisam ser melhor compreendidos na Amazônia e em outras áreas úmidas em risco (Kingsford 2000, Zahar et al. 2008, Ziegler et al. 2013, Junk et al. 2014). Além disso, essas informações devem ser consideradas ao licenciar e quantificar os impactos ambientais dessas empresas. Os Estudos de Impacto Ambiental (EIA) e os respectivos Relatórios de Impactos Ambientais (RIMA), devem caracterizar as condições ambientais de uma área antes da

aprovação de um projeto proposto, e deve indicar todos os impactos potenciais, bem como propor medidas de mitigação quando apropriado (Brasil 1986). No entanto, os EIA/RIMAs da Amazônia Brasileira são frequentemente desconsiderados durante a tomada de decisão (Cochrane et al. 2017, Ritter et al. 2017). Nossa sugestão para melhorar seu poder diagnóstico e preditivo, complementando os relatórios de impacto é a realização de pesquisas a jusante das áreas afetadas, bem como análises projetivas dinâmicas de mudanças e padrões de pulso de inundação previstos após o represamento considerando a vazão e o nível da água.

Embora tenhamos mapeado as áreas mais frágeis, ainda é difícil prever a duração exata e a extensão do processo de mortalidade de árvores que ainda ocorre devido à alteração do pulso de inundação. É provável, no entanto, que durará décadas (Assahira et al. 2017) e que as interações climáticas e de uso da terra provavelmente intensificarão os efeitos deletérios causados pelas barragens na Amazônia (Nobre et al. 2016). Uma vez que a alteração do pulso de inundação, mais de 30 anos após a perturbação, continua causando anomalias no crescimento e mortalidade de árvores, principalmente da espécie *E. tenuifolia*, o cenário é pessimista e a mortalidade massiva de árvores pode levar à perda de florestas nas baixas topografias de igapó, podendo provocar o colapso desse macro-habitat, afetando também os ambientes associados, tais como igapós em porções superiores e a fauna aquática. Esta espécie deve ser melhor estudada principalmente em relação às adaptações à inundação e questões ecofisiológicas que possibilitem uma melhor compreensão dos padrões de mortalidade. Esperamos que esses resultados sirvam de apoio para técnicos e tomadores de decisão, formulação de novas políticas públicas para a proteção de áreas úmidas da Amazônia, e sugerimos que mais estudos sejam feitos em áreas a jusante de barragens hidrelétricas na Amazônia, contemplando diferentes grupos vegetais e animais que possam estar sendo afetados por distúrbios hidrológicos.

Referências bibliográficas

Adams, W. 2000. Downstream impacts of dams. *WCD Thematic Review I*: 24.

Armstrong, W.; Drew, M.C. 2002. Root growth and metabolism under oxygen deficiency. *Plant Roots: The Hidden Half*: 729–761.

Assahira, C.; Resende, A.F. de; Trumbore, S.E.; Wittmann, F.; Cintra, B.B.L.; Batista, E.S.; et al. 2017. Tree mortality of a flood-adapted species in response of hydrographic changes caused by an Amazonian river dam. *Forest Ecology and Management* 396: 113–123.

Barichivich, J.; Gloor, E.; Peylin, P.; Brienen, R.J.W.; Schöngart, J.; Espinoza, J.C.; et al. 2018. Recent intensification of Amazon flooding extremes driven by strengthened Walker circulation. *Science Advances* 4: eaat8785.

Brasil. 1986. Resolução CONAMA nº 01, de 23 de janeiro de 1986. *CONAMA - Conselho Nacinal o Meio Ambiente*.

Castello, L.; Macedo, M.N. 2015a. Large-scale degradation of Amazonian freshwater ecosystems Large-scale degradation of Amazonian freshwater ecosystems. *Global Change Biology*.

Castello, L.; Macedo, M.N. 2015b. Large-scale degradation of Amazonian freshwater ecosystems. *Global Change Biology* 22: 990–1007.

Castello, L.; Mcgrath, D.G.; Hess, L.L.; Coe, M.T.; Lefebvre, P.A.; Petry, P.; et al. 2013. The vulnerability of Amazon freshwater ecosystems. *Conservation Letters* 6: 217–229.

Cochrane, S.M.V.; Matricardi, E.A.T.; Numata, I.; Lefebvre, P.A. 2017. Landsat-based analysis of mega dam flooding impacts in the Amazon compared to associated environmental impact assessments: Upper Madeira River example 2006–2015. *Remote Sensing Applications: Society and Environment* 7: 1–8.

Crawford, R.M.M.; Braendle, R. 2007. Oxygen deprivation stress in a changing environment. *Journal of Experimental Botany* 47: 145–159.

Duffy, P.B.; Brando, P.; Asner, G.P.; Field, C.B. 2015. Projections of future meteorological drought and wet periods in the Amazon. *Proceedings of the National Academy of Sciences* 112: 13172–13177.

Espinoza, J.C.; Ronchail, J.; Marengo, J.A.; Segura, H. 2018. Contrasting North–South changes in Amazon wet-day and dry-day frequency and related atmospheric features (1981–2017). *Climate Dynamics* 0: 0.

Fearnside, P.; Rosa, L.P.; Saut, P.; Guiana, F.; Paris, T.; Nations, U. 2006. Methane Quashes Green Credentials of Hydropower Preprint Analysis Quantifies Scientific Plagiarism. *Nature* 444: 524–525.

Fearnside, P.M. 1995. Hydroelectric Dams in Brazilian Amazonia As. *Environmental Conservation* 22: 7–19.

Fearnside, P.M. 2005. Deforestation in Brazilian Amazonia: History, rates, and consequences. *Conservation Biology* 19: 680–688.

Fearnside, P.M. 2013. Carbon credit for hydroelectric dams as a source of greenhouse-gas emissions: The example of Brazil's Teles Pires Dam. *Mitigation and Adaptation Strategies for Global Change* 18: 691–699.

Fearnside, P.M. 2015. Emissions from tropical hydropower and the IPCC. *Environmental Science and Policy* 50: 225–239.

Ferreira-Ferreira, J.; Silva, T.S.F.; Streher, A.S.; Affonso, A.G.; De Almeida Furtado, L.F.; Forsberg, B.R.; et al. 2014. Combining ALOS/PALSAR derived vegetation structure and inundation patterns to characterize major vegetation types in the Mamirauá Sustainable Development Reserve, Central Amazon floodplain, Brazil. *Wetlands Ecology and Management* 23: 41–59.

Ferreira, L.V. 2000. Effects of flooding duration on species richness, floristic composition and forest structure in river margin habitat in Amazonian blackwater floddplain forest: implications for desiong of protected areas. *Biodiversity and Conservation* 9: 1–14.

Fittkau, E.J.; Junk, W.; Klinge, H.; Sioli, H. 1975. Substrate and vegetation in the Amazon region. *Vegetation und substrat. Vaduz, J. Cramer*: 73–90.

Forsberg, B.R.; Melack, J.M.; Dunne, T.; Barthem, R.B.; Goulding, M.; Paiva, R.C.D.; et al. 2017. *The potential impact of new Andean dams on Amazon fluvial ecosystems*. Vol. 12.1–35p.

Fritts, H.C. 1976. *Tree Rings and Climate*. .

Gloor, M.; Brienen, R.J.W.; Galbraith, D.; Feldpausch, T.R.; Schöngart, J.; Guyot, J.L.; et al. 2013. Intensification of the Amazon hydrological cycle over the last two decades. *Geophysical Research Letters* 40: 1729–1733.

Householder, E.; De Assis, R.L.; Schöngart, J.; Junk, W.J.; Wittmann, F.; Piedade, M.T.F.F.; et al. 2012. Habitat specifity, endemism and the neotropical distribution of Amazonian white-water floodplain trees. *Ecography* 36: 690–707.

Jackson, M.B. 1990. Hormones and developmental change in plants subjected to submergence

or soil waterlogging. *Aquatic Botany* 38: 49–72.

Jesús, M.; Espinoza, P.; Janet, G.; Guillen, I.; Morales, M.S.; Arisméndiz, R.R. 2014. dendrocronológicos en la selva central del Perú. 62: 783–793.

Junk, W.J. 1989. *Flood tolerance and tree distribution in central Amazonian floodplains*. 47–64p.

Junk, W.J.; Mello, J.A.S.N. de. 1990. Impactos ecológicos das represas hidrelétricas na bacia amazônica brasileira. *Estudos Avançados* 4: 126–143.

Junk, W.J.; Bayley, P.B.; Sparks, R.E. 1989. The flood pulse concept in river-floodplain systems. *Proceedings of the International Large River Symposium* 106: 110–127.

Junk, W.J.; Ohly, J.J.; Piedade, M.T.F.; Soares, M.G.M. 2000. *Central Amazon floodplain : actual use and options for a sustainable management*. Backhuys Publishers, 584p.

Junk, W.J.; Wittmann, F.; Schöngart, J.; Piedade, M.T.F. 2015. A classification of the major habitats of Amazonian black-water river floodplains and a comparison with their white-water counterparts. *Wetlands Ecology and Management* 23: 677–693.

Junk, W.J.; Piedade, M.T.F.; Wittmann, F.; Schöngart, J.; Parolin, P. 2010. *Amazonian Floodplain Forests: Ecophysiology, Biodiversity and Sustainable Management*. Vol. 210.618p.

Junk, W.J.; Piedade, M.T.F.; Cunha, C.N. da; Wittmann, F.; Schöngart, J. 2018. Macrohabitat studies in large Brazilian floodplains to support sustainable development in the face of climate change. *Ecohydrology and Hydrobiology* 18: 334–344.

Junk, W.J.; Piedade, M.T.F.; Schöngart, J.; Cohn-Haft, M.; Adeney, J.M.; Wittmann, F. 2011. A classification of major naturally-occurring amazonian lowland wetlands. *Wetlands* 31: 623–640.

Junk, W.J.; Piedade, M.T.F.; Lourival, R.; Wittmann, F.; Kandus, P.; Lacerda, L.D.; et al. 2014. Brazilian wetlands: Their definition, delineation, and classification for research, sustainable management, and protection. *Aquatic Conservation: Marine and Freshwater Ecosystems* 24: 5–22.

Kemenes, A.; Forsberg, B.R.; Melack, J.M. 2007. Methane release below a tropical hydroelectric dam. *Geophysical Research Letters* 34: 1–5.

Kemenes, A.; Forsberg, B.R.; Melack, J.M. 2011. CO2 emissions from a tropical hydroelectric reservoir (Balbina, Brazil). *Journal of Geophysical Research: Biogeosciences* 116.

Kemenes, A.; Forsberg, B.R.; Melack, J.M. 2016. Downstream emissions of CH4and CO2from hydroelectric reservoirs (Tucurui, Samuel, and Curua-Una) in the Amazon basin. *Inland*

Waters 6: 295–302.

Kingsford, R.T. 2000. Ecological impacts of dams, water diversions and river management on floodplain wetlands in Australia. *Austral Ecology* 25: 109–127.

Lobo, G. de S.; Wittmann, F.; Piedade, M.T.F. 2019. Response of black-water floodplain (igapó) forests to flood pulse regulation in a dammed Amazonian river. *Forest Ecology and Management* 434: 110–118.

Luize, B.G.; Silva, T.S.F.; Wittmann, F.; Assis, R.L.; Venticinque, E.M. 2015. Effects of the Flooding Gradient on Tree Community Diversity in Várzea Forests of the Purus River, Central Amazon, Brazil. *Biotropica* 47: 137–142.

Luize, B.G.; Magalhães, J.L.L.; Queiroz, H.; Lopes, M.A.; Venticinque, E.M.; de Moraes Novo, E.M.L.; et al. 2018. The tree species pool of Amazonian wetland forests: Which species can assemble in periodically waterlogged habitats? *PLoS ONE* 13.

Malhi, Y.; Roberts, J.T.; Betts, R. a; Killeen, T.J.; Li, W.; Nobre, C. a. 2008. the Fate of the Amazon. *Science* 319: 169–172.

Marengo, J.A.; Espinoza, J.C. 2016. Extreme seasonal droughts and floods in Amazonia: Causes, trends and impacts. *International Journal of Climatology* 36: 1033–1050.

Marengo, J.A.; Tomasella, J.; Alves, L.M.; Soares, W.R.; Rodriguez, D.A. 2011. The drought of 2010 in the context of historical droughts in the Amazon region. *Geophysical Research Letters* 38: 1–5.

Marengo, J.A.; Souza Jr., C.M.; Thonicke, K.; Burton, C.; Halladay, K.; Betts, R.A.; et al. 2018. Changes in Climate and Land Use Over the Amazon Region: Current and Future Variability and Trends. *Frontiers in Earth Science* 6.

Melack, J.M.; Hess, L.L. 2010. Remote sensing of the distribution and extent of wetlands in the Amazon basin. In: *Amazonian Floodplain Forests*, Springer, p.43–59.

Montero, J.C.; Piedade, M.T.F.; Wittmann, F. 2014. Floristic variation across 600 km of inundation forests (Igapó) along the Negro River, Central Amazonia. *Hydrobiologia* 729: 229–246.

Neves, J.R.D. 2018. *Mudanças na fitofisionomia e estoque e produção de biomassa pelas alterações no ciclo hidrológico em florestas alagáveis de igapó na Amazônia Central*. Instituto Nacional de Pesquisas da Amazônia, 69pp.

Neves, J.R.D.; Piedade, M.T.F.; Resende, A.F. de; Feitosa, Y.O.; Schöngart, J. 2019. Impact of climatic and hydrological disturbances on black-water floodplain forests in Central Amazonia Juliana. *Biotropica*.

Nobre, C.A.; Sampaio, G.; Borma, L.S.; Castilla-Rubio, J.C.; Silva, J.S.; Cardoso, M. 2016. Land-use and climate change risks in the Amazon and the need of a novel sustainable development paradigm. *Proceedings of the National Academy of Sciences* 113: 10759–10768.

Pangala, S.R.; Enrich-Prast, A.; Basso, L.S.; Peixoto, R.B.; Bastviken, D.; Hornibrook, E.R.C.; et al. 2017. Large emissions from floodplain trees close the Amazon methane budget. *Nature* 552: 230–234.

Parolin, P. 2009. Submerged in darkness: Adaptations to prolonged submergence by woody species of the Amazonian floodplains. *Annals of Botany* 103: 359–376.

Parolin, P.; Waldhoff, D.; Piedade, M.T.F. 2010. Fruit and seed chemistry, biomass and dispersal. In: *Amazonian Floodplain Forests*, Springer, p.243–258.

Parolin, P.; De Simone, O.; Haase, K.; Waldhoff, D.; Rottenberger, S.; Kuhn, U.; et al. 2004. Central Amazonian Floodplain Forests: Tree Adaptations in a Pulsing System. *The Botanical Review* 70: 357–380.

Piedade, M.T.F.; Schongart, J.; Wittmann, F.; Parolin, P.; Junk, W.J. 2013. Impactos ecológicos da inundação e seca na vegetação das áreas alagáveis amazônicas. *Eventos climáticos extremos na Amazônia: causas e conseqüências*: 405–457.

Piedade, M.T.F.F.; Ferreira, C.S.; Wittmann, A. de O.; Buckeridge, M.S.; Parolin, P.; Oliveira-Wittmann, A.; et al. 2010. Biochemistry of Amazonian floodplain trees. In: *Amazonian Floodplain Forests: Ecophysiology, Biodiversity and Sustainable Management*, Springer, Dordrecht, p.127–140.

Prance, G.T. 1979. Notes on the Vegetation of Amazonia III. The Terminology of Amazonian Forest Types Subject to Inundation. *Brittonia* 31: 26.

Ritter, C.D.; McCrate, G.; Nilsson, R.H.; Fearnside, P.M.; Palme, U.; Antonelli, A. 2017. Environmental impact assessment in Brazilian Amazonia: Challenges and prospects to assess biodiversity. *Biological Conservation* 206: 161–168.

Rosenqvist, A.; Forsberg, B.R.; Pimentel, T.; Richey, J.E. 2002. Using JERS-1 L-band SAR to estimate methane emissions from the Jau/spl acute/ river floodplain (Amazon/Brazil). *IGARSS '98. Sensing and Managing the Environment. 1998 IEEE International Geoscience and Remote Sensing. Symposium Proceedings. (Cat. No.98CH36174)*: 1623–1625 vol.3.

Sauter, M. 2013. Root responses to flooding. *Current Opinion in Plant Biology* 16: 282–286.

Schöngart, J.; Junk, W.J. 2007. Forecasting the flood-pulse in Central Amazonia by ENSO-

indices. *Journal of Hydrology* 335: 124–132.

Schöngart, J.; Piedade, M.T.F.; Ludwigshausen, S.; Horna, V.; Worbes, M.; Schongart, J.; et al. 2002. Phenology and stem-growth periodicity of tree species in Amazonian floodplain forests. *Journal of Tropical Ecology* 18: 581–597.

Schöngart, J.; Junk, W.J.; Piedade, M.T.F.; Ayres, J.M.; Hüttermann, A.; Worbes, M. 2004. Teleconnection between tree growth in the Amazonian floodplains and the El Niño-Southern Oscillation effect. *Global Change Biology* 10: 683–692.

Scudeller, V.V.; Vegas-Vilarrúbia, T. 2018. Distribution and β-diversity of tree species in igapó forests (Negro River basin, Brazilian Amazon). *Journal of Vegetation Science*: 0–2.

Silva, T.S.F.; Melack, J.; Susin, S.A.; Ferreira-Ferreira, J.; Furtado, L.F. de A. 2015. Capturing the Dynamics of Amazonian Wetlands Using Synthetic Aperture Radar: Lessons Learned and Future Directions. *Remote Sensing of Wetlands*: 455–472.

Sioli, H. 1984. The Amazon and its main affluents: Hydrography, morphology of the river courses, and river types. : 127–165.

Speer, J.H. 2009. *Fundamentals of Tree-Ring Research*. 521p.

Timpe, K.; Kaplan, D. 2017. The changing hydrology of a dammed Amazon. *Science Advances* 3: 1–14.

Tomasella, J.; Borma, L.S.; Marengo, J.A.; Rodriguez, D.A.; Cuartas, L.A.; Nobre, C.A.; et al. 2010. The droughts of 1996-1997 and 2004-2005 in Amazonia: Hydrological response in the river main-stem. *Hydrological Processes* 25: 1228–1242.

Tomasella, J.; Pinho, P.F.; Borma, L.S.; Marengo, J.A.; Nobre, C.A.; Bittencourt, O.R.F.O.; et al. 2013. The droughts of 1997 and 2005 in Amazonia: Floodplain hydrology and its potential ecological and human impacts. *Climatic Change* 116: 723–746.

Voesenek, L.A.C.J.; Benschop, J.J.; Bou, J.; Cox, M.C.H.; Groeneveld, H.W.; Millenaar, F.F.; et al. 2003. Interactions between plant hormones regulate submergence-induced shoot elongation in the flooding-tolerant dicot Rumex palustris. *Annals of Botany* 91: 205–211.

Williams, G.P.; Wolman, M.G. 1984. Downstream effects of dams on alluvial rivers. *U.S. Geol. Surv., Prof. Pap.; (United States); Journal Volume: 1286*: 83.

Wittmann, F.; Schöngart, J.; Junk, W.J. 2010. Phytogeography, Species Diversity, Community Structure and Dynamics of Central Amazonian Floodplain Forests. .

Wittmann, F.; Schöngart, J.; Montero, J.C.; Motzer, T.; Junk, W.J.; Piedade, M.T.F.F.; et al. 2006. Tree species composition and diversity gradients in white-water forests across the Amazon Basin. *Journal of Biogeography* 33: 1334–1347.

Wittmann, F.; Anhuf, D.; Junk, W.J.; Wittmann, F.; Anhuft, D.; Junk, W.J. 2013. Tree species distribution and community structure of central Amazonian vairzea forests by remote-sensing techniques. 18: 805–820.

Woodhouse, I.H. 2017. *Introduction to microwave remote sensing*. CRC press, .

Worbes, M. 1985. Structural and other adaptations to long-term flooding by trees in Central Amazonia. *Amazoniana* 9: 459–484.

Worbes, M. 2002. One hundred years of tree-ring research in the tropics-a brief history and an outlook to future challenges. *Dendrochronologia* 20: 217–231.

Yoon, J.H.; Zeng, N. 2010. An Atlantic influence on Amazon rainfall. *Climate Dynamics* 34: 249–264.

Zahar, Y.; Ghorbel, A.; Albergel, J. 2008. Impacts of large dams on downstream flow conditions of rivers: Aggradation and reduction of the Medjerda channel capacity downstream of the Sidi Salem dam (Tunisia). *Journal of Hydrology* 351: 318–330.

Zeng, N.; Yoon, J.H.; Marengo, J.A.; Subramaniam, A.; Nobre, C.A.; Mariotti, A.; et al. 2008. Causes and impacts of the 2005 Amazon drought. *Environmental Research Letters* 3.

Ziegler, A.D.; Petney, T.N.; Grundy-Warr, C.; Andrews, R.H.; Baird, I.G.; Wasson, R.J.; et al. 2013. Dams and Disease Triggers on the Lower Mekong River. *PLoS Neglected Tropical Diseases* 7.